

Gas Generation Testing and Support for the Hanford Waste Treatment and Immobilization Plant

S. A. Bryan
D. M. Camaioni
T. G. Levitskaia
B. K. McNamara
R. L. Sell
L. M. Stock

June 2004

Battelle – Pacific Northwest Division
Richland, Washington 99352

LEGAL NOTICE

This report was prepared by Battelle Memorial Institute (Battelle) as an account of sponsored research activities. Neither Client nor Battelle nor any person acting on behalf of either:

MAKES ANY WARRANTY OR REPRESENTATION, EXPRESS OR IMPLIED, with respect to the accuracy, completeness, or usefulness of the information contained in this report, or that the use of any information, apparatus, process, or composition disclosed in this report may not infringe privately owned rights; or assumes any liabilities with respect to the use of, or for damages resulting from the use of, any information, apparatus, process, or composition disclosed in this report.

Reference herein to any specific commercial product, process, or service by trade name, trademark, manufacturer, or otherwise, does not necessarily constitute or imply its endorsement, recommendation, or favoring by Battelle. The views and opinions of authors expressed herein do not necessarily state or reflect those of Battelle.

Gas Generation Testing and Support for the Hanford Waste Treatment and Immobilization Plant

S. A. Bryan
D. M. Camaioni
T. G. Levitskaia
B. K. McNamara
R. L. Sell
L. M. Stock

L. H. For W.L. Tamosaitis
6/24/04

**ACCEPTED FOR
PROJECT USE**

June 2004

Test specification: 24590-PTF-TSP-RT-03-009, Rev. 0
Test plan: TP-RPP-WTP-283 Rev 0
Test exceptions: none
R&T focus area: Pretreatment
Test Scoping Statement(s): HG-1

Battelle - Pacific Northwest Division
Richland, Washington 99352

Completeness of Testing

This report describes the results of work and testing specified by test specification 24590-PTF-TSP-RT-03-009, Rev. 0 and test plan TP-RPP-WTP-283 Rev. 0, "Gas Generation Model Support." The work and any associated testing followed the quality assurance requirements outlined in the test specification and test plan. The descriptions provided in this test report are an accurate account of both the conduct of the work and the data collected. Test plan results are reported. Also reported are any unusual or anomalous occurrences that are different from expected results. The test results and this report have been reviewed and verified.

Approved:



Gordon H. Beeman, Manager
WTP R&T Support Project

6-15-04
Date

Testing Summary

Objectives

This project was initiated to support efforts by the Bechtel National, Inc., Research and Technology Department to provide design tools for estimating rates of hydrogen gas generation by waste streams in the Waste Treatment and Immobilization Plant (WTP). A model for predicting hydrogen generation rates in Hanford's stored tank wastes has been developed by Hu (1997, 2000, 2002). However, as the waste is processed in the WTP, its properties and conditions are subject to change. Assessments of which processing steps would most affect hydrogen generation identified several effects that needed to be understood (Sherwood and Stock 2003). These included the effects of beta/gamma and alpha radiolysis and of adding hydroxide, permanganate, air, sugar, and glass-forming materials at various stages in the processing prior to the vitrification step. While many issues could be resolved through technical evaluations of existing information, some issues required experimental testing. This report summarizes the experimental work. Six Technical Issue Reports (TIRs) were written to evaluate the major issues and are included as appendixes.

The objective of this experimental work is to assess the contribution of oxygen to the rate of hydrogen generation from actual and simulated Hanford waste. The data discussed in this report provide information on the gas generation capacity and reactivity of Hanford tank material.

Gas generation rates for various WTP flow sheet waste streams are estimated using the Hu (2002) model. This model was developed from an expansive information base that includes data on many of the 177 Hanford underground storage tanks, laboratory studies at Battelle – Pacific Northwest Division (PNWD), Argonne National Laboratory, and Georgia Institute of Technology tank waste characterization programs, and Hanford waste processing data from Los Alamos National Laboratory. The model used hydrogen gas generation data from wastes kept under an inert atmosphere.

Pulse jet mixers and other operations will introduce oxygen into the WTP waste streams. It is known that the waste stored at the Hanford tank farms (Mahoney et al. 1999) has been depleted in oxygen with a concomitant elevation in the hydrogen generation rate. Hydrogen gas generation rates were observed to increase for actual Hanford tank wastes exposed to an oxygen atmosphere (Person 1998; Pederson and Bryan 1996), an observation confirmed with waste simulants (Barefield et al. 1996; Pederson and Bryan 1996). Because the estimates of hydrogen generation in WTP waste streams is based on a model (Hu 2002) that excluded oxygen as a potential factor, we are exploring the effect of an oxygen atmosphere on the hydrogen generation rates of actual and simulated wastes under quiescent and stirring conditions.

Laboratory work was undertaken to determine the influence of oxygen on the hydrogen generation rates in actual wastes because Person (1996, 1998) had shown that the hydrogen generation rates for waste from Tank 241-SY-101 at temperatures over 70°C increased by more than an order of magnitude when exposed to oxygen. While not definitive, other work with wastes and waste simulants also suggests that exposing waste to oxygen could increase hydrogen production.

WTP personnel and PNWD selected five Hanford waste tank materials for investigation. Samples from three tanks (AN-107, U-106, and AN-102) were selected because of their high total organic carbon

(TOC) content. These wastes also had varying amounts of aluminum, a catalyst for the thermal generation of hydrogen. Another sample (AW-101) was selected because previous study suggested that it might be more reactive than predicted by the Hu correlation. The tests were carried out at 90°C because the hydrogen formation rates would be bounding and the product distributions would provide information about the propensity for methane and C₂ hydrocarbons. The hydrogen generation rates of the tank wastes were measured in the presence of 20% and 100% oxygen atmospheres. The results were very reproducible, and there were no significant differences in rates in the two atmospheres. The results of the first tests in 100% oxygen in a waste that had been exposed to 20% oxygen for about 500 hours were replicated with fresh samples of the waste in a 100% oxygen atmosphere.

The results show that oxygen increases the rates of hydrogen generation for wastes that have 1.5 to 3% TOC (by factors ranging from 4.0 to 14.4 for high TOC wastes) but does not appreciably alter the rates of hydrogen generation in wastes with low TOC content (factors range from 0.6 to 1.9 for low TOC wastes). These observations are compatible with previous observations by Person (1996, 1998). He found that oxygen accelerated hydrogen generation in Tank SY-101 waste with 3.5% TOC by a factor of more than 10, whereas there was little effect on the hydrogen generation rate for Tank AN-105 waste with 0.3% TOC. The results also are compatible with previous investigations with waste simulants (Barefield et al. 1996).

The experiments performed using actual waste with moderate to high TOC values indicated that hydrogen generation rates increase more in tank wastes exposed to air (20% or 100% oxygen atmosphere) than under inert cover gas. This factor was not addressed by the Hu model developed for predicting hydrogen generation rates in what are relatively quiescent air-free wastes. Assuming that air (with a 20% oxygen atmosphere) will be introduced into the wastes during pulse jet mixing and perhaps other WTP operations, the Hu correlation is not likely to be directly applicable for predicting rates.

This work documents the effect of various parameters on hydrogen generation from Hanford tank waste and details additional experiments to assess the role of oxygen on hydrogen generation rates from actual and simulated wastes. Results show that oxygen increases hydrogen generation from actual and simulated wastes. The specific objectives in the test plan governing this work^(a) are listed in the table.

Test Objective	Objective Met (Y/N)	Discussion
Evaluate Pretreatment Facility and front-end HLW vitrification facility flow sheets to identify operating conditions that significantly deviate from those modeled by Hu, including accident and upset conditions identified by HAZOP (2003) process.	Y	TIRs on pretreatment evaluations were written and submitted to WTP. These reports are included as appendixes to this report.
Laboratory test results provide a measure of the degree of conservatism associated with Hu model.	Y	Experimental work providing information on conservatism of the Hu model is the basis of this report.

(a) Bryan SA. 2003. "Gas Generation Model Support." Waste Treatment Plant Support Project Test Plan, TP-RPP-WTP-283 Rev 0, Battelle – Pacific Northwest Division, Richland, WA.

Test Exceptions

List Test Exceptions	Describe Test Exceptions
None.	N/A

Results and Performance Against Success Criteria

List Success Criteria	How Tests Did or Did Not meet Success Criteria
A successful program will provide sufficient, timely information to validate and/or enhance application of the Hu model for predicting hydrogen generation rates in the pretreatment facility and front end of the HLW Vitrification Facility.	<ul style="list-style-type: none"> ▪ TIRs detailing pretreatment evaluations were written and submitted to WTP and are also included as appendixes to this report. ▪ Experimental work providing information for the degree of conservatism of the Hu model is the basis of this report and a preceding interim report issued on 12/11/03. ▪ These reports were issued in a timely manner and within schedule.

Quality Requirements

PNWD implements the River Protection Project (RPP) WTP quality requirements by performing work in accordance with the PNWD Waste Treatment Plant Support Project Quality Assurance Project Plan (QAPjP) approved by the RPP-WTP Quality Assurance organization. This work was performed to the quality requirements of NQA-1-1989 Part I, Basic and Supplementary Requirements, and NQA-2a-1990, Part 2.7. In addition, 10 CFR 830 Subpart A applies for “Important to Safety” analyses. These quality requirements are implemented through PNWD’s *Waste Treatment Plant Support Project (WTPSP) Quality Assurance Requirements and Description Manual*. The analytical requirements are implemented through WTP Support Project’s Statement of Work (WTPSP-SOW-002, Rev.0), with the Radiochemical Processing Laboratory (RPL) Quantitative Gas Mass Spectrometry team.

Experiments that are not method-specific shall be performed in accordance with PNWD’s procedures QA-RPP-WTP-1101, “Scientific Investigations,” and QA-RPP-WTP-1201, “Calibration Control System,” ensuring that sufficient data are taken with properly calibrated measuring and test equipment to obtain quality results. Bechtel National, Inc.’s (BNI) QAPjP, PL-24590-QA00001, is not applicable because the work will not be performed to support environmental/regulatory testing, and the data will not be used as such.

PNWD addresses internal verification and validation activities by conducting an Independent Technical Review of the final data report in accordance with PNWD procedure QA-RPP-WTP-604. This review verifies that the reported results are traceable, that inferences and conclusions are soundly based, and the reported work satisfies the Test Plan objectives. This review procedure is part of PNWD’s *WTPSP Quality Assurance Requirements and Description Manual*.

R&T Test Conditions

Gas generation tests on actual radioactive tank wastes were conducted in the Radiochemical Processing Laboratory High-Level Radiation Facility (325A HLRF). Various Hanford tank samples were shipped from the 222-S Laboratory to PNWD for use in the testing, including Tanks AN-102, AN-106, AN-107, AW-101, and U 106 wastes. Gas generation tests on simulated AN-107 waste were conducted in nonradiological laboratories in the Radiochemical Processing Laboratory. Gas generation measurements using actual Hanford wastes were made using reaction vessels and a gas manifold system similar to those used in studies with simulated waste (Bryan and Pederson 1995) and described in reports detailing work with actual waste (Bryan et al. 1996; King et al. 1997). Experiments using simulated Hanford wastes used commercial Parr[®] reaction vessel systems for gas generation measurements.

Specific listed research and technology test conditions described in Test Specification 24590-PTF-RT-03-009 Rev 0^(a) are summarized in the following table.

List R&T Test Conditions	Were Test Conditions Followed?
Gas generation testing will be conducted at the High-Level Radiochemistry Facility (325A HLRF) in the RPL facility.	Yes, work was performed within the RPL facility.
Gas generation will be studied at high temperatures where reactions involving organic compounds occur rapidly.	Yes, gas generation was studied at high temperatures.
Additional tests may be required that involve external gamma radiation and internal alpha radiation sources.	Additional tests involving external gamma or internal alpha sources were not required.
Composition of gases generated will be measured by mass spectrometry in accordance with approved Battelle procedures.	Yes, PNWD's mass spectrometry laboratory performed all gas phase analyses as described.
The test plan will describe these (test specification) activities in detail.	Yes, test plan TP-RPP-WTP-283 Rev 0 describes the activities detailed in the test specification.
An initial Phase I experimental program will be developed to confirm application of the Hu model to the WTP.	Yes, Phase I experiments completed are reported in this document. In addition to experimental work TIRs were submitted to WPT evaluating the application of the Hu model for use by WTP.
A subsequent Phase II experimental program will provide information on how gas generation rates are affected by conditions unique to the WTP.	Phase II experiments were determined to be not needed and were not performed.

(a) Sherwood DJ. 2003. "Adaptation of the Tank Farm Correlation for Gas Generation to the WTP." Test Specification Document, 24590-PTF-TSP-RT-03-009 Rev. 0, Bechtel National Inc., Richland, WA.

Simulant Use

These tests used simulated waste based on the composition of Hanford Tank AN-107 waste. The work is described in Section 3 of this report. The test results based on the simulated AN-107 waste are compared with experimental work using actual waste (including actual AN-107 waste) in Section 2.

Discrepancies and Follow-on Tests

None.

References

Barefield EK, D Boatwright, A Deshpande, F Doctorovich, CL Liotta, HM Neumann, and S Seymore. 1996. *Mechanisms of Gas Generation from Simulated SY Tank Farm Wastes: FY 1994 Progress Report*. PNNL-11247, Pacific Northwest National Laboratory, Richland, WA.

Bryan SA and LR Pederson. 1995. *Thermal and Combined Thermal and Radiolytic Reactions Involving Nitrous Oxide, Hydrogen, and Nitrogen in the Gas Phase: Comparison of Gas Generation Rates in Supernate and Solid Fractions of Tank 241-SY-101 Simulated Wastes*. PNL-10490, Pacific Northwest Laboratory, Richland, WA.

Bryan SA, LR Pederson, CM King, SV Forbes, and RL Sell. 1996. *Gas Generation from Tank 241-SY-103 Waste*. PNL-10978, Pacific Northwest National Laboratory, Richland, WA.

Hu TA. 1997. *Calculations of Hydrogen Release Rate at Steady State for Double Shell Tanks*. HNF-SD-WM-CN-117, Lockheed Martin Hanford Corporation, Richland, WA.

Hu TA. 2000. *Empirical Rate Equation Model and Rate Calculation of Hydrogen Generation Rate for Hanford Waste Tanks*. HNF-3851 Rev. 0A, CH2M HILL Hanford Group, Richland, WA.

Hu TA. 2002. *Steady-State Flammable Gas Release Rate Calculations and Lower Flammability Level Evaluation for Hanford Tank Waste*. RPP-5926 Rev. 2, CH2M HILL Hanford Group, Richland, WA.

King CM, LR Pederson, and SA Bryan. 1997. *Thermal and Radiolytic Gas Generation from Tank 241-S-102 Waste*. PNNL-11600, Pacific Northwest National Laboratory, Richland, WA.

Mahoney LA, ZI Antoniak, JM Bates, and ME Dahl. 1999. *Retained Gas Sampler Program*. PNNL-13000, Pacific Northwest National Laboratory, Richland, WA.

Pederson LR and SA Bryan. 1996. *Status and Integration of Studies of Gas Generation in Hanford Wastes*. PNNL-11297, Pacific Northwest National Laboratory, Richland, WA.

Person JC. 1996. *Effects of Oxygen Cover Gas and NaOH Dilution on Gas Generation in Tank 241-SY-101 Waste*. WHC-SD-WM-DTR-043, Westinghouse Hanford Company, Richland, WA.

Person JC. 1998. *Gas Generation in Tank 241-AN-105 Waste with and Without Oxygen Reactions*. HNF-2038 Rev 0, Numatec Hanford Corp., Richland, WA.

Sherwood DJ and LM Stock. September 14, 2003. *An Assessment of the Applicability of the Hu Model for Hydrogen Generation to the WTP*. Bechtel National Inc., Richland, WA.

Acronyms and Abbreviations

BNI	Bechtel National, Inc.
C ₂ hydrocarbons	Hydrocarbons with two carbon atoms
DAC	Data Acquisition and Control
DOE	Department of Energy
DST	Double-Shell Tank
EDTA	Ethylenediaminetetraacetic acid
HEDTA	Hydroxyethyl ethylenediaminetetraacetic acid
HLRF	High-Level Radiation Facility
HGR	Hydrogen Generation Rate
HLW	High-Level Waste
ICP-AES	Inductively Coupled Plasma-Atomic Emission Spectroscopy
ID	Identification number or inner diameter
IDA	Iminodiacetic acid
LAW	Low-Activity Waste
MDL	Method Detection Limit
NTA	Nitrilotriacetic acid
ORP	DOE Office of River Protection
PNNL	Pacific Northwest National Laboratory
PNWD	Battelle – Pacific Northwest Division
QAPjP	Quality Assurance Project Plan
PJM	Pulse Jet Mixer
R/h	Rad per hour
REDOX	Reduction/Oxidation (Facility)
RPD	Relative Percent Difference
RPP	River Protection Project
SST	Single-Shell Tank
TC	Total Carbon
TIC	Total Inorganic Carbon
TIR	Technical Issue Report
TOC	Total Organic Carbon
TRU	Transuranic waste
UFP	Ultrafiltration Process
WTP	Waste Treatment Plant

Contents

Testing Summary	iii
Acronyms and Abbreviations	ix
1.0 Introduction	1.1
2.0 Gas Measurements on Actual Waste Samples.....	2.1
2.1 Experimental Conditions and Equipment Used for Gas Generation Tests on Actual Hanford Wastes	2.1
2.2 Hanford Tank Test Material	2.5
2.2.1 Hanford Waste Sample Description and Composite Information	2.5
2.2.2 Hanford Waste Sample Compositional Analyses	2.6
2.3 Gas Generation from Tank Waste Samples.....	2.8
2.3.1 Gas Generation from Various Hanford Tank Waste Samples	2.9
2.4 Discussion of Results: Gas Generation from Tank Waste Samples	2.28
3.0 Gas Generation Measurements Using Simulated AN-107 Waste	3.1
3.1 Experimental Conditions and Equipment Used for Gas Generation Tests on AN-107 Hanford Waste Simulant.....	3.1
3.1.1 Reaction Vessels	3.1
3.1.2 Gas Volume, Temperature, and Pressure Measurements.....	3.3
3.1.3 General Procedure	3.4
3.2 AN-107 Simulated Waste Composition and Preparation	3.5
3.3 Gas Generation Results from AN-107 Simulated Waste	3.9
3.3.1 General Observations.....	3.12
3.3.2 Effect of Organics	3.12
3.3.3 Effect of Stirring	3.13
3.3.4 Effect of Oxygen.....	3.14
3.3.5 Effect of Temperature	3.15
3.3.6 Effect of pH	3.15
4.0 Summary and Conclusions	4.1
5.0 References	5.1
Appendix A: Modeling Hydrogen Generation Rates in Wastes with Alpha Radiation.....	A.1
Appendix B: The Influence of Beta and Gamma Radiation on the Rate of Hydrogen Generation	B.1
Appendix C: The Influence of Oxygen on Hydrogen Generation Rates	C.1
Appendix D: The Influence of Hydroxide Ion on the Rate of Hydrogen Generation.....	D.1
Appendix E: Effect of Permanganate Addition on Predicting Hydrogen Generation Rates	E.1
Appendix F: Effect of Glass Forming Chemicals on Hydrogen Generation Rates.....	F.1

Figures

2.1	Reaction Vessel Used in Small-Scale Gas generation Tests.....	2.1
2.2	Reaction Vessel Holder with Ten Reaction Vessels Used in Gas Generation Tests	2.2
2.3	Diagram of Pressure Manifold System Used in Gas Generation Tests.....	2.3
2.4	Comparison of Hydrogen Generation Rates from Hanford Waste AN-102 under Various Cover Gases at 90°C	2.29
2.5	Comparison of Hydrogen Generation Rates from Hanford Waste AN-106 under Various Cover Gases at 90°C	2.29
2.6	Comparison of Hydrogen Generation Rates from Hanford Waste AN-107 under Various Cover Gases at 90°C	2.30
2.7	Comparison of Hydrogen Generation Rates from Hanford Waste AW-101 under Various Cover Gases at 90°C	2.30
2.8	Comparison of Hydrogen Generation Rates from Hanford Waste U-106 under Various Cover Gases at 90°C	2.31
2.9	Comparison of Hydrogen Generation Rates from Simulated Hanford Waste AN-107 under Various Cover Gases at 90°C	2.31
2.10	Measured Hydrogen Generation Rates under Inert and 20% Oxygen Atmosphere	2.33
2.11	Oxygen Depletion Rates for Various Hanford and Simulated Wastes	2.34
3.1	Schematic of Parr Reaction System Used for Stirred and Unstirred Simulated Waste Tests	3.3
3.2	Effect of Stirring on Hydrogen Generation	3.13
3.3	Effect of Temperature on H ₂ and N ₂ O Generation and O ₂ Depletion	3.14

Tables

2.1	Sample Masses and Vessel Volumes Used in Small-Scale Gas Generation Tests with Actual Hanford Wastes	2.4
2.2	Composite Information for Tank AN-102 Material	2.5
2.3	Composite Information for Tank AN-106 Material	2.5
2.4	Composite Information for Tank AN-107 Material	2.6
2.5	Composite Information for Tank AW-101 Material	2.6
2.6	Composite Information for Tank U-106 Material	2.6
2.7	Ion Chromatography Analysis of Tank Waste Material Used in Gas Generation Tests	2.7
2.8	Carbon Analysis of Tank Waste Material Used in Gas Generation Tests	2.7
2.9	Inductively Coupled Plasma-Atomic Emission Spectroscopy of Tank Waste Material Used in Gas Generation Tests	2.7
2.10	Alpha and Beta Radiochemical Analysis of Tank Waste Material Used in Gas Generation Tests	2.7
2.11	Summary of Tests with Actual Hanford Wastes	2.9
2.12	Mole Percent Composition Thermal Gas Sampled, Gas Formed, and Heating Times of Runs 1 and 2 Using AN-102 Waste, with 20% and 100% Oxygen Atmosphere as Initial Cover Gas	2.10
2.13	Mole Percent Composition Thermal Gas Sampled, Gas Formed, and Heating Times of Runs 3 and 4 Using AN-106 Waste, with 20% and 100% Oxygen Atmosphere as Initial Cover Gas	2.11
2.14	Mole Percent Composition Thermal Gas Sampled, Gas Formed, and Heating Times of Runs 5 and 6 Using AN-107 Waste, with 20% and 100% Oxygen Atmosphere as Initial Cover Gas	2.12
2.15	Mole Percent Composition Thermal Gas Sampled, Gas Formed, and Heating Times of Runs 7 and 8 Using AW-101 Waste, with 20% and 100% Oxygen Atmosphere as Initial Cover Gas	2.13
2.16	Mole Percent Composition Thermal Gas Sampled, Gas Formed, and Heating Times of Runs 9 and 10 Using U-106 Waste, with 20% and 100% Oxygen Atmosphere as Initial Cover Gas	2.14
2.17	Mole Percent Composition Thermal Gas Sampled, Gas Formed, and Heating Times of Runs 11 and 12 Using AN-102 Waste, 100% Ne and 100% Oxygen Atmosphere as Initial Cover Gas	2.15
2.18	Mole Percent Composition Thermal Gas Sampled, Gas Formed, and Heating Times of Runs 13 and 14 Using AN-106 Waste, 100% Ne and 100% Oxygen Atmosphere	2.16

2.19	Mole Percent Composition Thermal Gas Sampled, Gas Formed, and Heating Times of Runs 15 and 16 Using AN-107 Waste, 100% Ne and 100% Oxygen Atmosphere as Initial Cover Gas	2.17
2.20	Mole Percent Composition Thermal Gas Sampled, Gas Formed, and Heating Times of Runs 17 and 18 Using AW-101 Waste, 100% Ne and 100% Oxygen Atmosphere	2.18
2.21	Mole Percent Composition Thermal Gas Sampled, Gas Formed, and Heating Times of Runs 19 and 20 Using U-106 Waste, 100% Ne and 100% Oxygen Atmosphere as Initial Cover Gas	2.19
2.22	Gas Generation Rates from Thermal Treatment of AN-102 Waste (Runs 1 and 2) under 20% and 100% Oxygen Atmosphere as Initial Cover Gas	2.20
2.23	Gas Generation Rates from Thermal Treatment of AN-106 Waste (Runs 3 and 4) under 20% and 100% Oxygen Atmosphere as Initial Cover Gas	2.21
2.24	Gas Generation Rates from Thermal Treatment of AN-107 Waste (Runs 5 and 6) under 20% and 100% Oxygen Atmosphere as Initial Cover Gas	2.22
2.25	Gas Generation Rates from Thermal Treatment of AW-101 Waste (Runs 7 and 8) under 20% and 100% Oxygen Atmosphere as Initial Cover Gas	2.23
2.26	Gas Generation Rates from Thermal Treatment of U-106 Waste (Runs 9 and 10) under 20% and 100% Oxygen Atmosphere as Initial Cover Gas	2.24
2.27	Gas Generation Rates from Thermal Treatment of AN-102 Waste (Runs 11 and 12) under 100% Neon/100% Oxygen Atmosphere as Initial Cover Gas	2.25
2.28	Gas Generation Rates from Thermal Treatment of AN-106 Waste (Runs 13 and 14) under 100% Neon/100% Oxygen Atmosphere as Initial Cover Gas	2.25
2.29	Gas Generation Rates from Thermal Treatment of AN-107 Waste (Runs 15 and 16) under 100% Neon/100% Oxygen Atmosphere as Initial Cover Gas	2.26
2.30	Gas Generation Rates from Thermal Treatment of AW-101 Waste (Runs 17 and 18) under 100% Neon/100% Oxygen Atmosphere as Initial Cover Gas	2.26
2.31	Gas Generation Rates from Thermal Treatment of U-106 Waste (Runs 19 and 20) under 100% Neon/100% Oxygen Atmosphere as Initial Cover Gas	2.27
2.32	Hydrogen Generation Rates as a Function of Cover Gas	2.28
2.33	Generation Rates for All Major Gases Produced as a Function of Cover Gas	2.32
2.34	Oxygen Depletion Rates for Actual and Simulated Wastes.....	2.34
3.1	Summary of Tests Using Simulated AN-107 Waste.....	3.2
3.2	Composition of Tank AN-107 Supernate Simulant.....	3.6
3.3	Composition of AN-107 Simulant Calculated Based on Weighed Amounts of Reagents Used for Its Preparation	3.8
3.4	TOC/TIC Analyses Results of AN-107 Simulated Waste	3.9
3.5	Gas Composition of Parr Reactor Tests Containing AN-107 Simulated Waste	3.10

3.6	Gas Generation Rates for Parr Reactor Tests Using AN-107 Simulated Waste	3.11
4.1	Generation Rates for All Major Gases Produced as a Function of Cover Gas	4.1

1.0 Introduction

This report summarizes work performed as outlined in test plan TP-RPP-WTP-283 Rev. 0, "Gas Generation Model Support."^(a) The document describes research performed to measure gas generation from actual slurry samples taken from various Hanford waste tanks. Thermal gas generation tests have been conducted on five separate wastes and one waste simulant by Battelle – Pacific Northwest Division (PNWD) for the Office of River Protection (ORP) Waste Treatment Plant (WTP). This work was detailed in the test plan, which was written in response to the Bechtel National, Inc. (BNI) test specifications.^(b) There were no deviations from the stated test plan.

WTP Project personnel and PNWD selected five Hanford Site waste tank materials for investigation. Three samples (AN-107, U-106 and AN-102)^(c) were selected because of their high total organic carbon (TOC) content. These wastes also had different amounts of aluminum, a catalyst for the thermal generation of hydrogen. Another (AW-101) was selected because a previous study suggested that it might be more reactive than predicted by the Hu (1997, 2000, 2002) correlation. The tests were carried out at 90°C because the hydrogen formation rates would be bounding and the product distributions would provide information about the propensity for methane and C₂ hydrocarbons.

The gas generation tests on the actual Hanford waste samples focused on finding the effects of the addition of oxygen cover gas on the hydrogen generation rate as well as the effects of other gases. The actual tank samples were contained within a hot cell during testing. The tests established gas generation rates from actual waste samples as a function of oxygen presence and absence as a cover gas. From these results, the effect of oxygen addition to the waste was demonstrated.

The effect of stirring on oxygen reactivity with tank waste is important for assessing the effect that pulse jet mixers (PJM) may have on oxygenation of actual waste streams within the WTP. To assess the effects of stirring on oxygen cover gas tests, a nonradioactive waste simulant based on the composition of AN-107 was prepared and tested within a Parr[®] reactor system equipped with a mechanical stirrer. The Parr reactor tests established gas generation rates from simulated waste samples as a function of stirring and no-stirring conditions with oxygen cover gas. From these results, the effect of stirring under oxygen addition to the waste was determined.

The WTP flow sheet was evaluated to determine the applicability of the Hu correlation to predict hydrogen generation in the WTP. The evaluation concluded that, while applicable to many of the unit operations in the plant, the physical/chemical conditions for several process operations deviate from those for which the model was parameterized. Additional work was required to ascertain whether the Hu model was applicable, whether it could be adapted, or whether experimental tests should be performed. In some cases, such as the effect of hydroxide ion and permanganate additions and

(a) Bryan SA. 2003. *Gas Generation Model Support*. Battelle Test Plan TP-RPP-WTP-283 Rev. 0, Battelle – Pacific Northwest Division, Richland, WA.

(b) Sherwood DJ. 2003. "Adaptation of the Tank Farm Correlation for Gas Generation to the WTP." Test Specification Document, 24590-PTF-TSP-RT-03-009 Rev. 0, Bechtel National Inc., Richland, WA.

(c) Hanford waste tanks are designated with the prefix 241-. In this report, as in common usage, that prefix is omitted.

alpha radiolysis, the issues can be concluded by technical analyses of documented results and through chemical kinetic simulations. In other cases, such as the effects of oxygen saturation and acidification of the wastes, resolution required that experimental tests be performed. Some, such as alpha radiolysis, require the model to be adapted; others, such as acidification of the waste, may require substitute models or may be guided by results of experimental tests described within this report.

Section 2 of this report describes the gas generation measurements performed with the actual wastes, including the description of the test samples, the experimental conditions and equipment used for the tests, and the discussion of the results. Section 3 presents the gas generation experiments with simulated wastes under stirring and no-stirring conditions under oxygen atmosphere. Section 4 is a summary, and Section 5 contains the cited references.

The WTP flow sheet was reviewed to identify the process steps that would affect hydrogen generation rates (Sherwood and Stock 2003). The technical evaluation of the flow sheet was reported as a series of Technical Issue Reports (TIRs). The recommendations of these TIRs form the technical basis for performing the experimental work described in this report. The TIRs are summarized in Section 4 and included as appendixes. Appendix A analyzes the modeling of hydrogen generation rates in wastes with alpha radiation, Appendix B summarizes the influence of beta and gamma radiation on the rate of hydrogen generation, and Appendix C evaluates the influence of oxygen on hydrogen generation rates. Appendix D assesses the influence of hydroxide ion on the rate of hydrogen generation, Appendix E analyzes the effect of permanganate addition on predicting hydrogen generation rates, and Appendix F evaluates the effect of glass-forming chemicals on hydrogen generation rates.

PNWD implements the River Protection Project (RPP) WTP quality requirements by performing work in accordance with the PNWD Waste Treatment Plant Support Project Quality Assurance Project Plan (QAPjP) approved by the RPP-WTP Quality Assurance organization. This work will be performed to the quality requirements of NQA-1-1989 Part I, Basic and Supplementary Requirements, and NQA-2a-1990, Part 2.7. In addition, 10 CFR 830 Subpart A applies for “Important to Safety” analyses. These quality requirements are implemented through PNWD's *Waste Treatment Plant Support Project (WTPSP) Quality Assurance Requirements and Description Manual*. The analytical requirements are implemented through WTP Support Project's Statement of Work (WTPSP-SOW-002, Rev.0), with the Radiochemical Processing Laboratory (RPL) Quantitative Gas Mass Spectrometry team.

Experiments that are not method-specific shall be performed in accordance with PNWD's procedures QA-RPP-WTP-1101, “Scientific Investigations,” and QA-RPP-WTP-1201, “Calibration Control System,” ensuring that sufficient data are taken with properly calibrated measuring and test equipment to obtain quality results.

Bechtel National, Inc.'s (BNI) QAPjP, PL-24590-QA00001, is not applicable because the work will not be performed in support of environmental/regulatory testing, and the data will not be used as such.

PNWD addresses internal verification and validation activities by conducting an Independent Technical Review of the final data report in accordance with PNWD procedure QA-RPP-WTP-604. This review verifies that the reported results are traceable, that inferences and conclusions are soundly based, and the reported work satisfies the Test Plan objectives. This review procedure is part of PNWD's *WTPSP Quality Assurance Requirements and Description Manual*.

2.0 Gas Measurements on Actual Waste Samples

Gas generation tests on actual radioactive tank wastes were conducted in the 325 Building High-Level Radiation Facility (325A HLRF). Gas generation tests on simulated AN-107 waste were conducted in nonradiological laboratories in the 325 Building. The experimental conditions for tests on actual wastes and the apparatus and conditions for simulated waste experiments are described in Section 2.1. Hanford wastes are described in Section 2.2. Results of gas generation tests are presented in Section 2.3, including gas phase composition and gas generation rates from various Hanford wastes. Section 2.4 contains a discussion of the results of gas generation tests with actual Hanford tank wastes.

2.1 Experimental Conditions and Equipment Used for Gas Generation Tests on Actual Hanford Wastes

Gas generation measurements using actual Hanford wastes were made using reaction vessels and a gas manifold system similar to those used in studies with simulated waste (Bryan and Pederson 1995) and described in reports detailing work with actual waste (Bryan et al. 1996; King et al. 1997).^(a) Each vessel has a separate pressure transducer on an isolated gas manifold line. The entire surface of the reaction system exposed to the slurry sample is stainless steel, except for a copper gasket sealing the flange at the top of the reaction vessel. Figure 2.1 is a photograph of the reaction vessel showing the placement of the thermocouples at various locations on the outside of and within the reaction vessel. The location of reaction vessels within a carousel-style holder is depicted in Figure 2.2. There was no provision for stirring the contents of the reaction vessels containing actual wastes; the contents of these vessels were quiescent.



Figure 2.1. Reaction Vessel Used in Small-Scale Gas generation Tests

(a) Bryan SA, CM King, LR Pederson, and SV Forbes. 1996. *Thermal and Radiolytic Gas Generation from Tank 241-SY-103 Waste: Progress Report*. TWSFG96.17, Pacific Northwest National Laboratory, Richland, WA.

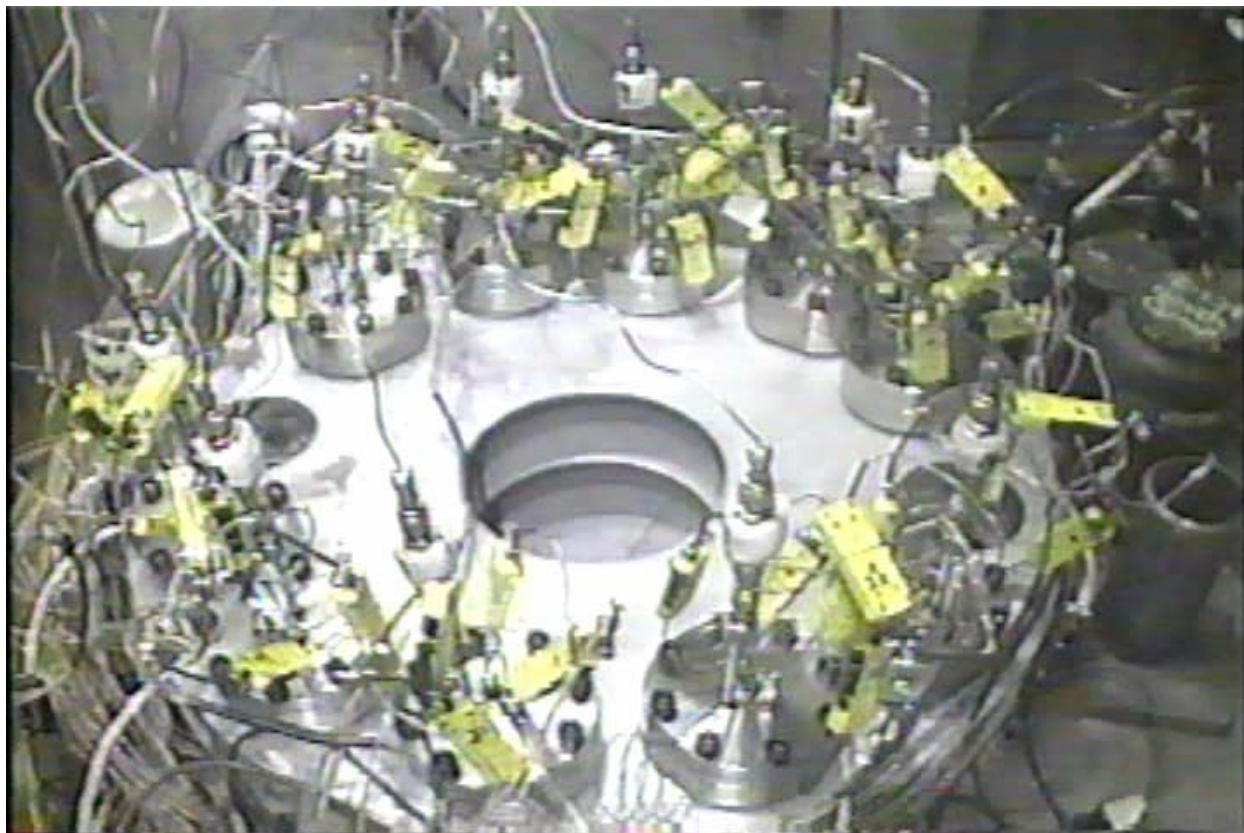


Figure 2.2. Reaction Vessel Holder with Ten Reaction Vessels Used in Gas Generation Tests (photograph taken inside the HLRF hot cell facility)

Figure 2.3 is a schematic diagram of the gas manifold system. Temperatures and pressures are recorded every 10 seconds on a Campbell Scientific CR10 data logger, and an average of the data is taken every 20 minutes and saved in a computer file.

The reaction vessels are cylinders of 316L stainless steel. The reaction space of the vessel is approximately 2 inches in diameter and 4 inches high. Each vessel was wrapped in heating tape and insulated. Two thermocouples were attached to the external body of the reaction vessel, one for temperature control and one for over-temperature protection. Two thermocouples were inserted through the lid. The thermocouple centered in the lower half of the vessel monitors the temperature of the liquid phase; the one centered in the upper half monitors the gas phase temperature within the reaction vessel. The reaction vessels were placed in a hot cell and connected by small inner-diameter tubing (0.1016 cm ID) to the gas manifold outside the hot cell. A stainless steel filter (60-micrometer pore size, Nupro[®]) protected the tubing and manifold from contamination. A thermocouple was attached to this filter as well.

The total gas in the system was calculated using the ideal gas law relationship from the pressure, temperature, and volume of the parts of the apparatus having different gas phase temperatures:

$$\text{moles}_{\text{total}} = \text{moles}_{\text{vessel}} + \text{moles}_{\text{filter}} + \text{moles}_{\text{manifold and tubing}}$$

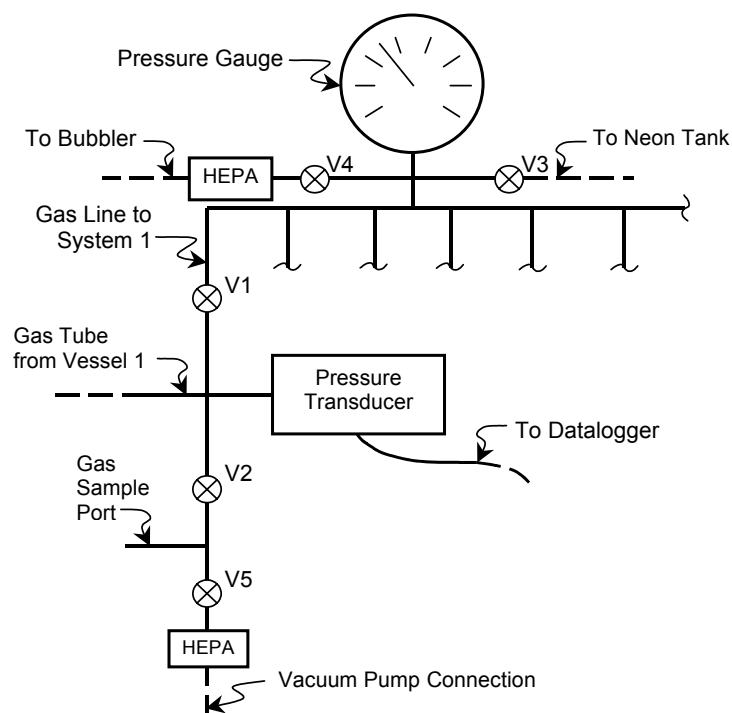


Figure 2.3. Diagram of Pressure Manifold System Used in Gas Generation Tests

The manifold and filter volumes were determined from pressure/volume relationships using a separate calibrated gas manifold system. The volume of each vessel was determined gravimetrically after filling it with water. These volumes are recorded in Table 2.1, along with the mass of slurry added to each vessel and the gas phase volume in the vessel after the sample was added. The reproducibility of the molar gas determination using this manifold system has been determined experimentally. The relative error for measuring moles of gas with the system has been determined. A detailed discussion of these points can be found in Bryan et al. (1996). In summary, the relative standard deviation for quantitative gas-phase measurements conducted over time and temperature ranges similar to those of the gas generation tests was typically less than 2%.

An atmospheric pressure gauge was attached to the data logger. The pressure in each system is given as the sum of atmospheric pressure and relative pressure in each system. Neon, because it leaks slower than helium from the system, was used as cover gas. For experiments using an atmosphere containing 20% oxygen, a special blend of oxygen in neon was purchased from A-L Compressed Gases. High-purity oxygen was used for those experiments requiring a 100% oxygen atmosphere. All gases were analyzed independently by mass spectrometry prior to use and determined to contain no impurities in concentrations significant enough to warrant correction.

At the start of each run, each system was purged by at least three cycles by pressurizing with neon at 45 psi (310 kPa) and then venting to the atmosphere. The systems were at atmospheric pressure and ambient temperature, about 745 mm Hg (99.3 kPa) and 32°C respectively, when sealed. The sample portion of the manifold was isolated (valves V1 and V2 closed) (see Figure 2.3) for the remainder of the run. The vessels were then heated, adjusting the set points to keep the waste material within 1°C of the desired liquid phase temperatures. The temperature of the gas phase was 5° to 25°C lower than that of the sample liquid phase.

Table 2.1. Sample Masses and Vessel Volumes Used in Small-Scale Gas Generation Tests with Actual Hanford Wastes

Run number	1	2	3	4	5	6	7	8	9	10
Sample	AN-102	AN-102	AN-106	AN-106	AN-107	AN-107	AW-101	AW-101	U-106	U-106
Sample mass, g	15.70	15.01	16.05	15.09	15.08	15.31	14.92	15.49	15.21	16.40
<i>Vessel Volumes</i>										
vessel ID	S-9	S-10	S-11	S-1	S-3	S-4	S-7	S-8	S-5	S-6
gas phase, mL	212.9	213.0	209.2	212.1	211.6	213.5	212.3	212.0	212.4	211.3
total, mL	223.7	223.4	222.4	224.5	222.4	224.5	222.5	222.6	222.9	222.7
Run number	11	12	13	14	15	16	17	18	19	20
Sample	AN-102	AN-102	AN-106	AN-106	AN-107	AN-107	AW-101	AW-101	U-106	U-106
Sample mass, g	14.77	15.39	15.01	14.70	15.84	15.31	15.23	14.95	14.52	14.95
<i>Vessel Volumes</i>										
vessel ID	S-20	S-21	S-13	S-12	S-14	S-40	S-18	S-19	S-16	S-17
gas phase, mL	212.8	211.6	206.5	209.5	212.3	211.7	213.4	212.2	212.3	212.6
total, mL	223.0	222.3	221.8	221.6	223.6	222.6	223.8	222.4	222.4	222.9

At the end of each run, the vessels were allowed to cool to ambient temperature, and then a sample of the gas was taken via a stainless steel collection bottle for analysis by a mass spectrometer. The collection bottles were equipped with a valve and had a volume of approximately 75 mL. The reaction vessel system, gas manifold, and gas collection system were suited for handling the relatively non-polar fixed gases such as H₂, N₂, N₂O, O₂, Ar, CO₂, and CH₄. The collection bottle, after being evacuated overnight at high vacuum, was attached to the gas sample port. Air was removed from the region between valves V2 and V5 (Figure 2.3) using a vacuum pump, then the gas sample was taken directly from the reaction vessel into the previously evacuated collection bottle. After the collection bottle was removed, the bottle and sample port were surveyed for radioactive contamination. No contamination was found at this point during these experiments. Typically, multiple gas samples were taken for each waste sample. Repeated gas sampling is discussed in more detail in Section 2.3, Gas Generation from Tank Waste Samples.

Analysis of the composition of the gas phase of each reaction vessel after each run was performed by mass spectral analysis according to analytical procedure PNNL-98523-284 Rev. 1. The amount of a specific gas formed during heating is given by the mole percent of each gas multiplied by the total moles of gas present in a system. For determining the extent of oxygen depletion during a reaction, the moles of oxygen present at the initiation of the experiment was subtracted from the moles of oxygen present at the end of each experiment. Duplicate samples, which were run in separate reaction vessels and sampled independently, were used to assess the reproducibility and uncertainty of the rate parameters.

Gases in the reaction system are well mixed (Bryan et al. 1996). The measured amount of argon in gas samples is an indicator of how much nitrogen and oxygen from air has leaked into the system (the N₂:Ar ratio in air is 83.6:1; the O₂:Ar ratio is 22.4:1; these ratios are regularly verified by mass spectrometry). The nitrogen produced in the vessel is the total nitrogen minus atmospheric nitrogen. Similarly, the oxygen within the reaction system is corrected for atmospheric contamination. The solubilities of nitrogen, hydrogen, methane, and nitrous oxide gases have been measured on simulated waste systems that are similar in composition to the liquid in the actual and simulated wastes used in this study (Pederson and Bryan 1996). Less than 0.01% of these gases dissolve in the condensed phase, so the loss of gases due to solubility is negligible.

2.2 Hanford Tank Test Material

The waste samples used in gas generation testing are a blend of samples received and processed by PNWD in FY 2003. The sample sources and description and compositing information are detailed in Section 2.2.1. The analyses of the composite samples for the Hanford waste samples are described in Section 2.2.2.

2.2.1 Hanford Waste Sample Description and Composite Information

Various Hanford tank samples were shipped from 222-S Laboratory to PNWD for use in gas generation testing. These samples include wastes from Tanks AN-102, AN-106, AN-107, AW-101, and U-106. Tables 2.2 through 2.6 contain the pertinent information for each composite waste sample used for gas generation testing. The specific analyses for each of the composite samples are detailed in Section 2.2.2.

Table 2.2. Composite Information for Tank AN-102 Material

Tank ID	Sample ID	Volume, mL	Description
AN-102	AN-102-DQO-ANIONS	125	DQO composite subsample; liquid w/10 mL settled solids.
AN-102	AN-102-DQO-CN	100	DQO composite subsample; 250 mL jar; liquid w/10 mL settled solids
AN-102	AN-102-DQO-MET-1	70	250 mL Jar; liquid w/10 mL settled solids.
AN-102 total composite mass, g			596.2

Table 2.3. Composite Information for Tank AN-106 Material

Tank ID	Sample ID	Volume, mL	Description
AN-106	6AN-02-01A	85	Clear liquid sample, dark settled solids, 0.5mL; 125 mL jar
AN-106	6AN-02-01B	109	Clear liquid sample; no solids; 125 mL jar
AN-106 total composite mass, g			250.8

Table 2.4. Composite Information for Tank AN-107 Material

Tank ID	Sample ID	Volume, mL	Description
AN-107	19225	97	Liquid sample, dark brown slurry; 125 mL jar
AN-107	19228	102	Liquid sample, dark brown slurry; 125 mL jar
AN-107	19229	103	Liquid sample, dark brown slurry; 125 mL jar
AN-107	19230	94	Liquid sample, dark brown slurry; 125 mL jar
AN-107 total composite mass, g			604.8

Table 2.5. Composite Information for Tank AW-101 Material

Tank ID	Sample ID	Volume, mL	Description
AW-101	19440	130	250 mL jar; clear liquid; 30 mL settled solids; Core C-306.
AW-101	19645	150	250 mL jar; clear liquid; 10 mL settled solids; Core C-306.
AW-101	19646	130	250 mL jar; dark sludge; Core C-306.
AW-101 total composite mass, g			493.0

Table 2.6. Composite Information for Tank U-106 Material.

Tank ID	Sample ID	Volume, mL	Description
U-106	14944	120	125 mL jar; drainable liquids, opaque, brown; Core C-147
U-106	10312	5	60 mL jar; drainable liquids, opaque, brown; Core C-147
U-106	U-106-5	35	125 mL jar; drainable liquids, opaque, brown; Core C-147
U-106 total composite mass, g			160.7

2.2.2 Hanford Waste Sample Compositional Analyses

Composite samples from wastes used for gas generation were analyzed by ion chromatography (IC), inductively coupled plasma-atomic absorption spectroscopy (ICP-AES), carbon analysis [total inorganic carbon (TIC), TOC, and total carbon (TC)], as well as radiochemical analysis (total alpha, beta, and Sr-90). The results of these analyses are presented in Tables 2.7 through 2.10. The TC analysis reported in Table 2.8 was performed by both the furnace method and the hot persulfate method. It has been

Table 2.7. Ion Chromatography Analysis of Tank Waste Material Used in Gas Generation Tests

Sample ID	Weight percent							
	F	Cl	NO ₂	Br	NO ₃	PO ₄	SO ₄	C ₂ O ₄
AN-102	0.12 J ^(a)	0.31	7.76	<dl ^(b)	18.29	0.05	0.89	0.03
AN-106	0.41 J ^(a)	0.12	1.95	<dl	5.13	0.11	0.36	0.10
AN-106 duplicate	0.39 J ^(a)	0.11	1.87	<dl	5.30	0.10	0.34	0.10
AN-107	0.18 J ^(a)	0.16	5.33	<dl	18.12	0.17	0.70	0.07
AW-101	0.12 J ^(a)	0.45	7.52	0.03 J ^(a)	12.78	0.01 J ^(a)	0.04	0.04
U-106	0.08 J ^(a)	0.40	7.95	<dl	18.32	0.06	0.54	0.07

(a) J = values above detection limit but below estimated quantitation limit.
(b) <dl = less than detection limit; detection limit = 0.013 µg/mL.

Table 2.8. Carbon Analysis of Tank Waste Material Used in Gas Generation Tests

Sample ID	Density of Sample (g/mL)	Free Hydroxide, M (first equivalence point) ^(a)	Weight Percent			
			TOC	TIC	TC(HP) ^(b)	TC (furn) ^(c)
AN-102	1.444	0.37	2.02	0.80	2.82	3.21
AN-106	1.215	1.83	0.12	0.70	0.83	0.80
AN-106 duplicate	1.215	^(d)	0.12	0.72	0.84	^(d)
AN-107	1.397	1.23	2.93	1.09	4.02	4.35
AW-101	1.464	4.95	0.18	0.12	0.30	0.29
U-106	1.446	0.36	2.77	0.75	3.53	3.46

(a) Measured in duplicate. (b) Hot persulfate method.
(c) Furnace method. (d) Not measured.

Table 2.9. Inductively Coupled Plasma-Atomic Emission Spectroscopy (ICP-AES) of Tank Waste Material Used in Gas Generation Tests

Sample ID	Density g/mL	ICP-AES, µg/mL											
		Al	K	Na	U	Cr	Fe	Mn	Ni	Pd	Rh	Ru	Sr
AN-102	1.444	6600	2400	220K	<dl ^(b)	175	22.8	3.03	480	16 J ^(a)	<dl ^(d)	28.5	2.76
AN-102 dup	1.444	6610	2380	220K	<dl ^(b)	174	16.4	3.09	479	17 J ^(a)	<dl ^(d)	28.6	2.76
AN-106	1.215	2130	8860	107K	<dl ^(b)	420	3.4 J ^(a)	<dl	1.9 ^(a)	<dl ^(c)	<dl ^(d)	<dl ^(e)	<dl ^(f)
AN-107	1.397	268	1540	198K	<dl ^(b)	182	1830	633	580	24 J ^(a)	<dl ^(d)	36.8	3.04
AW-101	1.464	28700	37500	239K	<dl ^(b)	108	15.2	8.28	6.9 ^(a)	<dl	<dl ^(d)	3.2 J ^(a)	0.25 ^(a)
U-105	1.446	12600	2310	24K	<dl ^(b)	488	80.4	10.3	617	19 J ^(a)	<dl ^(d)	29.8	4.23

(a) J = values above detection limit but below estimated quantitation limit.
(b) <dl = less than detection limit, 70 µg/mL.
(c) <dl = less than detection limit, 15 µg/mL.
(d) <dl = less than detection limit, 6 µg/mL.
(e) <dl = less than detection limit, 2 µg/mL.
(f) <dl = less than detection limit, 0.2 µg/mL.

Table 2.10. Alpha and Beta Radiochemical Analysis of Tank Waste Material Used in Gas Generation Tests

Sample ID	Total Alpha, μCi/mL	Total Beta, μCi/mL	Sr-90, μCi/g
AN-102	1.08E-01 ±4%	3.68E+02 ±4%	4.79E+01 ±3%
AN-102 duplicate	1.11E-01 ±4%	3.56E+02 ±4%	4.87E+01 ±3%
AN-106	<5e-3	6.00E+01 ±4%	<3E-01
AN-106 duplicate	<4e-3	5.87E+01 ±4%	<3E-01
AN-107	5.37E-01 ±2%	3.57E+02 ±4%	6.15E+01 ±3%
AW-101	<4e-3	2.52E+02 ±4%	2.93E-01 ±43%
U-106	2.22E-01 ±3%	2.72E+02 ±3%	3.87E+01 ±3%

established for Hanford wastes in general that the hot persulfate values are slightly lower than theoretical (~ 82% or more of the organic detected by this method) due to lack of detection of volatile organic compounds including NPH.^(a)The furnace method generally provides reasonable TOC results, tending to be slightly high (exceeding 100%of theoretical value) due to artifacts such as the decomposition of inorganic carbonate.^(a) The reported TOC values in Table 2.8 are calculated from the difference in the TIC and the TC (hot persulfate method). The TOC values in this table are for total TOC within the sample. For estimating gas generation, the “soluble” TOC, or the TOC-minus oxalate, is generally used. The oxalate values included in Table 2.7, coupled with the total sample TOC in Table 2.8, can be used to calculate TOC-minus-oxalate values.

2.3 Gas Generation from Tank Waste Samples

The percent composition and gas generation rates from actual Hanford wastes under thermal conditions in the presence and absence of oxygen are described in this section. The measurements were run in duplicate. For example, for waste sample AN-102, run numbers 1 and 2 are duplicate samples of each other. All thermal measurements were performed at 90°C except the first, which was run at 85°C. Each vessel was loaded with the appropriate waste composite. Gas samples were taken from the vessels periodically. During a specific experimental run, after each gas sample was taken, the vessel was purged with fresh cover gas to remove previously generated gases before resuming gas generation. For example, at the conclusion of Run 1a, a gas sample was taken, followed by repeated filling and venting of fresh cover gas before starting Run 1b (see Table 2.11 for run designations). Table 2.11 is a summary of the tests performed to assess the reactivity of oxygen with actual wastes.

(a) Stock LM and DM Camaioni. 2001. “Comments on Approach to Modeling Organic Emissions from the Hanford Low Activity Waste and High Level Waste Treatment Facility.” Letter Report, Pacific Northwest National Laboratory, Richland, WA.

Table 2.11. Summary of Tests with Actual Hanford Wastes

Reaction Conditions			Waste Samples, Masses, and Run Numbers									
Cover gas	Temp, °C	Time, hr	AN-102		AN-106		AN-107		AW-101		U-106	
			15.70g	15.01g	16.05g	15.09g	15.08g	15.31g	14.92g	15.49g	15.21g	16.40g
20% O ₂ , 80% Ne	85	17	1a	2a	3a	4a	5a	6a	7a	8a	9a	10a
	90	286	1b	2b	2b	4b	5b	6b	7b	8b	9b	10b
	90	50	1c	2c	3c	4c	5c	6c	7c	8c	9c	10c
	90	52	1d	2d	3d	4d	5d	6d	7d	8d	9d	10d
	90	100	1e	2e	3e	4e	5e	6e	7e	8e	9e	10e
	90	50	1f	2f	3f	4f	5f	6f	7f	8f	9f	10f
100% O ₂	90	50	1g	2g	3g	4g	5g	6g	7g	8g	9g	10g
			14.77g	15.39g	15.01g	14.70g	15.84g	15.31g	15.23g	14.95g	14.52g	14.95g
100% Ne	90	42	11a	12a	13a	14a	15a	16a	17a	18a	19a	20a
100% Ne	90	84	11b	12b	13b	14b	15b	16b	17b	18b	19b	20b
100% O ₂	90	40	11c	12c	13c	14c	15c	16c	17c	18c	19c	20c
100% O ₂	90	116	11d	12d	13d	14d	15d	16d	17d	18d	19d	20d

2.3.1 Gas Generation from Various Hanford Tank Waste Samples

This section contains the thermal gas generation data produced by heating material in duplicate reaction vessels at 85° in the presence of oxygen and 90°C in the presence and absence of oxygen. The total amount of gas produced versus heating time was calculated for all 20 reaction vessels. To obtain separate rates for each gas present, samples were analyzed by mass spectroscopy, which allows quantification of the concentrations of individual gases. The mole percent composition of these gas samples is given in Tables 2.12 through 2.21. Of more interest are the relative amounts of gases generated, which are presented in the shaded areas of the tables. These values have been corrected for atmospheric contamination. The gas composition formed during heating is derived from the composition of sampled gas by excluding the neon cover gas and any argon, nitrogen, or oxygen derived from atmospheric contamination. For example, if an analysis found 80% neon, 15% nitrous oxide, and 5% hydrogen, the composition of gas formed by excluding neon would be 75% N₂O and 25% hydrogen. The uncertainties in all the entries in these tables are approximately ±1 in the last digit.

The gas generation rates were determined for each gas sample from the heating time, the percent composition of the gas, the total moles of gas in each system when the sample was taken, and the weight of tank material present in each reaction vessel.

Argon was used to indicate atmospheric contamination because it was not present in the cover gas and was not produced from the waste. Any nitrogen (or oxygen) present could have been generated (or depleted) by the waste or result from atmospheric contamination. The percent nitrogen is given by the percent nitrogen found minus 83.6 times the percent argon in the sample (the ratio of nitrogen to argon in dry air is 83.6). The percent oxygen is given by the percent oxygen found minus 22.43 times the percent argon in the sample (the ratio of oxygen to argon in dry air is 22.43). Using the percent composition data, reaction times, and mass of each sample, rates of gas generation were determined as a function of temperature and are given in Tables 2.22 through 2.31. The ammonia value, when included in these tables, is an estimate and serves as an indicator that this gas was present. Because of ammonia's relatively high solubility, quantitation by means of gas phase measurement is not possible.

Table 2.12. Mole Percent Composition Thermal Gas Sampled (including Ne), Gas Formed (shaded), and Heating Times of Runs 1 and 2 Using AN-102 Waste, with 20% and 100% Oxygen Atmosphere as Initial Cover Gas

Gas Composition: Mole %																			
Run	Cover gas	Temp °C	Ne	Ar	H ₂	CO ₂	CH ₄	N ₂	O ₂	N ₂ O	NOx	NH ₃ (est)	C ₂ HCs	>C ₂ HCs	Total HCs	Time, h	Vessel ID	Sample mass, g	Mass spec ID
1a	20% O ₂ , 80% Ne	85	79.8	--	0.034	0.014	--	0.077	18.70	0.028	--	--	0.005	--	0.005	17	S-9	15.70	WTP25-50-9
					0.180	0.07	--	0.41	99.16	0.15	--	--	0.027	--	0.027				
1b	20% O ₂ , 80% Ne	90	67.8	--	1.07	--	0.004	9.75	1.69	19	--	--	0.087	--	0.087	286	S-9	15.70	WTP25-58-9
					3.386	--	0.013	30.85	5.35	60.12	--	--	0.275	--	0.275				
1c	20% O ₂ , 80% Ne	90	92.7	0.001	0.11	--	0.007	2.39	2.13	2.24	--	--	0.027	--	0.027	50	S-9	15.70	WTP25-60-9
					1.59	--	0.10	34.6	30.85	32.4	--	--	0.39	--	0.39				
1d	20% O ₂ , 80% Ne	90	86.1	0.001	0.038	--	0.008	2.16	9.80	1.51	--	--	0.026	--	0.026	52	S-9	15.70	WTP25-63-9
					0.28	--	0.059	16.0	72.37	11.15	--	--	0.192	--	0.192				
1e	20% O ₂ , 80% Ne	90	87.9	0.001	0.07	--	0.002	1.33	9.50	0.58	--	0.07	0.018	--	0.018	99	S-9	15.70	WTP25-65-9
					0.61	--	0.0	11.5	82.11	5.0	--	1	0.16	--	0.16				
1f	20% O ₂ , 80% Ne	90	82.9	0.002	0.035	0.036	0.00	0.52	15.30	0.016	--	0.02	0.009	0.001	0.01	49	S-9	15.70	WTP25-67-9
					0.22	0.2	0.0	2.8	96.37	0.1	--	0.1	0.06	0.01	0.06				
1g	100% O ₂	90	--	--	0.044	0.009	--	0.433	99.30	0.202	--	--	--	--	0	50	S-9	15.70	WTP25-70-9
					0.04	0.0	--	0.4	99.31	0.2	--	--	--	--	0.0				
2a	20% O ₂ , 80% Ne	85	79.4	0.004	0.03	0.039	--	0.239	19.00	0.009	--	--	0.003	--	0.003	17	S-10	15.01	WTP25-50-10
					0.16	0.2	--	1.2	98.34	0.05	--	--	0.016	--	0.016				
2b	20% O ₂ , 80% Ne	90	81.6	--	0.64	--	0.00	5.40	1.66	10	--	--	0.054	--	0.054	286	S-10	15.01	WTP25-58-10
					3.60	--	0.017	30.41	9.35	56.32	--	--	0.304	--	0.304				
2c	20% O ₂ , 80% Ne	90	85.1	0.001	0.055	0.004	0.01	1.74	10.20	2.4	--	--	0.016	--	0.016	50	S-10	15.01	WTP25-60-10
					0.38	0.0	0.055	12.04	70.57	16.61	--	--	0.11	--	0.11				
2d	20% O ₂ , 80% Ne	90	82.0	0.001	0.024	--	0.01	2.04	12.70	2.58	--	--	0.019	--	0.019	52	S-10	15.01	WTP25-63-10
					0.14	--	0.040	11.74	73.11	14.85	--	--	0.109	--	0.109				
2e	20% O ₂ , 80% Ne	90	83.2	0.001	0.042	--	0.00	3.29	9.40	2.93	--	0.09	0.025	--	0.025	100	S-10	15.01	WTP25-65-10
					0.27	--	0.0	20.8	59.46	18.5	--	1	0.16	--	0.16				
2f	20% O ₂ , 80% Ne	90	81.8	0.001	0.022	0.021	0.00	1.16	16.00	0.62	--	0.03	0.014	--	0.014	50	S-10	15.01	WTP25-67-10
					0.12	0.12	0.01	6.5	89.45	3.5	--	0.2	0.08	--	0.08				
2g	100% O ₂	90	--	0.002	0.026	--	--	0.81	97.90	0.357	--	--	0.012	--	0.012	50	S-10	15.01	WTP25-70-10
					0.03	--	--	0.7	98.87	0.4	--	--	0.01	--	0.01				

Table 2.13. Mole Percent Composition Thermal Gas Sampled (including Ne), Gas Formed (shaded), and Heating Times of Runs 3 and 4 Using AN-106 Waste, with 20% and 100% Oxygen Atmosphere as Initial Cover Gas

Gas Composition: Mole %																			
Run	Cover gas	Temp °C	Ne	Ar	H ₂	CO ₂	CH ₄	N ₂	O ₂	N ₂ O	NOx	NH ₃ (est)	C ₂ HCs	> C ₂ HCs	Total HCs	Time, h	Vessel ID	Sample mass, g	Mass spec ID
3a	20% O ₂ , 80% Ne	85	80	0.003	0.003	0.009	--	0.13	19.30	--	--	--	--	--	0	16	S-11	16.05	WTP25-50-11
					0.015	0.05	--	0.7	99.27	--	--	--	--	--	--				
3b	20% O ₂ , 80% Ne	90	91.4	0.001	0.0450	0.014	0.004	0.055	8.40	--	--	--	0.004	0.001	0.005	286	S-11	16.05	WTP25-58-11
					0.53	0.16	0.047	0.6	98.56	--	--	--	0.047	0.012	0.059				
3c	20% O ₂ , 80% Ne	90	81.2	0.001	0.0060	0.011	0.002	0.022	18.40	--	--	--	0.005	--	0.005	50	S-11	16.05	WTP25-60-11
					0.03	0.06	0.011	0.12	99.70	--	--	--	0.027	--	0.027				
3d	20% O ₂ , 80% Ne	90	81	--	0.0040	0.013	0.002	0.016	18.90	--	--	--	0.003	--	0.003	53	S-11	16.05	WTP25-63-11
					0.02	0.1	0.011	0.08	99.80	--	--	--	0.016	--	0.016				
3e	20% O ₂ , 80% Ne	90	81.6	0.001	0.0070	0.007	--	0.017	18.20	--	--	--	--	--	0	100	S-11	16.05	WTP25-65-11
					0.04	0.04	--	0.09	99.83	--	--	--	--	--	--				
3f	20% O ₂ , 80% Ne	90	80.6	0.001	0.0030	0.011	0.001	0.02	19.10	0.006	--	--	0.003		0.003	50	S-11	16.05	WTP25-67-11
					0.02	0.06	0.005	0.1	99.77	0.03	--	--	0.02	--	0.02				
3g	100 % O ₂	90		--	0.004	0.028	--	0.012	99.90	--	--	--	0.004	--	0.004	51	S-11	16.05	WTP25-70-11
					0.004	0.03	--	0.0	99.95	--	--	-	0.0	--	0.0				
4a	20% O ₂ , 80% Ne	85	80.1	0.006	0.005	0.013	--	0.065	19.40	--			--	--	0	17	S-1	15.09	WTP25-50-12
					0.026	0.07	--	0.34	99.57	--	--	--	--	--	0				
4b	20% O ₂ , 80% Ne	90	90.4	0.001	0.058	0.008	0.00	0.044	9.40	--	--	--	0.004	0.001	0.005	280	S-1	15.09	WTP25-58-12
					0.609	0.08	0.0	0.46	98.75	--	--	--	0.04	0.01	0.05				
4c	20% O ₂ , 80% Ne	90	81	--	0.006	0.009	0.00	0.017	18.80	--	--	--	--	--	--0	51	S-1	15.09	WTP25-60-12
					0.032	0.05	0.01	0.09	99.77	--	--	--	--	--	--				
4d	20% O ₂ , 80% Ne	90	80.2	--	0.002	0.01	0.00	0.014	19.50	--	--	--	0.002	--	0.002	28	S-1	15.09	WTP25-63-12
					0.010	0.06	0.01	0.07	99.85	--	--	--	0.010	--	0.010				
4e	20% O ₂ , 80% Ne	90	81.9	--	0.01	--	--	0.015	18.10	--	--	--	--	--	0	99	S-1	15.09	WTP25-65-12
					0.044	--	--	0.083	99.87	--	--	--	--	--	0				
4f	20% O ₂ , 80% Ne	90	80.5	0.001	0.00	0.01	--	0.013	19.10	--	--	--	0.003	--	0.003	50	S-1	15.09	WTP25-67-12
					0.021	0.02	--	0.07	99.84	--	--	--	0.02	--	0.02				
4g	100 % O ₂	90			0.004	0.022	--	0.006	99.90	--	--	--	0.003	--	0.003	50	S-1	15.09	WTP25-70-12

Table 2.14. Mole Percent Composition Thermal Gas Sampled (including Ne), Gas Formed (shaded), and Heating Times of Runs 5 and 6 Using AN-107 Waste, with 20% and 100% Oxygen Atmosphere as Initial Cover Gas

Gas Composition: Mole %																			
Run	Cover gas	Temp °C	Ne	Ar	H ₂	CO ₂	CH ₄	N ₂	O ₂	N ₂ O	NOx	NH ₃ (est)	C ₂ HCs	> C ₂ HCs	Total HCs	Time, h	Vessel ID	Sample mass, g	Mass spec ID
5a	20% O ₂ , 80% Ne	85	80.2	0.002	0.001	0.014	0.00	0.295	19.40	0.016	--	--	0.003	--	0.003	17	S-3	15.08	WTP25-50-3
					0.01	0.07	0.010	1.08	98.69	0.08	--	--	0.015	--	0.015				
5b	20% O ₂ , 80% Ne	90	84.5	0.02	0.026	--	0.00	6	2.89	6.4	--	--	0.023	--	0.023	285	S-3	15.08	WTP25-58-3
					0.20	--	0.015	33.10	18.49	48.02	--	--	0.17	--	0.17				
5c	20% O ₂ , 80% Ne	90	80.2	0.01	0.019	--	0.00	4.56	9.21	6	--	--	0.010	--	0.01	50	S-3	15.08	WTP25-60-3
					0.10	--	0.01	20.2	47.80	31.8	--	--	0.05	--	0.05				
5d	20% O ₂ , 80% Ne	90	76.9	0.005	0.02	--	0.00	8.8	2.97	11.2	--	--	0.025	--	0.025	52	S-3	15.08	WTP25-63-3
					0.09	--	0.01	37.5	12.75	49.6	--	--	0.11	--	0.11				
5e	20% O ₂ , 80% Ne	90	66.6	0.008	0.025	--	0.01	16.5	1.69	15.1	--	--	0.049	--	0.049	97	S-3	15.08	WTP25-65-3
					0.08	--	0.02	48.8	4.70	46.3	--	--	0.15	--	0.15				
5f	20% O ₂ , 80% Ne	90	89.8	0.014	0.017	--	0.01	5.4	2.13	2.61	--	--	0.019	0.001	0.02	50	S-3	15.08	WTP25-67-3
					0.19	--	0.1	48.9	20.86	29.6	--	--	0.22	0.01	0.23				
5g	100 % O ₂	90	0.283	0.016	0.03	0.05	0.01	2.21	96.60	0.71	--	--	0.013	0.001	0.014	49	S-3	15.08	WTP25-70-3
					0.03	0.046	0.0	1.0	98.20	0.7	--	--	0.01	0.00	0.01				
6a	20% O ₂ , 80% Ne	85	80.3	--	0.001	0.016	--	0.113	19.30	0.013	--	--	0.002	--	0.002	17	S-4	15.31	WTP25-50-4
					0.005	0.08	--	0.6	99.25	0.07	--	--	0.010	--	0.010				
6b	20% O ₂ , 80% Ne	90	77	0.001	0.037	--	0.01	7.2	1.31	14.3	--	--	0.025	--	0.025	286	S-4	15.31	WTP25-58-4
					0.162	--	0.022	31.5	5.73	62.51	--	--	0.109	--	0.109				
6c	20% O ₂ , 80% Ne	90	82.5	--	0.027	--	--	6	2.17	9.30	--	--	--	--	0	50	S-4	15.31	WTP25-60-4
					0.154	--	--	34.3	12.40	53.15	--	--	--	--	0				
6d	20% O ₂ , 80% Ne	90	73.1	0.001	0.019	--	0.01	11.5	2.37	12.9	--	--	0.040	--	0.04	52	S-4	15.31	WTP25-63-4
					0.071	--	0.03	42.9	8.83	48.1	--	--	0.15	--	0.15				
6e	20% O ₂ , 80% Ne	90	76.8	0.003	0.017	--	0.01	12.1	2.00	9.1	--	--	--	--	0	100	S-4	15.31	WTP25-65-4
					0.074	--	0.04	51.8	8.50	39.5	--	--	--	--	0				
6f	20% O ₂ , 80% Ne	90	94.5	0.002	0.016	0.013	0.01	2.11	2.14	1.04	--	--	0.013	0.001	0.014	49	S-4	15.31	WTP25-67-4
					0.305	0.2	0.2	38.6	40.37	19.8	--	--	0.2	0.02	0.3				
6g	100 % O ₂	90		0.006	0.025	0.016	0.00	1.39	97.90	0.63	--	--	0.011	0.001	0.012	49	S-4	15.31	WTP25-70-4

Table 2.15. Mole Percent Composition Thermal Gas Sampled (including Ne), Gas Formed (shaded), and Heating Times of Runs 7 and 8 Using AW-101 Waste, with 20% and 100% Oxygen Atmosphere as Initial Cover Gas

Gas Composition: Mole %																			
Run	Cover gas	Temp °C	Ne	Ar	H ₂	CO ₂	CH ₄	N ₂	O ₂	N ₂ O	NOx	NH ₃ (est)	C ₂ HCs	> C ₂ HCs	Total HCs	Time, h	Vessel ID	Sample mass, g	Mass spec ID
7a	20% O ₂ , 80% Ne	85	79.3	0.004	0.028	0.008	0.003	0.36	19.30	0.002	--	--	0.003	--	0.003	17	S-7	14.92	WTP25-50-7
					0.144	--	0.0155	0.56	99.21	0.01	--	--	0.015	--	0.015				
7b	20% O ₂ , 80% Ne	90	83.2	0.009	0.29	0.006	0.056	0.84	15.50	--	--	--	0.003	0.001	0.004	205	S-7	14.92	WTP25-58-7
					1.85	--	0.3533	1.08	96.65	--	--	--	0.019	0.006	0.025				
7c	20% O ₂ , 80% Ne	90	80.3	0.004	0.04	0.006	0.012	0.324	19.20	--	--	--	--	--	0	50	S-7	14.92	WTP25-60-7
					0.223	--	0.0622	0.38	99.18	--	--	--	--	--	0				
7d	20% O ₂ , 80% Ne	90	80.3	0.002	0.04	0.008	0.013	0.141	19.20	--	--	--	--	--	0	52	S-7	14.92	WTP25-63-7
					0.187	--	0.0674	0.3	99.41	--	--	--	--	--	0.000				
7e	20% O ₂ , 80% Ne	90	80.8	0.003	0.06	0.009	0.02	0.227	18.40	--	--	--	--	--	0	100	S-7	14.92	WTP25-65-7
					0.30	0.05	0.11	0.32	99.22	--	--	--	--	--	0.000				
7f	20% O ₂ , 80% Ne	90	80.2	0.004	0.03	0.018	0.012	0.285	19.30	--	--	--	--	--	0	49	S-7	14.92	WTP25-67-7
					0.14	0.09	0.06	0.18	99.48	--	--	--	--	--	0.00				
7g	100% O ₂	90	--	0.004	0.041	0.014	0.01	0.121	99.80	--	--	--	--	--	0	50	S-7	14.92	WTP25-70-7
					0.04	0.0	0.0	0.1	99.81	--	--	--	--	--	0.0				
8a	20% O ₂ , 80% Ne	85	79.5	--	0.029	0.015	0.00	0.044	19.20	0.003	--	--	0.003	--	0.003	17	S-8	15.49	WTP25-50-8
					0.15	0.1	0.02	0.2	99.50	0.02	--	--	0.016	--	0.016				
8b	20% O ₂ , 80% Ne	90	86.5	0.001	0.336	0.008	0.07	0.03	12.90	--	--	--	0.003	0.001	0.004	286	S-8	15.49	WTP25-58-8
					2.52	0.1	0.55	0.25	96.60	--	--	--	0.02	0.01	0.03				
8c	20% O ₂ , 80% Ne	90	80.8	--	0.027	0.008	0.01	0.028	19.00	0.005	--	--	--	--	0	50	S-8	15.49	WTP25-60-8
					0.14	0.0	0.06	0.15	99.59	0.03	--	--	--	--	0.000				
8d	20% O ₂ , 80% Ne	90	80.4	--	0.024	0.011	0.01	0.01	19.20	--	--	--	--	--	0	52	S-8	15.49	WTP25-63-8
					0.12	0.1	0.06	0.05	99.66	--	--	--	--	--	0.00				
8e	20% O ₂ , 80% Ne	90	80.6	--	0.036	0.012	0.02	0.02	18.80	--	--	--	--	--	0	99	S-8	15.49	WTP25-65-8
					0.19	0.1	0.08	0.11	99.56	--	--	--	--	--	0.000				
8f	20% O ₂ , 80% Ne	90	80.2	0.001	0.017	0.009	0.01	0.02	19.50	--	--	--	0.003	--	0.003	49	S-8	15.49	WTP25-67-8
					0.09	0.0	0.05	0.12	99.58	--	--	--	0.015	--	0.015				
8g	100% O ₂	90		0.016	0.038	0.019	0.01	1.24	98.60	--	--	--	--	--	0	50	S-8	15.49	WTP25-70-8
					0.04	0.0	0.01	1.2	98.69	--	--	--	--	--	0.0				

Table 2.16. Mole Percent Composition Thermal Gas Sampled (including Ne), Gas Formed (shaded), and Heating Times of Runs 9 and 10 Using U-106 Waste, with 20% and 100% Oxygen Atmosphere as Initial Cover Gas

Gas Composition: Mole %																			
Run	Cover gas	Temp °C	Ne	Ar	H ₂	CO ₂	CH ₄	N ₂	O ₂	N ₂ O	NOx	NH ₃ (est)	C ₂ HCs	> C ₂ HCs	Total HCs	Time, h	Vessel ID	Sample mass, g	Mass spec ID
9a	20% O ₂ , 80% Ne	85	80.7	0.002	0.04	0.01	--	0.172	19.00	0.012	--	--	0.005	--	0.005	17	S-5	15.21	WTP25-50-5
					0.209	0.05	--	0.5	99.19	0.06	--	--	0.026	--	0.026				
9b	20% O ₂ , 80% Ne	90	73.5	0.001	0.82	--	0.01	7.00	1.88	16.5	--	--	0.072	--	0.072	286	S-5	15.21	WTP25-58-5
					3.12	--	0.03	27	7.15	62.79	--	--	0.27	--	0.27				
9c	20% O ₂ , 80% Ne	90	82.3	--	0.146	--	0.01	5.00	2.16	10	--	--	0.043	--	0.043	50	S-5	15.21	WTP25-60-5
					0.84	--	0.05	29	12.44	57.61	--	--	0.25	--	0.25				
9d	20% O ₂ , 80% Ne	90	85.9	--	0.095	--	0.01	4.41	2.70	6.6	--	--	0.046	--	0.046	52	S-5	15.21	WTP25-63-5
					0.685	--	0.07	31.82	19.48	47.62	--	--	0.33	--	0.33				
9e	20% O ₂ , 80% Ne	90	89.4	--	0.096	--	0.002	3.68	2.63	3.59	--	0.15	--	--	0	100	S-5	15.21	WTP25-65-5
					0.946	--	0.02	36.26	25.92	35.38	--	1	--	--	0				
9f	20% O ₂ , 80% Ne	90	86.0	0.001	0.032	--	0.007	1.14	12.00	0.7	--	0.02	0.013	--	0.013	50	S-5	15.21	WTP25-67-5
					0.230	--	0.01	8.19	86.23	5.03	--	--	0.09	--	0.09				
9g	100% O ₂	90		--	0.028	--	--	1.47	97.80	0.58	--	--	0.015	--	0.015	49	S-5	15.21	WTP25-70-5
					0.028	--	--	1.5	97.89	0.6	--	--	0.0	--	0.0				
10a	20% O ₂ , 80% Ne	85	80.3	0.002	0.036	0.015	0.00	0.201	19.00	0.009	--	--	0.005	--	0.005	17	S-6	16.4	WTP25-50-6
					0.19	--	0.005	0.6	99.04	0.05	--	--	0.026	--	0.026				
10b	20% O ₂ , 80% Ne	90	93.1	0.001	0.33	--	0.003	0.69	4.80	0.81	--	--	0.03	--	0.03	286	S-6	16.4	WTP25-58-6
					4.97	--	0.05	10.4	72.03	12.2	--	--	0.45	--	0.45				
10c	20% O ₂ , 80% Ne	90	82.5	--	0.03	0.040	0.002	0.318	15.80	0.459	--	--	--	--	0	51	S-6	16.4	WTP25-60-6
					0.19	--	0.012	1.9	94.78	2.75	--	--	--	--	0				
10d	20% O ₂ , 80% Ne	90	83.1	--	0.04	--	0.001	1.1	13.70	1.95	--	--	0.016	--	0.016	52	S-6	16.4	WTP25-63-6
					0.22	--	0.006	6.5	81.43	11.59	--	--	0.095	--	0.095				
10e	20% O ₂ , 80% Ne	90	76.1	--	0.11	--	0.001	6.9	2.53	13.6	--	0.08	0.059	--	0.059	99	S-6	16.4	WTP25-65-6
					0.49	--	0.00	29.6	10.87	58.4	--	--	0.25	--	0.25				
10f	20% O ₂ , 80% Ne	90	78.5	0.001	0.08	--	0.002	6.5	2.16	12	--	0.08	0.086	--	0.086	50	S-6	16.4	WTP25-67-6
					0.40	--	0.01	31.1	10.33	57.4	--	--	0.41	--	0.41				
10g	100% O ₂	90	0.303	0.01	0.055	0.077	0.001	4.28	90.50	4.41	--	--	0.049	--	0.049	49	S-6	16.4	WTP25-70-6
					0.06	0.1	0.001	3.6	91.51	4.5	--	--	0.0	--	0.0				

Table 2.17. Mole Percent Composition Thermal Gas Sampled (including Ne), Gas Formed (shaded), and Heating Times of Runs 11 and 12 Using AN-102 Waste, 100% Ne and 100% Oxygen Atmosphere as Initial Cover Gas

Gas Composition: Mole%																				
Run	Cover gas	Temp °C	Ne	Ar	H ₂	CO ₂	CH ₄	N ₂	O ₂	N ₂ O	NOx	NH ₃ (est)	C ₂ HCs	> C ₂ HCs	Total HCs	Time, h	Vessel ID	Sample mass, g	Mass spec ID	
11a	100% Ne	90	99.2	0.001	0.042	0.01	0.003	0.128	0.03	0.11	0.182	--	0.004	--	0.004	42	S-20	14.77	WTP25-78-9	
					8.17	2.724	0.6	24.9	6.03	21.4	35.4	--	0.78	--	1					
11b	100% Ne	90	99.1	0.001	0.022	0.03	0.004	0.142	0.01	0.169	0.282	--	0.005	--	0.005	84	S-20	14.77	WTP25-83-9	
					3.25	4.882	0.6	21.0	1.33	25.0	41.7	--	0.74	--	1					
11c	100% O ₂	90	--	--	0.065	--	--	0.256	99.40	0.248	--	--	0.018	--	0.018	40	S-20	14.77	WTP25-85-9	
					0.07	--	--	0.3	99.41	0.2	--	--	0.02	--	0					
11d	100% O ₂	90	--	0.001	0.142	--	0.002	5.3	86.90	6.8	0.315	--	0.067	--	0.067	116	S-20	14.77	WTP25-88-9	
					0.14	--	0.002	5.3	86.99	6.8	0.3	--	0.07	--	0					
12a	100% Ne	90	99.3	0.001	0.056	0.02	0.004	0.182	0.03	0.169	0.191	--	0.005	--	0.005	42	S-21	15.39	WTP25-78-10	
					8.55	2.290	0.6	27.8	5.04	25.8	29.2	--	0.76	--	1					
12b	100% Ne	90	98.9	0.001	0.029	0.03	0.01	0.191	0.01	0.223	0.389	--	0.005	--	0.005	84	S-21	15.39	WTP25-83-10	
					3.24	2.796	0.6	21.4	1.57	24.9	43.5	--	0.56	--	1					
12c	100% O ₂	90	--	0.001	0.087	--	--	0.381	99.00	0.412	--	--	0.022	--	0.022	40	S-21	15.39	WTP25-85-10	
					0.09	--	--	0.4	99.10	0.4	--	--	0.02	--	0					
12d	100% O ₂	90	--	0.001	0.131	--	0.001	6	84.60	8.4	0.385	--	0.061	0.001	0.062	116	S-21	15.39	WTP25-88-10	
					0.13	--	0.001	6.0	84.60	8.4	0.4	--	0.06	0.00	0					

2.15

Table 2.18. Mole Percent Composition Thermal Gas Sampled (including Ne), Gas Formed (shaded), and Heating Times of Runs 13 and 14 Using AN-106 Waste, 100% Ne and 100% Oxygen Atmosphere

Gas Composition: Mole %																			
Run	Cover gas	Temp °C	Ne	Ar	H ₂	CO ₂	CH ₄	N ₂	O ₂	N ₂ O	NO _x	NH ₃ (est)	C ₂ HCs	> C ₂ HCs	Total HCs	Time, h	Vessel ID	Sample mass, g	Mass spec ID
13a	100% Ne	90	99.7	0.001	0.005	0.01	--	0.06	0.04	--	--	--	--	--	0	42	S-13	15.01	WTP25-78-11
					4.46	4.464	--	53.6	37.50	--	--	--	--	--	0				
13b	100% Ne	90	99.7	0.001	0.004	--	--	0.012	0.01	0.007	0.02	--	--	--	0	84	S-13	15.01	WTP25-83-11
					7.55	--	--	22.6	18.87	13.2	37.7	--	--	--	0				
13c	100% O ₂	90	--	--	0.009	0.02	--	0.012	99.90	--	--	--	0.004	--	0.004	39	S-13	15.01	WTP25-85-11
					0.01	0.022	--	0.0	99.95	--	--	--	0.00	--	0				
13d	100% O ₂	90	--	--	0.019	0.02	--	0.015	99.90	--	--	--	0.003	--	0.003	116	S-13	15.01	WTP25-88-11
					0.02	0.019	--	0.0	99.94	--	--	--	0.00	--	0				
14a	100% Ne	90	99.8	0.001	0.004	0.01	0.003	0.072	0.05	0.006	0.02	--	--	--	0	41	S-12	14.7	WTP25-78-12
					2.23	2.793	1.7	40.2	25.70	3.4	11.2	--	--	--	0				
14b	100% Ne	90	99.8	0.001	0.006	--	0.002	0.018	0.01	0.023	0.129	--	--	--	0	84	S-12	14.7	WTP25-83-12
					3.23	--	1.1	9.7	4.30	12.4	69.4	--	--	--	0				
14c	100% O ₂	90	--	--	0.012	0.02	--	0.012	99.90	--	--	--	0.003	0.001	0.004	41	S-12	14.7	WTP25-85-12
					0.012	0.020	--	0.0	99.95	--	--	--	0.00	0.00	0				
14d	100% O ₂	90	--	--	0.022	0.02	--	0.008	99.90	--	--	--	--	--	0	116	S-12	14.7	WTP25-88-12
					0.022	0.022	--	0.0	99.95	--	--	--	--	--	0				

Table 2.19. Mole Percent Composition Thermal Gas Sampled (including Ne), Gas Formed (shaded), and Heating Times of Runs 15 and 16 Using AN-107 Waste, 100% Ne and 100% Oxygen Atmosphere as Initial Cover Gas

Gas Composition: Mole%																			
Run	Cover gas	Temp °C	Ne	Ar	H ₂	CO ₂	CH ₄	N ₂	O ₂	N ₂ O	NO _x	NH ₃ (est)	C ₂ HCs	> C ₂ HCs	Total HCs	Time, h	Vessel ID	Sample mass, g	Mass spec ID
15a	100% Ne	90	98.5	0.004	0.003	0.03	0.01	0.52	0.09	0.27	0.6	--	--	--	0	43	S-14	15.84	WTP25-78-3
					0.25	2.743	0.4	22.4	1.89	22.4	49.9	--	--	--	0				
15b	100% Ne	90	97.8	0.007	0.001	0.04	0.01	0.82	0.09	0.43	0.82	--	0.004	--	0.004	84	S-14	15.84	WTP25-83-3
					0.06	2.454	0.4	18.6	5.20	25.1	47.9	--	0.23	--	0				
15c	100% O ₂	90	--	0.004	0.003	0.01	--	0.427	99.40	0.103	--	--	0.006	--	0.006	39	S-14	15.84	WTP25-85-3
					0.003	0.006	--	0.2	99.70	0.1	--	--	0.01	--	0				
15d	100% O ₂	90	--	0.014	0.011	0.01	0.003	2.72	96.50	0.7	--	--	0.016	--	0.016	116	S-14	15.84	WTP25-88-3
					0.011	0.006	0.003	1.7	97.59	0.7	--	--	0.02	--	0				
16a	100% Ne	90	98.3	--	0.002	0.02	0.01	0.191	0.02	0.331	1.02	--	--	--	0	42	S-40	15.31	WTP25-78-4
					0.125	0.940	0.6	12.0	1.13	20.7	63.9	--	--	--	0				
16b	100% Ne	90	96.7	0.001	0.002	0.04	0.02	0.277	0.00	0.51	2.44	--	0.004	--	0.004	84	S-40	15.31	WTP25-83-4
					0.060	1.057	0.6	8.4	0.06	15.4	73.7	--	0.12	--	0				
16c	100% O ₂	90	--	--	0.003	0.02	--	0.209	99.60	0.134	--	--	0.006	0.001	0.007	39	S-40	15.31	WTP25-85-4
					0.003	0.018	--	0.2	99.63	0.1	--	--	0.01	0.00	0				
16c	100% O ₂	90	--	--	0.008	0.03	0.003	1.44	98.00	0.48	--	--	0.014	0.001	0.015	116	S-40	15.31	WTP25-88-4
					0.008	0.029	0.003	1.4	98.00	0.5	--	--	0.01	0.00	0				

Table 2.20. Mole Percent Composition Thermal Gas Sampled (including Ne), Gas Formed (shaded), and Heating Times of Runs 17 and 18 Using AW-101 Waste, 100% Ne and 100% Oxygen Atmosphere

Gas Composition: Mole%																			
Run	Cover gas	Temp °C	Ne	Ar	H ₂	CO ₂	CH ₄	N ₂	O ₂	N ₂ O	NOx	NH ₃ (est)	C ₂ HCs	> C ₂ HCs	Total HCs	Time, h	Vessel ID	Sample mass, g	Mass spec ID
17a	100% Ne	90	99.1	0.002	0.066	0.01	0.01	0.243	0.04	0.174	0.341	--	--	--	0	42	S-18	15.23	WTP25-78-7
					8.32	0.883	1.8	20.1	2.34	21.9	43.0	--	--	--	0				
17b	100% Ne	90	98.5	0.003	0.108	0.01	0.02	0.338	0.04	0.415	0.57	--	--	--	0	84	S-18	15.23	WTP25-83-7
					8.12	0.602	1.7	12.8	2.63	31.2	42.9				0				
17c	100% O ₂	90	--	0.001	0.146	0.01	0.01	0.083	99.70	--	--	--	--	--	0	40	S-18	15.23	WTP25-85-7
					0.15	0.011	0.0	0.1	99.75	--	--	--	--	--	0				
17d	100% O ₂	90	--	0.003	0.265	0.02	0.03	0.222	99.40	--	--	--	--	--	0	116	S-18	15.23	WTP25-88-7
					0.27	0.019	0.0	0.1	99.63	--	--	--	--	--	0				
18a	100% Ne	90	98.8	0.008	0.041	0.01	0.01	0.78	0.20	0.024	0.087	--	--	--	0	42	S-19	14.95	WTP25-78-8
					9.93	2.665	2.7	47.2	10.66	5.8	21.1	--	--	--	0				
18b	100% Ne	90	97.9	0.011	0.121	0.03	0.03	1.06	0.21	0.23	0.34	--	--	--	0	84	S-19	14.95	WTP25-83-8
					10.13	2.094	2.3	18.8	17.42	19.3	28.5	--	--	--	0				
18c	100% O ₂	90	--	0.005	0.134	0.01	0.01	0.51	99.30	--	--	--	--	--	0	41	S-19	14.95	WTP25-85-8
					0.13	0.012	0.0	0.2	99.67	--	--	--	--	--	0				
18d	100% O ₂	90	--	0.044	0.192	0.03	0.03	4.03	95.60	--	--	--	--	--	0	116	S-19	14.95	WTP25-88-8
					0.20	0.029	0.0	0.5	99.27	--	--	--	--	--	0				

Table 2.21. Mole Percent Composition Thermal Gas Sampled (including Ne), Gas Formed (shaded), and Heating Times of Runs 19 and 20 Using U-106 Waste, 100% Ne and 100% Oxygen Atmosphere as Initial Cover Gas

Gas Composition: Mole%																				
Run	Cover gas	Temp °C	Ne	Ar	H ₂	CO ₂	CH ₄	N ₂	O ₂	N ₂ O	NO _x	NH ₃ (est)	C ₂ HCs	> C ₂ HCs	Total HCs	Time, h	Vessel ID	Sample mass, g	Mass spec ID	
19a	100% Ne	90	99.6	0.001	0.055	0.01	0.002	0.124	0.02	0.152	0.08	--	--	--	0	42	S-16	14.52	WTP25-78-5	
					12.0	2.832	0.4	27.0	5.01	33.1	17.4	--	--	--	0					
19b	100% Ne	90	99.4	0.001	0.033	0.02	0.004	0.098	0.004	0.156	0.217	--	0.003	--	0.003	84	S-16	14.52	WTP25-83-5	
					6.1	4.275	0.7	18.2	0.74	29.0	40.3	--	0.56	--	1					
19c	100% O ₂	90	--	--	0.039	--	--	0.01	99.80	0.056	--	--	0.010	--	0.01	41	S-16	14.52	WTP25-85-5	
					0.039	--	--	0.0	99.88	0.1	--	--	0.01	--	0					
19d	100% O ₂	90	--	--	0.046	0.04	--	0.373	99.40	0.036	--	--	0.014	--	0.014	116	S-16	14.52	WTP25-88-5	
					0.046	0.044	--	0.4	99.49	0.0	--	--	0.01	--	0					
20a	100% Ne	90	99.5	--	0.054	0.03	0.003	0.106	0.03	0.074	0.14	--	--	--	0	42	S-17	14.95	WTP25-78-6	
					12	7.727	0.7	24.1	6.59	16.8	31.8	--	--	--	0					
20b	100% Ne	90	99.3	0.001	0.027	0.02	0.003	0.073	0.01	0.131	0.227	--	0.004	--	0.004	84	S-17	14.95	WTP25-83-6	
					5.42	3.012	0.6	14.7	1.20	26.3	45.6	--	0.80	--	1					
20c	100% O ₂	90	--	--	0.046	--	--	0.12	99.70	0.068	--	--	0.012	--	0.012	39	S-17	14.95	WTP25-85-6	
					0.05	--	--	0.1	99.75	0.1	--	--	0.01	--	0					
20d	100% O ₂	90	--	--	0.058	0.01	--	0.336	99.40	0.147	--	--	0.016	--	0.016	116	S-17	14.95	WTP25-88-6	
					0.06	0.005	--	0.3	99.44	0.1	--	--	0.02	--	0					

Table 2.22. Gas Generation Rates from Thermal Treatment of AN-102 Waste (Runs 1 and 2) under 20% and 100% Oxygen Atmosphere as Initial Cover Gas (gas generation or depletion rates expressed in moles of gas generated per kg of total sample per day, or mol kg⁻¹ day⁻¹)

Gas Generation (or depletion) Rates: mol/kg/day																	
Run	Cover gas	Temp °C	H ₂	CO ₂	CH ₄	N ₂	O ₂	N ₂ O	NOx	NH ₃ (est)	C ₂ HCs	> C ₂ HCs	Total HCs	Time, h	Vessel ID	Sample mass, g	Mass spec ID
1a	20% O ₂ , 80% Ne	85	2.7E-4	1.1E-4	--	6.2E-4	-1.0E-2	2.3E-4	--	--	4.0E-5	--	4.0E-5	17	S-9	15.70	WTP25-50-9
1b	20% O ₂ , 80% Ne	90	5.8E-4	--	2.2E-6	5.3E-3	-8.3E-3	1.0E-2	--	--	4.7E-5	--	4.7E-5	286	S-9	15.70	WTP25-58-9
1c	20% O ₂ , 80% Ne	90	2.5E-4	--	1.6E-5	5.5E-3	-4.8E-2	5.2E-3	--	--	6.2E-5	--	6.2E-5	50	S-9	15.70	WTP25-60-9
1d	20% O ₂ , 80% Ne	90	9.1E-5	--	1.9E-5	5.1E-3	-2.8E-2	3.6E-3	--	--	6.2E-5	--	6.2E-5	52	S-9	15.70	WTP25-63-9
1e	20% O ₂ , 80% Ne	90	8.7E-5	--	2.5E-6	1.7E-3	-1.6E-2	7.2E-4	--	8.7E-5	2.2E-5	--	2.2E-5	99	S-9	15.70	WTP25-65-9
1f	20% O ₂ , 80% Ne	90	9.0E-5	9.3E-5	5.2E-6	1.1E-3	-1.4E-2	4.1E-5	--	5.2E-5	2.3E-5	2.6E-6	2.6E-5	49	S-9	15.70	WTP25-67-9
1g	100% O ₂	90	1.1E-4	2.3E-5	--	1.1E-3	-1.9E-2	5.2E-4	--	--	--	--	--	50	S-9	15.70	WTP25-70-9
2a	20% O ₂ , 80% Ne	85	2.6E-4	3.3E-4	--	2.0E-3	-8.0E-3	7.7E-5	--	--	2.6E-5	--	2.6E-5	17	S-10	15.01	WTP25-50-10
2b	20% O ₂ , 80% Ne	90	3.0E-4	--	1.4E-6	2.6E-3	-8.9E-3	4.7E-3	--	--	2.6E-5	--	2.6E-5	286	S-10	15.01	WTP25-58-10
2c	20% O ₂ , 80% Ne	90	1.5E-4	1.1E-5	2.1E-5	4.6E-3	-2.9E-2	6.3E-3	--	--	4.2E-5	--	4.2E-5	50	S-10	15.01	WTP25-60-10
2d	20% O ₂ , 80% Ne	90	6.3E-5	--	1.9E-5	5.4E-3	-2.1E-2	6.8E-3	--	--	5.0E-5	--	5.0E-5	52	S-10	15.01	WTP25-63-10
2e	20% O ₂ , 80% Ne	90	5.7E-5	--	1.4E-6	4.5E-3	-1.6E-2	4.0E-3	--	1.2E-4	3.4E-5	--	3.4E-5	100	S-10	15.01	WTP25-65-10
2f	20% O ₂ , 80% Ne	90	5.9E-5	5.7E-5	2.7E-6	3.1E-3	-1.2E-2	1.7E-3	--	8.1E-5	3.8E-5	--	3.8E-5	50	S-10	15.01	WTP25-67-10
2g	100% O ₂	90	7.0E-5	--	--	2.0E-3	-2.4E-2	9.6E-4	--	--	3.2E-5	--	3.2E-5	50	S-10	15.01	WTP25-70-10

Table 2.23. Gas Generation Rates from Thermal Treatment of AN-106 Waste (Runs 3 and 4) under 20% and 100% Oxygen Atmosphere as Initial Cover Gas (gas generation or depletion rates expressed in moles of gas generated per kg of total sample per day, or mol kg⁻¹ day⁻¹)

Gas Generation (or depletion) Rates: mol/kg/day																	
Run	Cover gas	Temp °C	H ₂	CO ₂	CH ₄	N ₂	O ₂	N ₂ O	NO _x	NH ₃ (est)	C ₂ HCs	> C ₂ HCs	Total HCs	Time, h	Vessel ID	Sample mass, g	Mass spec ID
3a	20% O ₂ , 80% Ne	85	2.4E-5	7.2E-5	--	1.0E-3	-6.1E-3	--	--	--	--	--	--	16	S-11	16.05	WTP25-50-11
3b	20% O ₂ , 80% Ne	90	1.8E-5	5.5E-6	1.6E-6	2.2E-5	-5.7E-3	--	--	--	1.6E-6	3.9E-7	2.0E-6	286	S-11	16.05	WTP25-58-11
3c	20% O ₂ , 80% Ne	90	1.5E-5	2.8E-5	5.1E-6	5.6E-5	-4.9E-3	--	--	--	1.3E-5	--	1.3E-5	50	S-11	16.05	WTP25-60-11
3d	20% O ₂ , 80% Ne	90	9.9E-6	3.2E-5	4.9E-6	3.9E-5	-3.4E-3	--	--	--	7.4E-6	--	7.4E-6	53	S-11	16.05	WTP25-63-11
3e	20% O ₂ , 80% Ne	90	9.1E-6	9.1E-6	--	2.2E-5	-2.9E-3	--	--	--	--	--	--	100	S-11	16.05	WTP25-65-11
3f	20% O ₂ , 80% Ne	90	7.8E-6	2.8E-5	2.6E-6	5.2E-5	-2.8E-3	1.6E-5	--	--	7.8E-6	--	7.8E-6	50	S-11	16.05	WTP25-67-11
3g	100% O ₂	90	1.0E-5	7.1E-5	--	3.1E-5	-5.7E-3	--	--	--	1.0E-5	--	1.0E-5	51	S-11	16.05	WTP25-70-11
4a	20% O ₂ , 80% Ne	85	4.1E-5	1.1E-4	--	5.4E-4	-6.3E-3	--	--	--	--	--	--	17	S-1	15.09	WTP25-50-12
4b	20% O ₂ , 80% Ne	90	2.5E-5	3.4E-6	1.7E-6	1.9E-5	-5.7E-3	--	--	--	1.7E-6	4.3E-7	2.1E-6	280	S-1	15.09	WTP25-58-12
4c	20% O ₂ , 80% Ne	90	1.6E-5	2.4E-5	5.4E-6	4.6E-5	-4.0E-3	--	--	--	--	--	--	51	S-1	15.09	WTP25-60-12
4d	20% O ₂ , 80% Ne	90	9.9E-6	4.9E-5	9.9E-6	6.9E-5	-2.8E-3	--	--	--	9.9E-6	--	9.9E-6	28	S-1	15.09	WTP25-63-12
4e	20% O ₂ , 80% Ne	90	1.1E-5	--	--	2.1E-5	-3.3E-3	--	--	--	--	--	--	99	S-1	15.09	WTP25-65-12
4f	20% O ₂ , 80% Ne	90	1.1E-5	3.0E-5	--	3.6E-5	-2.9E-3	--	--	--	8.2E-6	--	8.2E-6	50	S-1	15.09	WTP25-67-12
4g	100% O ₂	90	1.1E-5	6.1E-5	--	1.7E-5	-7.0E-3	--	--	--	8.3E-6	--	8.3E-6	50	S-1	15.09	WTP25-70-12

Table 2.24. Gas Generation Rates from Thermal Treatment of AN-107 Waste (Runs 5 and 6) under 20% and 100% Oxygen Atmosphere as Initial Cover Gas (gas generation or depletion rates expressed in moles of gas generated per kg of total sample per day, or mol kg⁻¹ day⁻¹)

Gas Generation (or depletion) Rates: mol/kg/day																	
Run	Cover gas	Temp °C	H ₂	CO ₂	CH ₄	N ₂	O ₂	N ₂ O	NO _x	NH ₃ (est)	C ₂ HCs	> C ₂ HCs	Total HCs	Time, h	Vessel ID	Sample mass, g	Mass spec ID
5a	20% O ₂ , 80% Ne	85	8.3E-6	1.2E-4	1.7E-5	1.7E-3	-5.8E-3	1.3E-4	--	--	2.5E-5	--	2.5E-5	17	S-3	15.08	WTP25-50-3
5b	20% O ₂ , 80% Ne	90	1.2E-5	--	8.9E-7	2.0E-3	-8.3E-3	2.8E-3	--	--	1.0E-5	--	1.0E-5	285	S-3	15.08	WTP25-58-3
5c	20% O ₂ , 80% Ne	90	5.2E-5	--	2.7E-6	1.0E-2	-3.0E-2	1.6E-2	--	--	2.7E-5	--	2.7E-5	50	S-3	15.08	WTP25-60-3
5d	20% O ₂ , 80% Ne	90	5.5E-5	--	5.5E-6	2.3E-2	-4.5E-2	3.1E-2	--	--	6.9E-5	--	6.9E-5	52	S-3	15.08	WTP25-63-3
5e	20% O ₂ , 80% Ne	90	4.4E-5	--	1.4E-5	2.8E-2	-2.7E-2	2.7E-2	--	--	8.7E-5	--	8.7E-5	97	S-3	15.08	WTP25-65-3
5f	20% O ₂ , 80% Ne	90	4.1E-5	--	3.2E-5	1.0E-2	-5.0E-2	6.3E-3	--	--	4.6E-5	2.4E-6	4.8E-5	50	S-3	15.08	WTP25-67-3
5g	100% O ₂	90	6.1E-5	9.2E-05	1.0E-5	1.9E-3	-9.3E-2	1.4E-3	--	--	2.6E-5	2.0E-6	2.9E-5	49	S-3	15.08	WTP25-70-3
6a	20% O ₂ , 80% Ne	85	7.5E-6	1.2E-4	--	8.5E-4	-6.0E-3	9.8E-5	--	--	1.5E-5	--	1.5E-5	17	S-4	15.31	WTP25-50-4
6b	20% O ₂ , 80% Ne	90	1.8E-5	--	2.4E-6	3.5E-3	-8.7E-3	6.9E-3	--	--	1.2E-5	--	1.2E-5	286	S-4	15.31	WTP25-58-4
6c	20% O ₂ , 80% Ne	90	7.0E-5	--	--	1.5E-2	-4.8E-2	2.4E-2	--	--	--	--	--	50	S-4	15.31	WTP25-60-4
6d	20% O ₂ , 80% Ne	90	5.4E-5	--	2.0E-5	3.3E-2	-4.6E-2	3.7E-2	--	--	1.1E-4	--	1.1E-4	52	S-4	15.31	WTP25-63-4
6e	20% O ₂ , 80% Ne	90	2.5E-5	--	1.4E-5	1.7E-2	-2.5E-2	1.3E-2	--	--	--	--	--	100	S-4	15.31	WTP25-65-4
6f	20% O ₂ , 80% Ne	90	3.6E-5	2.9E-5	2.0E-5	4.5E-3	-4.8E-2	2.3E-3	--	--	2.9E-5	2.2E-6	3.1E-5	49	S-4	15.31	WTP25-67-4
6g	100% O ₂	90	4.8E-5	3.1E-5	5.7E-6	1.9E-3	-9.3E-2	1.2E-3	--	--	2.1E-5	1.9E-6	2.3E-5	49	S-4	15.31	WTP25-70-4

Table 2.25. Gas Generation Rates from Thermal Treatment of AW-101 Waste (Runs 7 and 8) under 20% and 100% Oxygen Atmosphere as Initial Cover Gas (gas generation or depletion rates expressed in moles of gas generated per kg of total sample per day, or mol kg⁻¹ day⁻¹)

Gas Generation (or depletion) Rates: mol/kg/day																	
Run	Cover gas	Temp °C	H ₂	CO ₂	CH ₄	N ₂	O ₂	N ₂ O	NOx	NH ₃ (est)	C ₂ HCs	> C ₂ HCs	Total HCs	Time, h	Vessel ID	Sample mass, g	Mass spec ID
7a	20% O ₂ , 80% Ne	85	2.4E-4	6.8E-5	2.6E-5	9.3E-4	-5.3E-3	1.7E-5	--	--	2.6E-5	--	2.6E-5	17	S-7	14.92	WTP25-50-7
7b	20% O ₂ , 80% Ne	90	1.9E-4	3.9E-6	3.6E-5	1.1E-4	-3.5E-3	--	--	--	1.9E-6	6.4E-7	2.6E-6	205	S-7	14.92	WTP25-58-7
7c	20% O ₂ , 80% Ne	90	1.2E-4	1.7E-5	3.4E-5	2.1E-4	-2.7E-3	--	--	--	--	--	--	50	S-7	14.92	WTP25-60-7
7d	20% O ₂ , 80% Ne	90	9.8E-5	2.2E-5	3.5E-5	1.6E-4	-2.5E-3	--	--	--	--	--	--	52	S-7	14.92	WTP25-63-7
7e	20% O ₂ , 80% Ne	90	7.8E-5	1.3E-5	2.9E-5	8.5E-5	-2.7E-3	--	--	--	--	--	--	100	S-7	14.92	WTP25-65-7
7f	20% O ₂ , 80% Ne	90	7.7E-5	5.1E-5	3.4E-5	9.8E-5	-2.4E-3	--	--	--	--	--	--	49	S-7	14.92	WTP25-67-7
7g	100% O ₂	90	1.2E-4	4.1E-5	2.9E-5	3.5E-4	-2.3E-3	--	--	--	--	--	--	50	S-7	14.92	WTP25-70-7
8a	20% O ₂ , 80% Ne	85	2.4E-4	1.2E-4	2.4E-5	3.6E-4	-5.7E-3	2.4E-5	--	--	2.4E-5	--	2.4E-5	17	S-8	15.49	WTP25-50-8
8b	20% O ₂ , 80% Ne	90	1.4E-4	3.3E-6	3.1E-5	1.4E-5	-3.7E-3	--	--	--	1.3E-6	4.2E-7	1.7E-6	286	S-8	15.49	WTP25-58-8
8c	20% O ₂ , 80% Ne	90	7.2E-5	2.1E-5	2.9E-5	7.5E-5	-3.3E-3	1.3E-5	--	--	--	--	--	50	S-8	15.49	WTP25-60-8
8d	20% O ₂ , 80% Ne	90	6.2E-5	2.8E-5	2.8E-5	2.6E-5	-2.4E-3	--	--	--	--	--	--	52	S-8	15.49	WTP25-63-8
8e	20% O ₂ , 80% Ne	90	4.9E-5	1.6E-5	2.2E-5	2.7E-5	-1.9E-3	--	--	--	--	--	--	99	S-8	15.49	WTP25-65-8
8f	20% O ₂ , 80% Ne	90	4.6E-5	2.4E-5	2.4E-5	6.5E-5	-1.6E-3	--	--	--	8.1E-6	--	8.1E-6	49	S-8	15.49	WTP25-67-8
8g	100% O ₂	90	1.0E-4	5.2E-5	2.4E-5	3.4E-3	-1.1E-2	--	--	--	--	--	--	50	S-8	15.49	WTP25-70-8

Table 2.26. Gas Generation Rates from Thermal Treatment of U-106 Waste (Runs 9 and 10) under 20% and 100% Oxygen Atmosphere as Initial Cover Gas (gas generation or depletion rates are expressed in moles of gas generated per kg of total sample per day, or mol kg⁻¹ day⁻¹)

Gas Generation (or depletion) Rates: mol/kg/day																	
Run	Cover gas	Temp °C	H ₂	CO ₂	CH ₄	N ₂	O ₂	N ₂ O	NOx	NH ₃ (est)	C ₂ HCs	> C ₂ HCs	Total HCs	Time, h	Vessel ID	Sample mass, g	Mass spec ID
9a	20% O ₂ , 80% Ne	85	3.3E-4	8.1E-5	--	7.2E-4	-1.0E-2	9.8E-5	--	--	4.1E-5	--	4.1E-5	17	S-5	15.21	WTP25-50-5
9b	20% O ₂ , 80% Ne	90	4.2E-4	--	3.6E-6	3.6E-3	-8.5E-3	8.5E-3	--	--	3.7E-5	--	3.7E-5	286	S-5	15.21	WTP25-58-5
9c	20% O ₂ , 80% Ne	90	3.9E-4	--	2.1E-5	1.3E-2	-4.9E-2	2.7E-2	--	--	1.1E-4	--	1.1E-4	50	S-5	15.21	WTP25-60-5
9d	20% O ₂ , 80% Ne	90	2.3E-4	--	2.5E-5	1.1E-2	-4.6E-2	1.6E-2	--	--	1.1E-4	--	1.1E-4	52	S-5	15.21	WTP25-63-5
9e	20% O ₂ , 80% Ne	90	1.2E-4	--	2.5E-6	4.6E-3	-2.5E-2	4.5E-3	--	1.9E-4	--	--	--	100	S-5	15.21	WTP25-65-5
9f	20% O ₂ , 80% Ne	90	8.1E-5	--	2.5E-6	2.9E-3	-2.4E-2	1.8E-3	--	5.1E-5	3.3E-5	--	3.3E-5	50	S-5	15.21	WTP25-67-5
9g	100% O ₂	90	7.3E-5	--	--	3.8E-3	-3.3E-2	1.5E-3	--	--	3.9E-5	--	3.9E-5	49	S-5	15.21	WTP25-70-5
10a	20% O ₂ , 80% Ne	85	2.8E-4	1.2E-4	7.7E-6	9.0E-4	-8.7E-3	6.9E-5	--	--	3.9E-5	--	3.9E-5	17	S-6	16.40	WTP25-50-6
10b	20% O ₂ , 80% Ne	90	1.2E-4	--	1.1E-6	2.6E-4	-7.0E-3	3.1E-4	--	--	1.1E-5	--	1.1E-5	286	S-6	16.40	WTP25-58-6
10c	20% O ₂ , 80% Ne	90	7.9E-5	9.9E-5	4.9E-6	7.8E-4	-1.2E-2	1.1E-3	--	--	--	--	--	51	S-6	16.40	WTP25-60-6
10d	20% O ₂ , 80% Ne	90	8.8E-5	--	2.4E-6	2.6E-3	-1.7E-2	4.6E-3	--	--	3.8E-5	--	3.8E-5	52	S-6	16.40	WTP25-63-6
10e	20% O ₂ , 80% Ne	90	1.6E-4	--	1.4E-6	9.6E-3	-2.3E-2	1.9E-2	--	1.1E-4	8.2E-5	--	8.2E-5	99	S-6	16.40	WTP25-65-6
10f	20% O ₂ , 80% Ne	90	2.2E-4	--	5.2E-6	1.7E-2	-4.5E-2	3.1E-2	--	2.1E-4	2.2E-4	--	2.2E-4	50	S-6	16.40	WTP25-67-6
10g	100% O ₂	90	1.2E-4	1.7E-4	2.2E-6	7.9E-3	-6.6E-2	9.9E-3	--	--	1.1E-4	--	1.1E-4	49	S-6	16.40	WTP25-70-6

Table 2.27. Gas Generation Rates from Thermal Treatment of AN-102 Waste (Runs 11 and 12) under 100% Neon/100% Oxygen Atmosphere as Initial Cover Gas (gas generation/depletion rates expressed in moles of gas generated per kg of total sample per day, or mol kg⁻¹ day⁻¹)

Gas Generation (or depletion) Rates: mol/kg/day																	
Run	Cover gas	Temp °C	H ₂	CO ₂	CH ₄	N ₂	O ₂	N ₂ O	NOx	NH ₃ (est)	C ₂ HCs	>C ₂ HCs	Total HCs	Time, h	Vessel ID	Sample mass, g	Mass spec ID
11a	100% Ne	90	1.4E-4	4.7E-5	1.0E-5	4.3E-4	1.0E-4	3.7E-4	6.1E-4	--	1.3E-5	--	1.3E-5	42	S-20	14.77	WTP25-78-9
11b	100% Ne	90	3.7E-5	5.5E-5	6.7E-6	2.4E-4	1.5E-5	2.8E-4	4.7E-4	--	8.4E-6	--	8.4E-6	84	S-20	14.77	WTP25-83-9
11c	100% O ₂	90	2.1E-4	--	--	8.4E-4	-3.3E-2	8.2E-4	--	--	5.9E-5	--	5.9E-5	40	S-20	14.77	WTP25-85-9
11d	100% O ₂	90	1.5E-4	--	2.1E-6	5.5E-3	-3.4E-2	7.1E-3	3.3E-4	--	7.0E-5	--	7.0E-5	116	S-20	14.77	WTP25-88-9
12a	100% Ne	90	1.9E-4	5.0E-5	1.3E-5	6.0E-4	1.1E-4	5.6E-4	6.3E-4	--	1.7E-5	--	1.7E-5	42	S-21	15.39	WTP25-78-10
12b	100% Ne	90	4.8E-5	4.1E-5	8.3E-6	3.2E-4	2.3E-5	3.7E-4	6.4E-4	--	8.3E-6	--	8.3E-6	84	S-21	15.39	WTP25-83-10
12c	100% O ₂	90	2.7E-4	1.5E-4	--	1.2E-3	-3.5E-2	1.1E-3	--	--	6.9E-5	--	6.9E-5	40	S-21	15.39	WTP25-85-10
12d	100% O ₂	90	1.2E-4	--	9.5E-7	5.7E-3	-3.9E-2	8.0E-3	3.7E-4	--	5.8E-5	9.5E-7	5.9E-5	116	S-21	15.39	WTP25-88-10

Table 2.28. Gas Generation Rates from Thermal Treatment of AN-106 Waste (Runs 13 and 14) under 100% Neon/100% Oxygen Atmosphere as Initial Cover Gas (gas generation/depletion rates expressed in moles of gas generated per kg of total sample per day, or mol kg⁻¹ day⁻¹)

Gas Generation (or depletion) Rates: mol/kg/day																	
Run	Cover gas	Temp °C	H ₂	CO ₂	CH ₄	N ₂	O ₂	N ₂ O	NOx	NH ₃ (est)	C ₂ HCs	>C ₂ HCs	Total HCs	Time, h	Vessel ID	Sample mass, g	Mass spec ID
13a	100% Ne	90	1.7E-5	1.7E-5	--	2.0E-4	1.4E-4	--	--	--	--	--	--	42	S-13	15.01	WTP25-78-11
13b	100% Ne	90	6.8E-6	--	--	2.0E-5	1.7E-5	1.2E-5	3.4E-5	--	--	--	--	84	S-13	15.01	WTP25-83-11
13c	100% O ₂	90	3.2E-5	7.9E-5	--	4.3E-5	-8.0E-3	--	--	--	1.4E-5	--	1.4E-5	39	S-13	15.01	WTP25-85-11
13d	100% O ₂	90	2.2E-5	2.2E-5	--	1.7E-5	-7.7E-3	--	--	--	3.4E-6	--	3.4E-6	116	S-13	15.01	WTP25-88-11
14a	100% Ne	90	1.4E-5	1.7E-5	1.0E-5	2.5E-4	1.6E-4	2.1E-5	6.9E-5	--	--	--	--	41	S-12	14.70	WTP25-78-12
14b	100% Ne	90	1.0E-5	1.7E-5	3.4E-6	3.1E-5	1.4E-5	3.9E-5	2.2E-4	--	--	--	--	84	S-12	14.70	WTP25-83-12
14c	100% O ₂	90	4.1E-5	6.9E-5	--	4.1E-5	-8.7E-3	--	--	--	1.0E-5	3.4E-6	1.4E-5	41	S-12	14.70	WTP25-85-12
14d	100% O ₂	90	2.5E-5	2.5E-5	--	9.2E-6	-8.4E-3	--	--	--	--	--	--	116	S-12	14.70	WTP25-88-12

Table 2.29. Gas Generation Rates from Thermal Treatment of AN-107 Waste (Runs 15 and 16) under 100% Neon/100% Oxygen Atmosphere as Initial Cover Gas (gas generation/depletion rates expressed in moles of gas generated per kg of total sample per day, or mol kg⁻¹ day⁻¹)

Gas Generation (or depletion) Rates: mol/kg/day																	
Run	Cover gas	Temp °C	H ₂	CO ₂	CH ₄	N ₂	O ₂	N ₂ O	NOx	NH ₃ (est)	C ₂ HCs	> C ₂ HCs	Total HCs	Time, h	Vessel ID	Sample mass, g	Mass spec ID
15a	100% Ne	90	9.5E-6	1.0E-4	1.6E-5	8.5E-4	7.2E-5	8.4E-4	1.9E-3	--	--	--	--	43	S-14	15.84	WTP25-78-3
15b	100% Ne	90	1.6E-6	6.8E-5	1.1E-5	5.2E-4	1.4E-4	7.0E-4	1.3E-3	--	6.5E-6	--	6.5E-6	84	S-14	15.84	WTP25-83-3
15c	100% O ₂	90	9.8E-6	2.0E-5	--	5.8E-4	-2.4E-2	3.4E-4	--	--	2.0E-5	--	2.0E-5	39	S-14	15.84	WTP25-85-3
15d	100% O ₂	90	1.0E-5	5.7E-6	2.8E-6	1.5E-3	-2.6E-2	6.6E-4	--	--	1.5E-5	--	1.5E-5	116	S-14	15.84	WTP25-88-3
16a	100% Ne	90	6.4E-6	4.8E-5	2.9E-5	6.1E-4	5.8E-5	1.1E-3	3.3E-3	--	--	--	--	42	S-40	15.31	WTP25-78-4
16b	100% Ne	90	3.3E-6	5.7E-5	3.3E-5	4.5E-4	3.3E-6	8.3E-4	4.0E-3	--	6.5E-6	--	6.5E-6	84	S-40	15.31	WTP25-83-4
16c	100% O ₂	90	9.6E-6	5.8E-5	--	6.7E-4	-3.2E-2	4.3E-4	--	--	1.9E-5	3.2E-6	2.2E-5	39	S-40	15.31	WTP25-85-4
16d	100% O ₂	90	7.5E-6	2.7E-5	2.8E-6	1.3E-3	-2.5E-2	4.5E-4	--	--	1.3E-5	9.4E-7	1.4E-5	116	S-40	15.31	WTP25-88-4

Table 2.30. Gas Generation Rates from Thermal Treatment of AW-101 Waste (Runs 17 and 18) under 100% Neon/100% Oxygen Atmosphere as Initial Cover Gas (gas generation/depletion rates expressed in moles of gas generated per kg of total sample per day, or mol kg⁻¹ day⁻¹)

Gas Generation (or depletion) Rates: mol/kg/day																	
Run	Cover gas	Temp °C	H ₂	CO ₂	CH ₄	N ₂	O ₂	N ₂ O	NOx	NH ₃ (est)	C ₂ HCs	> C ₂ HCs	Total HCs	Time, h	Vessel ID	Sample mass, g	Mass spec ID
17a	100% Ne	90	2.2E-4	2.4E-5	4.7E-5	5.4E-4	6.3E-5	5.9E-4	1.1E-3	--	--	--	--	42	S-18	15.23	WTP25-78-7
17b	100% Ne	90	1.8E-4	1.4E-5	3.9E-5	4.3E-4	2.1E-5	7.0E-4	9.6E-4	--	--	--	--	84	S-18	15.23	WTP25-83-7
17c	100% O ₂	90	5.0E-4	3.8E-5	3.1E-5	2.1E-4	-8.5E-3	--	--	--	--	--	--	40	S-18	15.23	WTP25-85-7
17d	100% O ₂	90	3.1E-4	2.2E-5	3.0E-5	6.4E-5	-6.4E-3	--	--	--	--	--	--	116	S-18	15.23	WTP25-88-7
18a	100% Ne	90	1.3E-4	3.6E-5	3.6E-5	6.4E-4	1.4E-4	7.8E-5	2.8E-4	--	--	--	--	42	S-19	14.95	WTP25-78-8
18b	100% Ne	90	1.9E-4	4.0E-5	4.3E-5	3.6E-4	3.3E-4	3.7E-4	5.4E-4	--	--	--	--	84	S-19	14.95	WTP25-83-8
18c	100% O ₂	90	4.4E-4	4.0E-5	3.0E-5	4.8E-4	-2.0E-2	--	--	--	--	--	--	41	S-19	14.95	WTP25-85-8
18d	100% O ₂	90	2.2E-4	3.2E-5	2.9E-5	5.0E-4	-1.4E-2	--	--	--	--	--	--	116	S-19	14.95	WTP25-88-8

Table 2.31. Gas Generation Rates from Thermal Treatment of U-106 Waste (Runs 19 and 20) under 100% Neon/100% Oxygen Atmosphere as Initial Cover Gas (gas generation/depletion rates expressed in moles of gas generated per kg of total sample per day, or mol kg⁻¹ day⁻¹)

Gas Generation (or depletion) Rates: mol/kg/day																	
Run	Cover gas	Temp °C	H ₂	CO ₂	CH ₄	N ₂	O ₂	N ₂ O	NO _x	NH ₃ (est)	C ₂ HCs	> C ₂ HCs	Total HCs	Time, h	Vessel ID	Sample mass, g	Mass spec ID
19a	100% Ne	90	1.9E-4	4.6E-5	7.0E-6	4.3E-4	8.1E-5	2.8E-4	2.8E-4	--	--	--	--	42	S-16	14.52	WTP25-78-5
19b	100% Ne	90	5.8E-5	4.0E-5	7.0E-6	1.7E-4	7.0E-6	2.7E-4	3.8E-4	--	5.3E-6	--	5.3E-6	84	S-16	14.52	WTP25-83-5
19c	100% O ₂	90	1.3E-4	--	--	3.4E-5	-2.5E-2	1.9E-4	--	--	3.4E-5	--	3.4E-5	41	S-16	14.52	WTP25-85-5
19d	100% O ₂	90	5.0E-5	4.8E-5	--	4.1E-4	-1.8E-2	3.9E-5	--	--	1.5E-5	--	1.5E-5	116	S-16	14.52	WTP25-88-5
20a	100% Ne	90	1.8E-4	1.2E-4	1.0E-5	3.6E-4	9.9E-5	2.5E-4	4.8E-4	--	--	--	--	42	S-17	14.95	WTP25-78-6
20b	100% Ne	90	4.6E-5	2.6E-5	5.2E-6	1.3E-4	1.0E-5	2.3E-4	3.9E-4	--	6.9E-6	--	6.9E-6	84	S-17	14.95	WTP25-83-6
20c	100% O ₂	90	1.6E-4	1.7E-5	--	4.1E-4	-2.6E-2	2.3E-4	--	--	4.1E-5	--	4.1E-5	39	S-17	14.95	WTP25-85-6
20d	100% O ₂	90	6.1E-5	5.3E-6	--	3.5E-4	-1.9E-2	1.6E-4	--	--	1.7E-5	--	1.7E-5	116	S-17	14.95	WTP25-88-6

2.4 Discussion of Results: Gas Generation from Tank Waste Samples

The objective of this work is to assess the contribution of oxygen on the rate of hydrogen generation from Hanford waste. The gas generation rates of Hanford wastes in contact with various atmospheric gases (100% Ne; 20% O₂ in Ne; and 100% O₂) were measured and recorded in the previous section. The effect of added oxygen on hydrogen generation rates can be seen by comparing the results of these tests.

Table 2.32 summarizes hydrogen gas generation rates from the various Hanford wastes studied as a function of the cover gases used in this work. The second to last column in this table gives the enhancement of the hydrogen generation rate under a 20% oxygen cover gas compared with the rate observed for the same waste under similar conditions using 100% neon cover gas. The 20% oxygen in Ne values in Table 2.32 are averages of all hydrogen measurements under that cover gas for each respective waste; the same is the case for the 100% oxygen experiments. The enhancement of hydrogen generation in systems containing oxygen cover gas compared to the rate of hydrogen generation with an inert cover gas ranges from a high of 14.4 for AN-107 to a low of 0.6 for AW-101. The last column in the table contains the calculated hydrogen generation rate based on the Hu correlation.^(a) The hydrogen enhancements under oxygen cover gas for various wastes are shown graphically in Figures 2.4 through 2.9.

Table 2.33 contains the generation rates for all major gases produced as a function of cover gas. This table includes the standard deviation for generation rates determined from the averages of replicate runs. The gas generation values summarized in Tables 2.32 and 2.33 for the 100% neon cover gas are the second value measured in sequence for that system. With one exception, all 100% neon experiments showed a marked decrease in hydrogen generation rate from the first experiment to the second in each successive pair (compare, for example, hydrogen generation rates from experiment 11a with 11b or 12a with 12b from Table 2.27). The decrease in hydrogen generation rate with each successive 100% Ne experiment is consistent with residual dissolved oxygen remaining in the system during the first experiment reacting and increasing the hydrogen generation rate. The second

Table 2.32. Hydrogen Generation Rates as a Function of Cover Gas

Hanford waste type	Cover gas						Ratio: H ₂ generation rate in 20% O ₂ :100% Ne	Hu Correlation at 90°C mol H ₂ /kg/day
	100% Ne		20% O ₂ in Ne		100% O ₂			
	mol H ₂ /kg/d	std dev	mol H ₂ /kg/d	std dev	mol H ₂ /kg/d	std dev		
AN-102	4.25E-05	7.90E-06	1.89E-04	1.56E-04	1.14E-04	3.27E-05	4.4	4.03E-04
AN-106	8.48E-06	2.44E-06	1.65E-05	9.65E-06	1.71E-05	7.63E-06	1.9	1.68E-05
AN-107	2.44E-06	1.15E-06	3.52E-05	2.10E-05	3.17E-05	2.69E-05	14.4	1.65E-04
AW-101	1.88E-04	6.92E-06	1.17E-04	6.95E-05	1.88E-04	9.57E-05	0.6	6.32E-05
U-106	5.21E-05	8.09E-06	2.10E-04	1.22E-04	7.70E-05	3.24E-05	4.0	4.09E-04
AN-107 simulat	3.22E-05	--	2.02E-04	6.18E-05	1.07E-04	2.30E-05	6.3	--

(a) Stock LM and DJ Sherwood. 2003. *The Prediction of Hydrogen Formation in WTP Operations. The Applicability of the Hu Correlation.* Interim Report, Bechtel National, Inc., Richland, WA.

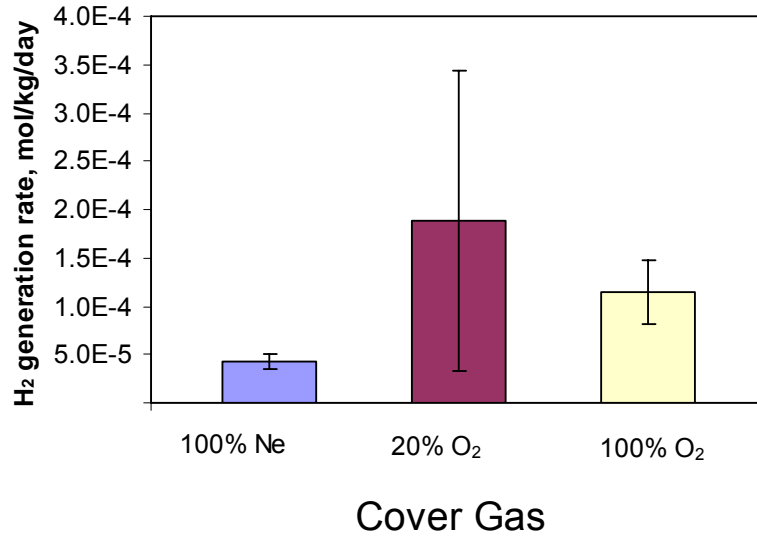


Figure 2.4. Comparison of Hydrogen Generation Rates from Hanford Waste AN-102 under Various Cover Gases at 90°C

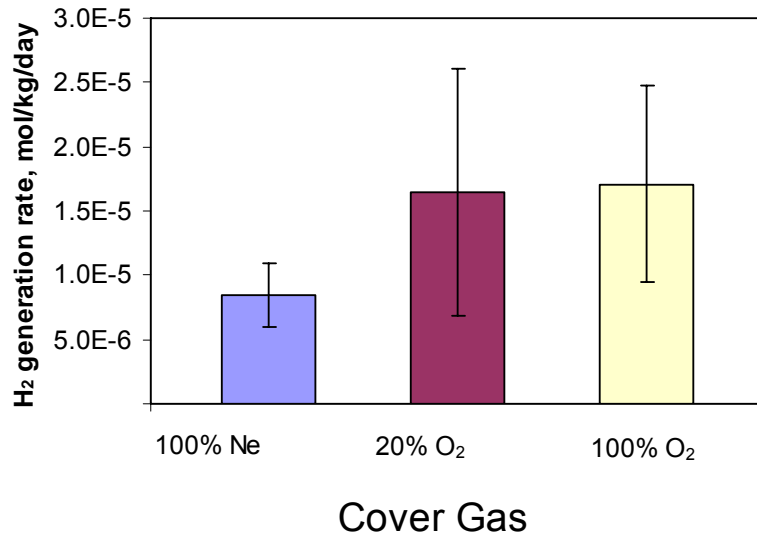


Figure 2.5. Comparison of Hydrogen Generation Rates from Hanford Waste AN-106 under Various Cover Gases at 90°C

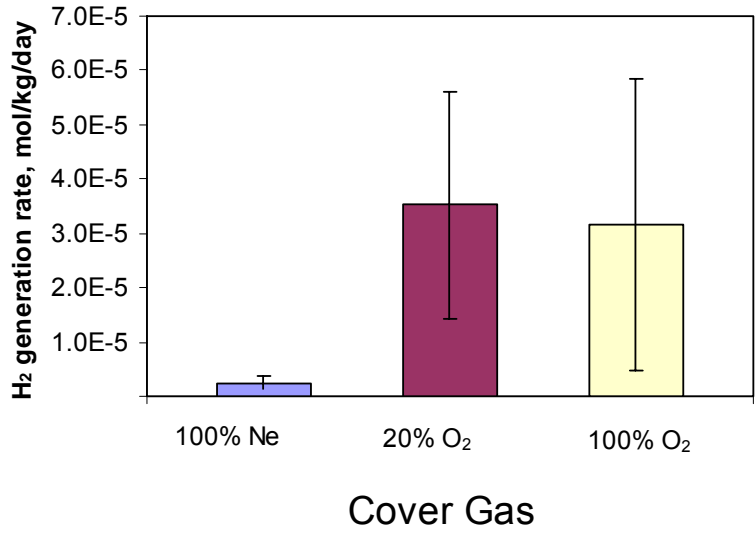


Figure 2.6. Comparison of Hydrogen Generation Rates from Hanford Waste AN-107 under Various Cover Gases at 90°C

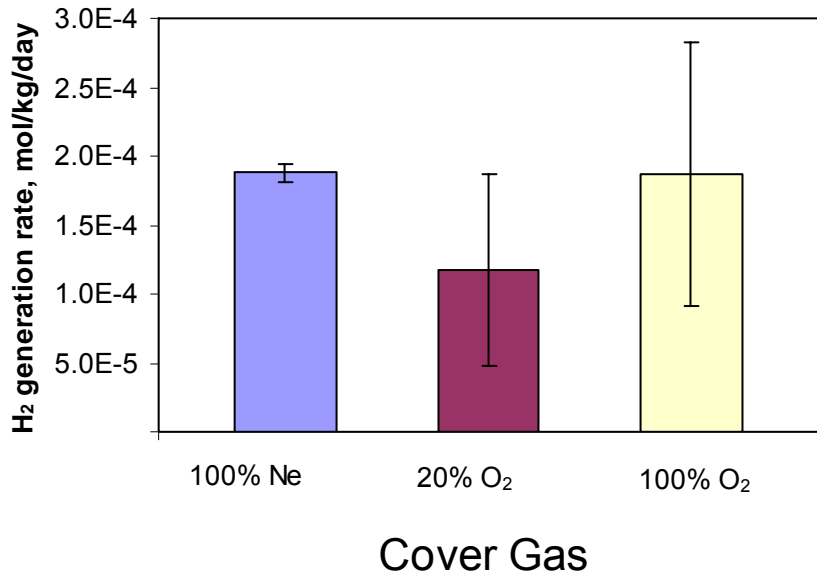


Figure 2.7. Comparison of Hydrogen Generation Rates from Hanford Waste AW-101 under Various Cover Gases at 90°C

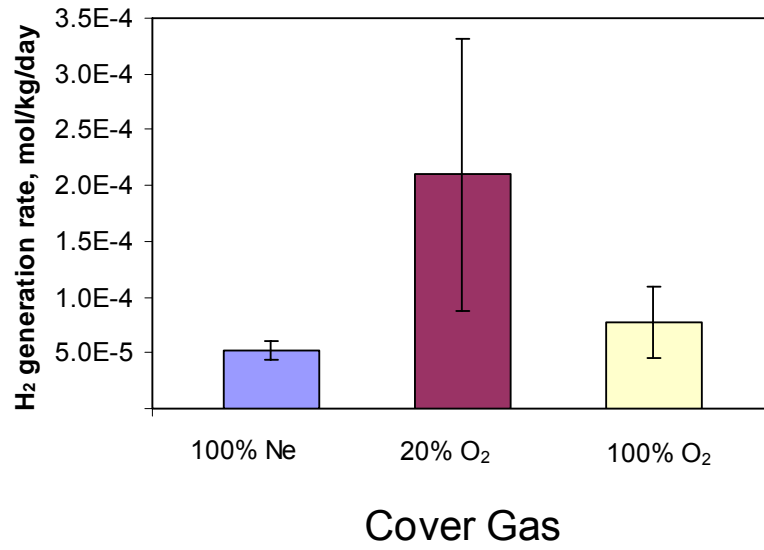


Figure 2.8. Comparison of Hydrogen Generation Rates from Hanford Waste U-106 under Various Cover Gases at 90°C

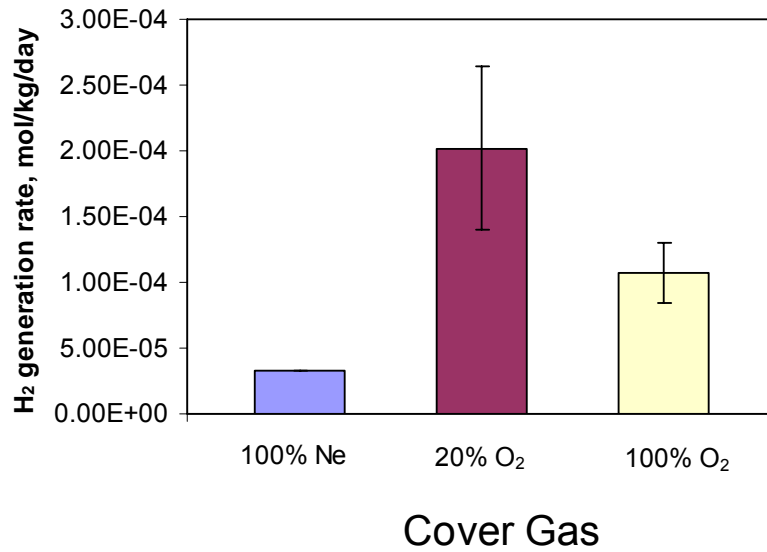


Figure 2.9. Comparison of Hydrogen Generation Rates from Simulated Hanford Waste AN-107 under Various Cover Gases at 90°C

Table 2.33. Generation Rates for All Major Gases Produced as a Function of Cover Gas. This table contains the standard deviation for generation rates determined from the averages of replicate runs.

Hanford waste type	Cover gas	H ₂		CO ₂		CH ₄		N ₂		N ₂ O		Total HC's	
		rate, mol/kg/d	std dev	rate, mol/kg/d	std dev	rate, mol/kg/d	std dev	rate, mol/kg/d	std dev	rate, mol/kg/d	std dev	rate, mol/kg/d	std dev
AN-102	100% Ne	4.25E-05	7.90E-06	4.84E-05	9.83E-06	7.49E-06	1.12E-06	2.77E-04	5.54E-05	3.26E-04	6.09E-05	8.33E-06	6.92E-08
	20% O ₂ in Ne	1.89E-04	1.56E-04	1.21E-04	1.24E-04	9.01E-06	8.48E-06	3.46E-03	1.82E-03	3.65E-03	3.25E-03	3.96E-05	1.38E-05
	100% O ₂	1.14E-04	3.27E-05	2.33E-05	--	1.52E-06	8.01E-07	3.58E-03	2.38E-03	4.14E-03	3.95E-03	4.03E-05	3.12E-05
AN-106	100% Ne	8.48E-06	2.44E-06	1.70E-05	--	3.40E-06	--	2.54E-05	7.33E-06	2.55E-05	1.93E-05	--	--
	20% O ₂ in Ne	1.65E-05	9.65E-06	3.54E-05	3.10E-05	4.45E-06	2.89E-06	1.63E-04	3.11E-04	1.55E-05	--	4.18E-06	4.69E-06
	100% O ₂	1.71E-05	7.63E-06	4.48E-05	2.49E-05	--	--	1.84E-05	8.89E-06	--	--	5.47E-06	4.63E-06
AN-107	100% Ne	2.44E-06	1.15E-06	6.27E-05	8.11E-06	2.20E-05	1.49E-05	4.84E-04	4.81E-05	7.65E-04	9.14E-05	6.51E-06	5.90E-09
	20% O ₂ in Ne	3.52E-05	2.10E-05	8.83E-05	5.13E-05	1.28E-05	9.87E-06	1.26E-02	1.10E-02	1.39E-02	1.29E-02	3.66E-05	3.62E-05
	100% O ₂	3.17E-05	2.69E-05	3.88E-05	3.70E-05	5.39E-06	3.48E-06	1.67E-03	2.79E-04	9.41E-04	4.64E-04	2.02E-05	6.86E-06
AW-101	100% Ne	1.88E-04	6.92E-06	2.67E-05	1.86E-05	4.10E-05	2.86E-06	3.94E-04	5.24E-05	5.34E-04	2.38E-04	--	--
	20% O ₂ in Ne	1.17E-04	6.95E-05	3.26E-05	3.39E-05	2.94E-05	4.70E-06	1.79E-04	2.55E-04	1.83E-05	5.69E-06	5.20E-06	9.56E-06
	100% O ₂	1.88E-04	9.57E-05	3.66E-05	1.25E-05	2.81E-05	2.53E-06	1.07E-03	1.54E-03	--	--	--	--
U-106	100% Ne	5.21E-05	8.09E-06	3.31E-05	1.03E-05	6.09E-06	1.31E-06	1.49E-04	3.28E-05	2.49E-04	3.42E-05	6.07E-06	1.14E-06
	20% O ₂ in Ne	2.10E-04	1.22E-04	9.85E-05	1.71E-05	7.03E-06	8.15E-06	5.59E-03	5.64E-03	9.50E-03	1.10E-02	6.10E-05	6.40E-05
	100% O ₂	7.70E-05	3.24E-05	7.55E-05	8.72E-05	2.25E-06	--	3.13E-03	3.59E-03	2.90E-03	4.72E-03	4.54E-05	4.45E-05

experiment in the pair would be devoid of this entrained oxygen and thus yield a more accurate representation of an inert cover gas experiment. The one exception to the second experiment in the pair yielding lower generation rates is the AW-101 waste. This waste is interesting in that it shows a trend that is opposite that of the other wastes studied; the hydrogen generation rate for this waste decreases with increased oxygen cover gas. Still, the second experiment under 100% neon was used for the AW-101 waste (17b and 18b, Table 2.30) because they too would best represent the system under an inert atmosphere.

Data from AN-107 simulated waste from Section 3 are also shown in Table 2.32 for comparison with actual waste data. The data for the simulated waste experiments and the experimental procedure are discussed in detail in Section 3, Gas Generation Measurements Using Simulated AN-107 Waste.

A comparison of the measured hydrogen generation rate under inert atmosphere and 20% oxygen atmosphere is shown graphically in Figure 2.10. This figure plots measured hydrogen rates against predicted rates for the Hanford wastes using the Hu correlation.^(a) The figure also contains measured and predicted data from other Hanford tanks for comparison. It is interesting to observe that all the waste tanks currently measured under inert atmosphere are conservatively predicted by the Hu model with one exception—AW-101. All of the waste tanks currently measured show enhancement with added oxygen atmosphere with the one exception—AW-101. Why the current Hanford wastes are over-predicted by the Hu model is not known, but there are differences in the treatment of the current samples and the wastes included in the Hu correlation database. The Hanford wastes in this current study were all subjected to moderately high thermal treatment (90°C) with no external radiolysis to ensure that the gas generation was dominated by thermolysis over all other pathways. The data in the Hu correlation database includes Hanford waste under moderately low temperatures (~30° to ~50°C) with a relatively high self-radiolysis

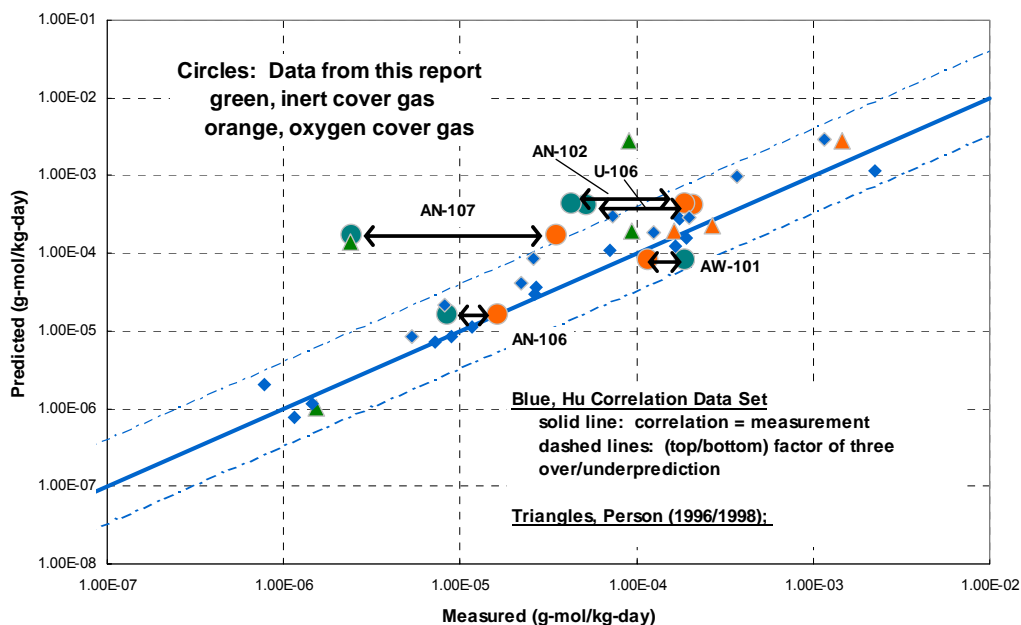


Figure 2.10. Measured Hydrogen Generation Rates Under Inert and 20% Oxygen Atmosphere

(a) Stock LM and DJ Sherwood. 2003. *The Prediction of Hydrogen Formation in WTP Operations. The Applicability of the Hu Correlation.* Interim Report, Bechtel National, Inc., Richland, WA.

source (~100 to 700 R/h). In some low dose-rate, low-TOC wastes, some of the Hu correlation hydrogen generation data were dominated by a steel corrosion term. The wastes in the current study were measured under substantially different conditions (higher temperature and lower dose rates) than those in the Hu correlation [moderately low temperatures (~30° to 50°C) and moderately high dose rates].

The arrows on Figure 2.10 indicate the amount of enhancement for the wastes in this current study (in the case of AW-101, the arrows denote a decrease) due to added oxygen atmosphere on the hydrogen generation rate compared to the inert atmosphere. Though it may be interesting to speculate on why the Hanford waste data measured in this study under inert or oxygen atmosphere are conservatively predicted by the Hu correlation, it may not be a valid question to ask, due to the nature of the differences in which the data were measured. The observation in this work that an oxygen atmosphere increases hydrogen generation in actual tank waste confirms past work by Person (1996) and Barefield and coworkers (1996).

The oxygen depletion rates for various actual and simulated Hanford wastes are shown in Table 2.34. A plot of the depletion rates as a function of TOC content is shown in Figure 2.11. The trend shown in the figure indicates that oxygen depletion depends on the amount of organic content available for reacting and thereby depleting the oxygen from the gas phase.

Table 2.34. Oxygen Depletion Rates for Actual and Simulated Wastes

Tank Type	Cover Gas, 20% O ₂ in Neon		
	O ₂ depletion, mol/kg/day	Standard dev	TOC (minus oxalate), wt%
AN-102	-1.83E-02	1.19E-02	1.99
AN-106	-4.23E-03	1.41E-03	0.02
AN-107	-2.90E-02	1.82E-02	2.86
AW-101	-3.13E-03	1.26E-03	0.14
U-106	-2.30E-02	1.58E-02	2.70
AN-107 simulant	-1.18E-02	4.44E-03	1.37
AN-107 simulant, no-organics	-1.94E-03	3.25E-04	0

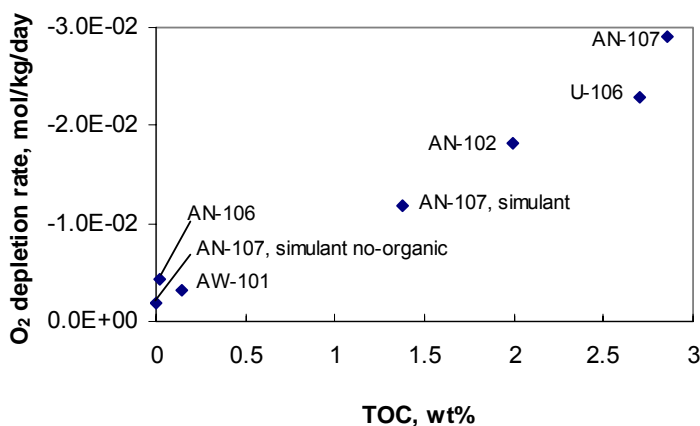


Figure 2.11. Oxygen Depletion Rates for Various Hanford and Simulated Wastes; cover gas was 20% oxygen in neon; TOC value is minus oxalate.

3.0 Gas Generation Measurements Using Simulated AN-107 Waste

The percent composition and rates for gas generation from simulated AN-107 waste under thermal conditions in the presence and absence of oxygen are described in this section. The effect of stirring the simulated AN-107 waste under an oxygen atmosphere is studied, and the gas generation results of those studies are presented. Testing a simulated waste (AN-107) allows use of a stirred reactor within an open lab setting (nonradiologically controlled environment) where the complicated stirred Parr reactor systems can be deployed in a cost-effective and timely manner to address the concerns of this task. The effect of the following on gas generation rate was investigated: 1) added organics, 2) varied pH, 3) stirring, 4) oxygen content of the cover gas, and 5) reaction temperature.

Section 3.1 contains the experimental conditions and equipment used for gas generation tests on AN-107 simulated wastes. The composition of the simulated AN-107 waste is discussed in Section 3.2; gas generation results from AN-107 simulated waste are summarized in Section 3.3.

3.1 Experimental Conditions and Equipment Used for Gas Generation Tests on AN-107 Hanford Waste Simulant

A test matrix of the planned experiments to examine the effects of stirring and not stirring on hydrogen gas generation using an organic-containing AN-107 waste simulant is given in Table 3.1. Four simulant solutions were tested: the baseline AN-107 simulant solution formulated as described in Section 3.2, the base AN-107 simulant without organics added, and two baseline AN-107 simulant solutions neutralized with nitric acid to a final pH of ~ 7.5 and ~ 4.5 . The baseline and organic-free simulants were tested under stirred and non-stirred conditions; the neutralized simulants were tested under stirred conditions. Neon was the cover gas. For experiments in an atmosphere containing 20% oxygen, a special blend of O₂ in neon was used.

3.1.1 Reaction Vessels

Reactions were carried out in two matched Parr reaction vessels. The reactors were assembled and interfaced to a dedicated computer through an analog-to-digital converter. The DAC converter was supplied by Parr, and scaled voltages were logged in real time by Parr instrument software through a National Instruments GPIB interface card. A single controller allowed adjustment and readout of temperature set points and stir rates (rpm) from one Parr reactor. The analog outputs from each controller were fed through the DAC to the computer.

The Parr reactors needed to be disassembled and new simulant added for each run. The top flange containing valving, temperature, and stirring apparatus was fixed to the reactor chamber flange with six 9/16-inch bolts in a sleeve arrangement. A Teflon gasket allowed a vacuum to be maintained between the two sides of the reactor. Prior to adding simulant, the integrity of the sealed reactor was checked on a low-pressure vacuum line. The reactor chamber was pumped down to 1×10^{-6} torr over a few hours.

Table 3.1. Summary of Tests Using Simulated AN-107 Waste

Run	AN-107 simulant conditions	Al content, mg/L	pH	TOC mg/L	TIC mg/L	Stirring	Cover gas % O ₂	Reaction temp °C	Mass of stimulant g	Density g/mL	Reaction time h	Gas pressure at termination torr	Sample ID
1	Standard	386	>14	21,300	16,800	Yes	0	90	107.8	1.437	48	769	WTP26-65-A
2	Standard	386	>14	21,300	16,800	Yes	20	60	106	1.437	60	648	WTP26-50-A
3	Standard	386	>14	21,300	16,800	Yes	20	60	106	1.437	48	600	WTP26-85-A
4	Standard	386	>14	21,300	16,800	Yes	20	90	106	1.437	43	996	WTP26-24-A
5	Standard	386	>14	21,300	16,800	Yes	20	90	106	1.437	40	618	WTP26-33-A
6	Standard	386	>14	21,300	16,800	Yes	20	120	106	1.437	59	706	WTP26-50-B
7	Standard	386	>14	21,300	16,800	Yes	20	120	106	1.437	48	646	WTP26-85-B
8	Standard	386	>14	21,300	16,800	Yes	100	90	100.7	1.437	44	96	WTP26-70-A
9	Standard	386	>14	21,300	16,800	Yes	100	90	107.8	1.437	48	56.7	WTP26-80-A
10	Standard	386	>14	21,300	16,800	No	0	90	107.7	1.437	48	762	WTP26-65-B
11	Standard	386	>14	21,300	16,800	No	20	90	106	1.437	43	1647	WTP26-24-B
12	Standard	386	>14	21,300	16,800	No	20	90	106	1.437	40	682	WTP26-33-B
13	Standard	386	>14	21,300	16,800	No	100	90	104.5	1.437	44	612	WTP26-70-B
14	pH = 4.17	306	4.17	16,870	13,300	Yes	20	90	102	1.387	93	2278	WTP26-43-A
15	pH = 4.62	309	4.62	17,080	13,500	Yes	20	90	102	1.387	45	948	WTP26-90-A
16	pH = 7.35	325	7.35	17,940	14,150	Yes	20	90	102	1.386	45	915	WTP26-90-B
17	pH = 7.55	328	7.55	18,100	14,280	Yes	20	90	102	1.386	93	2000	WTP26-43-B
18	Organic-free	386	>14	N/A	N/A	Yes	0	90	100.1	1.415	48	773	WTP26-75-A
19	Organic-free	386	>14	N/A	N/A	Yes	20	90	104	1.415	99.5	557	WTP26-39-A
20	Organic-free	386	>14	N/A	N/A	No	0	90	100	1.415	48	767	WTP26-75-B
21	Organic-free	386	>14	N/A	N/A	No	20	90	104	1.415	99.5	735	WTP26-39-B

3.1.2 Gas Volume, Temperature, and Pressure Measurements

The volumes, V_1 , V_2 , and V_3 , of the reactors shown in Figure 3.1 were measured on a calibrated vacuum line. V_1 included the volume of the reactor chamber out to the sampling port (valve) shown in Figure 3.1a. Cover gas was added to the reactor chamber through a gas inlet that contacted the solution. Gas samples were taken from the reactor through a gas outlet that was raised above the reacted solution. All pressure measurements were made on a calibrated vacuum line with volume-calibrated sampling bulbs.

The Parr reactors were equipped with a set point control and readout for temperature (Figure 3.1b). The set point control thermocouple (T_1), which was placed in the solution phase, was used to maintain a desired solution temperature. The temperature of the headspace above the solution was also monitored by a second thermocouple (T_2).

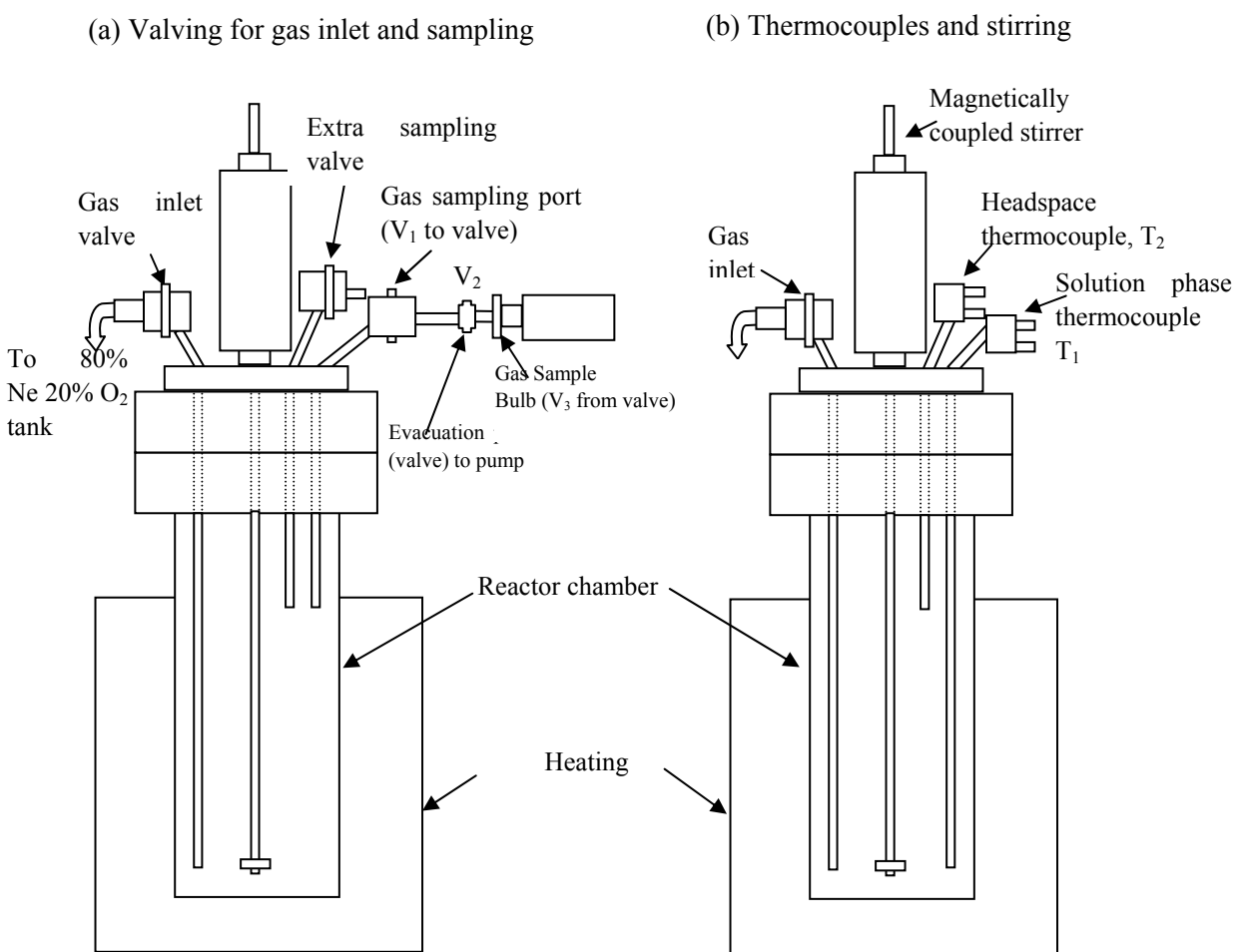


Figure 3.1. Schematic of Parr Reaction System Used for Stirred and Unstirred Simulated Waste Tests; (a) positioning of valves for volume measurements V_1 , V_2 , V_3 , gas inlet and outlet ports and magnetically coupled stirrer; gas inlet purged gas through the solution; gas sampling line 2 inches above solution level to prevent forced excursions of simulant into sampling bulb; (b) positioning of thermocouples T_1 and T_2

3.1.3 General Procedure

In every experiment, the Parr reactor chamber was charged with about 75 mL of AN-107 simulant and sealed. The chamber was evacuated by a roughing pump. The stirrer motor was turned on, and the cover gas, which was 100% neon, a mixture of 80% neon and 20% oxygen (A-L Compressed Gases), or 100% oxygen, was added to the chamber through the gas inlets to a pressure of about two atmospheres. This purge gas mixture was allowed to equilibrate while stirring for five minutes and was then evacuated from the chamber. This step was repeated at least four times. A final gas purge was allowed to equilibrate with the solution while stirring for 20 minutes and was then evacuated. An overpressure (approximately 25 psi) of the 80% neon-20% oxygen mixture was then added. The chamber was then opened to the atmosphere through a water bubbler to reduce the chamber pressure to atmospheric pressure, which was measured with a barometer. The temperature inside the reactor chamber was ramped to 90°C. The solution in the reactor chamber generally reached a steady oscillation at the set-point temperature (1°C) within one hour. The reactions were allowed to run for 1.5 to 4 days, and the reactors were then cooled to room temperature.

After the reaction mixture had cooled, the gas volume in the reactor chamber, V1, was expanded through the sampling port, V2, and into a removable sampling bulb, V3, as shown in Figure 3.1a. The valves at the sampling port and sampling bulb were closed and the sampling bulb disconnected and sent to the mass spectrometry facility for analysis. The sampling bulb was attached to an evacuated vacuum line, and the gas pressure in the bulb was measured. From the measured pressure and known volumes, the pressure in the reactor chamber at the time of termination was calculated using ideal gas law relations. The gas sampling bulb was attached to the sampling port of a Finnegan MAT-271 mass spectrometer, and the constituents of the gas-phase sample were characterized and quantified. Using the data output of the mass spectrometer analysis, which is the mole percentage of each gas component and the final pressure in the reaction vessel, the number of moles of each gas in the final reaction gas mixture was calculated using ideal gas law relations. Room temperature measured by the headspace thermocouple was used in the calculations. The partial vapor pressure was calculated as described in Norton and Pederson (1994). In each experiment, air contamination was determined based on the mole fraction of argon gas obtained by the mass spectrometry analysis; the final amount of oxygen in the reaction mixture was corrected accordingly. For determining oxygen depletion during a reaction, the moles of oxygen present at the start of the experiment were subtracted from the moles of oxygen present at the end of each experiment.

The rate of gas generation or depletion is normalized to the amount of simulant used in the experiment and was calculated using the following equation:

$$\text{Rate} = n_{\text{gas component}} / \{\text{weight simulant (kg)} \times \text{time (days)}\}$$

The standard error was normally within 20% as estimated from a combination of the duplicate measurements, volumetric error, and analytical precision. This equation for reaction rate differs from the traditional one ($\text{rate} = dC/dt$) as being normalized for the amount of simulant used in the reaction. Accordingly, the rate values obtained here cannot be used for determining the corresponding rate constant.

3.2 AN-107 Simulated Waste Composition and Preparation

Table 3.2 lists the AN-107 supernatant simulant composition that was used in the Parr reactor experiments. Two simulant solutions were prepared, one with and one without organic additives. The recipe for the AN-107 supernatant simulant and guidelines for its preparation were adopted from Eibling and Nash (2001). Table 3.3 contains the composition of AN-107 simulant based on the weighed amounts of reagents used for its preparation. The salt mixing consisted of three solutions. Solution A contained acidic compounds, including transition metal salts and organic complexing agents (Table 3.2). In Solution B, aluminate ion was generated by mixing the sodium hydroxide and the aluminum nitrate solutions; the nonreactive salts were dissolved in the resulting basic solution (see Table 3.2). Acidic solution A and basic solution B were blended to produce caustic Solution C. Residual salts, including sodium nitrate and reactive salts sodium carbonate and sodium nitrite, were added to Solution C. Water was added to adjust the final volume to 2 L. The color of the final solution was dark brown. The simulant without organics generated a heavy, dark-brown precipitate. The supernate phase was clear, colorless liquid. The simulant with organics produced a moderate amount of solids that remained dispersed in the liquid phase for about two days and then formed a light precipitate. To measure the density of the resulting simulants, the solutions were homogenized by mixing with the magnetic stirrer for 2 hours, after which aliquots were withdrawn and weighed. The density of the resulting simulants with and without organics was 1.437 ± 0.001 and 1.415 ± 0.001 g/mL, respectively, measured at 21°C.

To evaluate the effect of pH on gas generation, two additional simulant solutions containing organics were prepared. To make mildly caustic and acidic solutions, 85 and 80 mL of the simulant were mixed with 15 and 21 mL of concentrated nitric acid, respectively, using the procedure described below. The pH values of the final solutions were measured as 7.55 and 4.174, respectively. To duplicate the solutions, these procedures were repeated, and a second set of neutralized solutions with pH of 7.35 and 4.62 was prepared. The pH values of the simulant solutions were determined using a Mettler DL-21 automatic titrator equipped with a combination Ross[®] pH electrode (ATI Orion, Boston, MA). The pH electrode was calibrated with standard pH 4 and pH 10 buffer solutions. The density of the resulting simulant solution with pH of 7.550 and 4.174 was 1.386 ± 0.006 and 1.387 ± 0.007 g/mL, respectively, measured at 21°C.

The neutralization of the simulant with nitric acid may possibly chemically modify or even destroy the organic constituents present in the solution and thus alter its gas generation behavior. To evaluate whether the organic content of the simulant changes upon neutralization, two additional simulant solutions were prepared and analyzed for carbon content. One sample was purposely highly loaded with nitric acid to determine whether the formed precipitate would remove some organics from the supernate solution. The second solution was made so that it remained in the homogeneous liquid phase and contained more nitric acid than neutralized samples used in the gas generation experiment described above. Two acidic simulant solutions were prepared by neutralizing the baseline simulant containing organics with nitric acid. Two simulant aliquots, 50 mL each, were withdrawn and mixed with 14 and 28 mL of concentrated nitric acid, respectively. Mixing was done by drop-wise addition of the concentrated nitric acid to the stirred simulant solution. This procedure was conducted in the ventilated hood. Upon addition of nitric acid, the solid phase of the baseline simulant dissolved and the brown color changed to pale green. The more acidic solution produced large amount of white crystalline solid, which was separated. The baseline simulant, resulting acidic solutions, and crystalline precipitate were subjected to TOC and TIC analyses performed by the hot persulfate wet oxidation method. Results are reported in Table 3.4.

Table 3.2. Composition of Tank AN-107 Supernate Simulant

Chemical name	Chemical formula	Chemical manufacturer	Chemical Grade	Formula weight	Amount used to prepare 2 L of stimulant, g		Molar concentration		Solution
					w/o organics	with organics	w/o organics	with organics	
Acetic acid, sodium salt 99+%	CH ₃ CO ₂ Na	Aldrich	ACS reagent	82.03	N/A	2.8353	N/A	1.73E-02	A
Aluminum nitrate nonahydrate	Al(NO ₃) ₃ ·9H ₂ O	Aldrich	ACS reagent	375.14	10.734	10.7373	1.43E-02	1.43E-02	B
Ammonium molybdate	(NH ₄) ₆ Mo ₇ O ₂₄ ·4H ₂ O	Baker	Reagent	1235.954	0.1322	0.132	5.35E-05	5.34E-05	A
Ammonium nitrate	NH ₄ NO ₃	Aldrich	ACS reagent	80.04	0.1449	0.1443	9.05E-04	9.01E-04	A
Barium nitrate	Ba(NO ₃) ₂	Baker & Adamson	Reagent	261.38	0.0287	0.028	5.49E-05	5.36E-05	A
Boric acid	H ₃ BO ₃	Baker & Adamson	ACS reagent	61.84	0.4005	0.4	3.24E-03	3.23E-03	A
Cadmium nitrate	Cd(NO ₃) ₂ ·4H ₂ O	Mallinckrodt	analytical reagent	308.47	0.3538	0.3535	5.73E-04	5.73E-04	A
Calcium nitrate, tetrahydrate	Ca(NO ₃) ₂ ·4H ₂ O	Aldrich	ACS reagent	236.15	6.9648	6.9642	1.47E-02	1.47E-02	A
Cerous nitrate	Ce(NO ₃) ₃ ·6H ₂ O	MCB	--	434.25	0.328	0.3274	3.78E-04	3.77E-04	A
Cesium nitrate	CsNO ₃	Research Chem Corp.	99.9%	194.91	0.0552	0.0554	1.42E-04	1.42E-04	B
Citric acid	C ₆ H ₈ O ₇ ·H ₂ O	Aldrich	ACS reagent	192.12	N/A	18.885	N/A	4.91E-02	A
Copper (II) nitrate hemipentahydrate	Cu(NO ₃) ₂ ·2.5H ₂ O	Aldrich	ACS reagent	232.59	0.2217	0.2216	4.77E-04	4.76E-04	A
EDTA	C ₁₀ H ₁₂ N ₂ O ₈	Aldrich	ACS reagent	292.24	N/A	11.4	N/A	1.95E-02	A
Ferric nitrate	Fe(NO ₃) ₃ ·9H ₂ O	Baker	Reagent	404	24.45	24.45	3.03E-02	3.03E-02	A
Formic acid, sodium salt	HCO ₂ Na	Aldrich	ACS reagent	68.01	N/A	31.42	N/A	2.31E-01	A
HEDTA	C ₁₀ H ₁₈ N ₂ O ₇	Sigma	99+%, Lot # 18F0528	344.2	N/A	4.3333	N/A	6.29E-03	A
Iminodiacetic acid, disodium salt, hydrate	HN(CH ₂ CO ₂ Na) ₂ ·H ₂ O	Aldrich	98%	177.07	N/A	16.33	N/A	4.61E-02	A
Lanthanum nitrate	La(NO ₃) ₃ ·6H ₂ O	TRONA	Lot # LX0504	627.02	0.2845	0.2846	2.27E-04	2.27E-04	A
Lead nitrate	Pb(NO ₃) ₂	Baker & Adamson	Reagent	331.23	1.2412	1.2409	1.87E-03	1.87E-03	A
Magnesium nitrate	Mg(NO ₃) ₂ ·6H ₂ O	Baker	Reagent	256.41	0.5286	0.5276	1.03E-03	1.03E-03	A
Manganese (II) chloride	MnCl ₂	Aldrich	Reagent	125.84	2.5745	2.5738	1.02E-02	1.02E-02	A
Neodymium nitrate, anhydrous	Nd(NO ₃) ₃	Research Chem Corp.	99.9%	330.25	0.439	0.4392	6.65E-04	6.65E-04	A
Nickelous nitrate	Ni(NO ₃) ₂ ·6H ₂ O	Baker & Adamson	purified	290.82	5.2533	5.2532	9.03E-03	9.03E-03	A
Nitrilotriacetic acid	C ₆ H ₉ NO ₆	Sigma	99+%, Lot # 37F0669	191.14	N/A	1.141	N/A	2.98E-03	A

Table 3.2 (contd)

Chemical name	Chemical formula	Chemical manufacturer	Chemical grade	Formula weight	Amount used to prepare 2 L of simulant		Molar concentration		Solution
					with organics	w/o organics	with organics	w/o organics	
Potassium nitrate	KNO ₃	Mallinckrodt	analytical reagent	101.1	9.2118	9.2103	4.56E-02	4.56E-02	B
Silver nitrate	AgNO ₃	Aldrich	ACS reagent	169.88	0.0458	0.0462	1.35E-04	1.36E-04	A
Sodium carbonate	Na ₂ CO ₃	Aldrich	ACS reagent	105.99	297.5	297.48	1.40E+00	1.40E+00	C
Sodium chloride	NaCl	JT Baker	ultrapure bioreagent	58.44	3.6385	3.6394	3.11E-02	3.11E-02	B
Sodium chromate	Na ₂ CrO ₄ ·4H ₂ O	Baker & Adamson	reagent	234.06	1.096	1.096	2.34E-03	2.34E-03	B
Sodium fluoride	NaF	Aldrich	ACS reagent	41.99	0.5874	0.5918	6.99E-03	7.05E-03	B
Sodium gluconate	C ₆ H ₁₁ O ₇ Na	Sigma	99+%, Lot# 31H0575	218.1	N/A	7.8552	N/A	1.80E-02	A
Sodium glycolate	HOCH ₂ COONa	Pfalz & Bauer	99+%	98	N/A	48.61	N/A	2.48E-01	A
Sodium hydroxide	NaOH	Baker	reagent	40	50.526	50.53	6.32E-01	6.32E-01	B
Sodium nitrate	NaNO ₃	Fisher	ACS reagent	84.99	589.34	589.33	3.47E+00	3.47E+00	C
Sodium nitrite 97%	NaNO ₂	Aldrich	ACS reagent	69	182.978	182.98	1.33E+00	1.33E+00	C
Sodium oxalate	Na ₂ C ₂ O ₄	Mallinckrodt	ACS reagent	134	N/A	2.5155	N/A	9.39E-03	A
Sodium phosphate, tribasic	Na ₃ PO ₄ ·12H ₂ O	Baker & Adamson	reagent	380.16	8.8864	8.889	1.17E-02	1.17E-02	B
Sodium sulfate 98%	Na ₂ SO ₄	Aldrich	--	142.04	24.398	24.405	8.59E-02	8.59E-02	B
Strontium nitrate, anhydrous	Sr(NO ₃) ₂	Mallinckrodt	analytical reagent	211.63	0.0332	0.0329	7.84E-05	7.77E-05	A
Zinc nitrate	Zn(NO ₃) ₂ ·6H ₂ O	MCB	reagent	297.49	0.4127	0.4125	6.94E-04	6.93E-04	A
Zirconyl nitrate	ZrO(NO ₃) ₂ ·H ₂ O	Fairmont	--	249.25	0.382	0.3824	7.66E-04	7.67E-04	A

Table 3.3. Composition of AN-107 Simulant Calculated Based on Weighed Amounts of Reagents Used for Its Preparation

Component	Molar concentration, mol/L		Concentration, mg/L		mg/L, measured ^(a)
	w/o organics	with organics	w/o organics	with organics	with organics
Ag	1.35E-04	1.36E-04	15	15	--
Al	1.43E-02	1.43E-02	386	386	--
B	3.24E-03	3.23E-03	35	35	--
Ba	5.49E-05	5.36E-05	7.5	7.4	--
Ca	1.47E-02	1.47E-02	591	591	--
Ce	3.78E-04	3.77E-04	53	53	--
Cr	2.34E-03	2.34E-03	122	122	--
Cs	1.42E-04	1.42E-04	19	19	--
Cu	4.77E-04	4.76E-04	30	30	--
Fe	3.03E-02	3.03E-02	1,690	1,690	--
K	4.56E-02	4.56E-02	1,781	1,781	--
La	2.27E-04	2.27E-04	32	32	--
Mg	1.03E-03	1.03E-03	25	25	--
Mn	1.02E-02	1.02E-02	562	562	--
Mo	3.74E-04	3.74E-04	36	36	--
Na	7.08E+00	7.70E+00	162,716	177,092	--
Nd	6.65E-04	6.65E-04	96	96	--
Ni	9.03E-03	9.03E-03	530	530	--
Pb	1.87E-03	1.87E-03	388	388	--
Sr	7.84E-05	7.77E-05	6.9	6.8	--
Zn	6.94E-04	6.93E-04	45	45	--
Zr	7.66E-04	7.67E-04	70	70	--
Chloride	5.16E-02	5.16E-02	1,829	1,829	--
Carbonate	1.40E+00	1.40E+00	84,206	84,200	--
Fluoride	6.99E-03	7.05E-03	133	134	--
Hydroxide	6.32E-01	6.32E-01	10,737	10,738	--
Nitrate	3.68E+00	3.68E+00	228,145	228,140	--
Nitrite	1.33E+00	1.33E+00	60,993	60,993	--
Phosphate	1.17E-02	1.17E-02	1,110	1,111	--
Sulfate	8.59E-02	8.59E-02	8,245	8,247	--
Acetate	N/A	1.73E-02	--	--	--
Citrate	N/A	4.91E-02	--	--	--
EDTA	N/A	1.95E-02	--	--	--
Formate	N/A	2.31E-01	--	--	--
Gluconate	N/A	1.80E-02	--	--	--
Glycolate	N/A	2.48E-01	--	--	--
HEDTA	N/A	6.29E-03	--	--	--
Iminodiacetate	N/A	4.61E-02	--	--	--
Nitriloacetate	N/A	2.98E-03	--	--	--
Oxalate	N/A	9.39E-03	--	--	--
TOC, mg/L	--	--	--	19,724	21,300
TIC, mg/L	--	--	--	16,840	16,800
TC, mg/L	--	--	--	36,564	38,100

(a) Analytical measurements of baseline AN-107 simulant (Table 3.4 data) are duplicate averages.

Table 3.4. TOC/TIC Analyses Results of AN-107 Simulated Waste

RPL Number	Sample ID	TIC MDL (µgC/mL)	TIC Results (µgC/mL)	TOC MDL (µgC/mL)	TOC Results (µgC/mL)	TC Results (µgC/mL)
(a) Liquid samples						
04-00179	AN 107 baseline	27	16,300	73	20,600	36,900
04-00179 Dup	AN 107 baseline duplicate	27	17,300	73	22,000	39,300
	RPD (%)	--	6%	--	6%	6%
04-00181	AN 107 5M HNO ₃ liquid	7	150	18	13,000	13,150
04-00180	AN 107 pH 3	27	100	0	15,800	15,900
QC Sample performance						
04-00180	AN 107 pH 3 matrix spike	27	3,800	0	19,200	23,000
04-00180	Recovery	--	100%	--	86%	93%
Blank Spike/LCS 1	Recovery	--	101%	--	99%	--
(b) Solid samples						
04-00182	AN 107 5M HNO ₃ solids	28	<28	78	3,990	3,990
04-00182 Dup	AN 107 5M HNO ₃ solids	14	<14	40	3,810	3,810
	RPD (%)	--	NA	--	4%	4%
04-00182 MS	Recovery	--	97%	--	92%	95%
Blank Spike/LCS	Recovery	--	101%	--	99%	
TIC = total inorganic carbon		µgC = micrograms of carbon				
TOC = total organic carbon		TC = total carbon (sum of TIC and TOC)				
MDL = method detection limit		RPD = relative percent difference				
NA = not applicable; RPD calculated only when both sample and duplicate >5xMDL.						

3.3 Gas Generation Results from AN-107 Simulated Waste

The percent composition and generation rates for gas generation from AN-107 simulated Hanford waste under thermal conditions in the presence and absence of oxygen and under stirred and unstirred conditions are described in this section. Each vessel was loaded with the appropriate simulated waste. Gas samples were taken from the vessels at the end of the experiment.

To obtain separate rates for each gas present, gas samples were analyzed by mass spectroscopy. The mole percent composition of these gas samples is given in Table 3.5. The composition of gas formed during heating is derived from the composition of sampled gas by excluding the neon cover gas, argon, and nitrogen and oxygen from atmospheric contamination.

The gas generation rates were determined for each gas sample from the heating time, the percent composition of the gas, the total moles of gas in each system when the sample was taken, and the mass of simulated tank waste material present in each reaction vessel. Gas generation rate information is shown in Table 3.6.

Table 3.5. Gas Composition of Parr Reactor Tests Containing AN-107 Simulated Waste
(see Section 3.1 for specific experimental conditions for each run number)

Composition of Gas, mol%																			
Run	pH	% O ₂	Temp, °C	Ar	Ne	H ₂	CO ₂	CO	He	CH ₄	N ₂	O ₂	N ₂ O	NO _x	C ₂ H _x	>C ₂ HCs	Sum, %	N ₂ /Ar	sample ID
Standard AN-107 Simulant, Stirred Condition																			
1	>14	0	90	<0.001	95.2	0.06	0.037	0.012	<0.001	0.027	0.108	0.003	1.05	3.36	<0.001	<0.001	99.86	N/A	WTP26-65-A
2	>14	20	60	0.278	69.6	0.036	0.063	0.07	0.009	0.002	23.6	5.7	0.014	<0.005	<0.001	<0.001	99.09	84.9	WTP26-50-A
3	>14	20	60	0.005	98.9	0.039	0.01	0.041	0.013	<0.001	0.284	0.7	0.016	<0.005	<0.001	0.001	100.0	56.8	WTP26-85-A
4	>14	20	90	0.145	94.4	0.191	0.012	0.02	0.009	<0.001	3.08	2	0.139	<0.005	<0.001	<0.001	99.85	21.2	WTP26-24-A
5	>14	20	90	0.028	95.1	0.339	0.033	0.01	0.009	0.002	2.25	1.01	0.177	<0.005	0.003	<0.001	98.93	80.5	WTP26-33-A
6	>14	20	120	0.28	60.4	1.17	0.139	0.04	<0.001	0.002	24.4	6.2	6.2	0.56	<0.001	0.001	99.11	87.1	WTP26-50-B
7	>14	20	120	0.004	91.6	1.25	<0.005	<0.01	0.011	<0.001	0.91	0.015	5.3	0.86	<0.001	<0.001	99.95	227	WTP26-85-B
8	>14	100	90	0.008	5.1	1.62	0.141	0.22	<0.001	0.022	0.57	89.8	0.48	<0.005	0.014	0.03	98.00	71.3	WTP26-70-A
9	>14	100	90	0.055	2.16	2.55	0.2	0.46	<0.001	0.022	4.06	89.5	0.81	<0.005	0.016	0.1	99.88	73.8	WTP26-80-A
Standard AN-107 Simulant, Unstirred Condition																			
10	>14	0	90	<0.001	97.6	0.066	0.03	0.027	<0.001	0.004	0.106	0.007	1.38	0.47	<0.001	<0.001	99.69	N/A	WTP26-65-B
11	>14	20	90	0.011	86	0.203	0.024	<0.01	0.009	<0.001	0.99	12.7	0.028	<0.005	<0.001	<0.001	99.95	90	WTP26-24-B
12	>14	20	90	0.018	88.6	0.5	0.035	0.03	0.01	<0.001	1.45	8.9	0.124	<0.005	<0.001	<0.001	99.65	80.6	WTP26-33-B
13	>14	100	90	<0.001	0.79	0.286	0.054	<0.01	<0.001	<0.001	0.04	98.3	0.145	<0.005	<0.001	0.001	99.62	N/A	WTP26-70-B
Variable pH AN-107 Simulant, Stirred Condition																			
14	4.17	20	90	0.019	74.3	<0.001	13.5	<0.01	0.008	0.03	5.7	5.4	0.94	<0.005	0.021	0.107	100.01	300	WTP26-43-A
15	4.62	20	90	0.005	61.5	<0.001	26	<0.01	<0.001	0.096	4.9	0.022	2.6	4.7	0.055	0.11	99.98	980	WTP26-90-A
16	7.35	20	90	0.003	65.7	0.002	28.2	<0.01	<0.001	0.025	1.11	4.48	0.397	0.051	0.018	0.03	100.01	370	WTP26-90-B
17	7.55	20	90	0.003	85.4	0.002	6.3	<0.01	0.01	0.019	1.54	6.2	0.339	<0.005	0.013	0.057	99.88	513	WTP26-43-B
Organic free AN-107 Simulant, Stirred Condition																			
18	>14	0	90	0.003	99.7	0.002	0.056	<0.01	<0.001	<0.001	0.169	<0.001	0.012	<0.005	<0.001	<0.001	99.94	56.33	WTP26-75-A
19	>14	20	90	0.148	75.4	0.018	<0.005	<0.01	0.01	0.001	12.6	9.9	0.034	<0.005	0.003	<0.001	97.97	85.14	WTP26-39-A
Organic free AN-107 Simulant, Unstirred Condition																			
20	>14	0	90	0.001	99.7	0.003	0.04	<0.01	<0.001	<0.001	0.092	0.037	0.023	<0.005	<0.001	<0.001	99.90	92	WTP26-75-B
21	>14	20	90	0.009	83.7	0.038	0.011	0.02	0.01	<0.001	0.628	13.8	0.013	<0.005	0.004	<0.001	98.22	69.78	WTP26-39-B

Table 3.6. Gas Generation Rates for Parr Reactor Tests Using AN-107 Simulated Waste (see Section 3.1 for specific experimental conditions for each run number; blank cells indicate the analyte was below the detection limit)

Run	pH	% O ₂	Temp, °C	Component Rate, mol/kg/day										Sample ID
				H ₂	CO ₂	CO	CH ₄	N ₂	O ₂	N ₂ O	NO _x	C ₂ H _x	>C ₂ HCs	
Standard AN-107 Simulant, Stirred Condition														
1	>14	0	90	3.22E-05	1.98E-05	6.44E-06	1.45E-05	--	-1.61E-06	5.63E-04	1.80E-03	--	--	WTP26-65-A
2	>14	20	60	1.22E-05	2.13E-05	2.37E-05	6.76E-07	--	(a)	4.73E-06	--	--	--	WTP26-50-A
3	>14	20	60	1.62E-05	4.16E-06	1.71E-05	--	--	-1.00E-02	6.66E-06	--	--	4.16E-07	WTP26-85-A
4	>14	20	90	1.37E-04	8.63E-06	1.44E-05	--	--	-1.79E-02	1.00E-04	--	--	--	WTP26-24-A
5	>14	20	90	1.63E-04	1.59E-05	4.81E-06	9.62E-07	--	-1.13E-02	8.51E-05	--	1.44E-06	--	WTP26-33-A
6	>14	20	120	4.02E-04	4.78E-05	--	6.87E-07	--	(a)	2.13E-03	1.92E-04	--	3.44E-07	WTP26-50-B
7	>14	20	120	5.61E-04	--	4.93E-06	--	--	(b)	2.83E-03	3.86E-04	--	--	WTP26-85-B
8	>14	100	90	1.11E-04	9.62E-06	1.50E-05	1.50E-06	--	-4.95E-02	3.27E-05	--	9.55E-07	2.05E-06	WTP26-70-A
9	>14	100	90	8.17E-05	6.41E-06	1.47E-05	7.05E-07	--	-4.37E-02	2.60E-05	--	5.13E-07	3.20E-06	WTP26-80-A
Standard AN-107 Simulant, Unstirred Condition														
10	>14	0	90	3.22E-05	1.46E-05	--	1.95E-06	--	-3.41E-06	6.72E-04	2.29E-04	--	--	WTP26-65-B
11	>14	20	90	2.42E-04	2.86E-05	--	--	--	-1.08E-02	3.34E-05	--	--	--	WTP26-24-B
12	>14	20	90	2.66E-04	1.86E-05	--	--	--	-7.25E-03	6.59E-05	--	--	--	WTP26-33-B
13	>14	100	90	1.27E-04	2.39E-05	--	--	1.77E-05	-9.32E-03	6.42E-05	--	--	4.43E-07	WTP26-70-B
Variable pH AN-107 Simulant, Stirred Condition, 90°C														
14	4.17	20	90	--	1.08E-02	--	2.39E-05	3.28E-03	-1.08E-02	7.49E-04	--	1.67E-05	8.53E-05	WTP26-43-A
15	4.62	20	90	--	1.83E-02	--	6.74E-05	3.15E-03	(b)	1.83E-03	3.30E-03	3.86E-05	7.72E-05	WTP26-90-A
16	7.35	20	90	6.56E-07	9.25E-03	--	8.20E-06	2.82E-04	-3.94E-03	1.30E-04	--	--	--	WTP26-90-B
17	7.55	20	90	1.60E-06	5.02E-03	--	1.52E-05	9.02E-04	-1.21E-02	2.70E-04	--	1.04E-05	4.55E-05	WTP26-43-B
Organic free AN-107 Simulant, Stirred Condition														
18	>14	0	90	2.16E-06	6.03E-05	--	--	--	--	1.29E-05	--	--	--	WTP26-75-A
19	>14	20	90	3.18E-06	--	--	1.77E-07	--	-2.17E-03	6.01E-06	--	--	--	WTP26-39-A
Organic free AN-107 Simulant, Unstirred Condition														
20	>14	0	90	1.60E-06	2.14E-05	--	--	--	--	1.23E-05	--	--	--	WTP26-75-B
21	>14	20	90	8.89E-06	2.57E-06	4.68E-06	--	--	-1.71E-03	3.04E-06	--	9.35E-07	--	WTP26-39-B
(a) The number cannot be determined due to amount of air contamination.														
(b) All oxygen was consumed before the reaction terminated.														

3.3.1 General Observations

Experimental conditions for the gas generation tests with AN-107 simulant solutions are shown in Table 3.1. Final gas pressure in the reaction vessels at the time the reaction was terminated was calculated based on the measured pressure in the mass spectrometer sampling bulb and the known total volume of the reaction and sampling systems. The final gas pressure for experiments 4 and 11 was overestimated because of large uncertainty in the total volume of the system for these particular experiments. Both experiments were duplicated (runs 5 and 12) and comparable results obtained. The initial gas pressure in each reaction vessel was equal to atmospheric pressure and measured prior to the start of each run. Accordingly, gas pressure at termination below the atmospheric pressure indicates that the consumption of the cover gas was greater than gas generation during the reaction. Gas pressure at termination well above the atmospheric pressure suggests the opposite. It can be seen that the final gas pressure for the experiments conducted using oxygen-free cover gas (runs 1, 10, 18, and 20) and organic-free simulant (runs 18-21) is very close to atmospheric pressure presumably due to low chemical activity in those systems. Final gas pressure in the experiments using the standard simulant composition and cover gas containing 20% oxygen (runs 5-7 and 13) is slightly below atmospheric pressure. Very low gas pressure at termination was observed for the standard simulant under stirring conditions and 100% oxygen cover gas (runs 8 and 9), indicating that most of the oxygen was chemically consumed during the reaction. The final gas pressure in the nonstirred sample under the same conditions of 100% oxygen (run 13) was only slightly lower than atmospheric pressure, suggesting a much smaller extent of chemical activity. The neutralized simulant (runs 14-17) demonstrated final gas pressure much higher than atmospheric pressure, which consistently increased with reaction time.

Results of the mass spectrometry analyses for each sample are given in Table 3.5. Argon gas can be introduced in the sample by two pathways, by the residual air dissolved in the simulant and not fully removed prior the reaction or by air contamination during sampling for the mass spectrometry analysis. The systems were sparged with cover gas prior to the start of each experiment. High argon content indicates appreciable air contamination and was found in samples 2, 4, 6, and 19. The hydrogen generation determined for the experiments performed in duplicate (runs 2 and 3, 4 and 5, 6 and 7, 8 and 9, 11 and 12, Tables 3.5 and 3.6) are reproducible and in excellent agreement.

3.3.2 Effect of Organics

Hydrogen generation was lower for the organic-free simulant than for the standard simulant composition under the same conditions (runs 18 and 1, 19 and 4 /5, 20 and 10, 21 and 11/12, respectively). This result is expected because oxidative decomposition of the organic material in the simulant is the primary process producing hydrogen. The same trend is observed for N_2O gas, which is also presumably produced during the breakdown of the organic material. The release of CO_2 was comparable for the organic-free and standard simulant compositions. Production of other gases was negligible for the organic-free simulant. The general conclusion that organic-free simulant is chemically inert is supported by the low rates of oxygen depletion observed for runs 19 and 21 compared with corresponding runs 4/5 and 11/12 using the standard simulant.

3.3.3 Effect of Stirring

The effect of stirring on gas generation from the standard simulant at 90°C was studied using cover gas containing 0, 20, or 100% oxygen (stirred runs 1, 4/5, and 8/9; nonstirred runs 10–13). Results are shown in Figure 3.2. Product gas of similar composition was observed for both samples with neon (runs 1 and 10). This result can be explained by the effect of elevated temperature and internal sample composition on gas generation; the oxygen-free cover gas does not participate in the reaction and ensures its insensitivity to the stirring. Surprisingly, the hydrogen generation rates determined using the nonstirred simulant and 20% oxygen cover gas was slightly higher than that obtained using stirred simulant (runs 4/5 and 11/12). The corresponding rates of oxygen depletion were similar. For the 100% oxygen cover gas, stirred and nonstirred samples generated hydrogen at similar rates; depletion of oxygen was slightly faster for the stirred simulant (runs 8/9 and 13). Stirring had no effect on the organic-free simulant using 100% neon or 20% oxygen cover gas (runs 18-21).

The effect of stirring is complex because it affects several things, including oxygen diffusion in the simulant, the interfacial area between simulant and cover gas, and the state of the simulant itself. Overall, based on the results obtained with the AN-107 simulant, definitive conclusions on the effects of stirring on gas generation cannot be drawn.

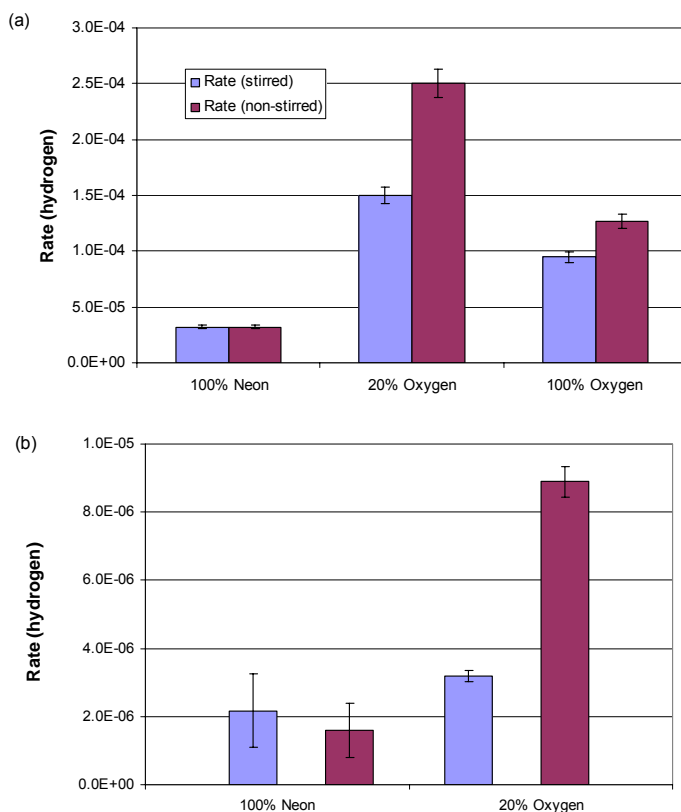


Figure 3.2. Effect of Stirring on Hydrogen Generation; (a) standard (b) organic-free AN-107 Simulants; n = moles of H₂ produced; duplicate data are averaged; hydrogen rate is in mol H₂/kg/day

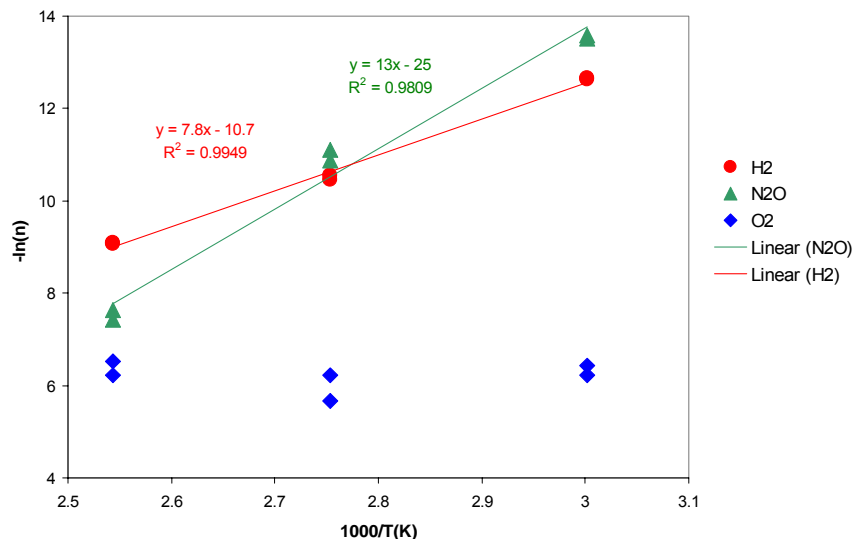


Figure 3.3. Effect of Temperature on H₂ and N₂O Generation and O₂ Depletion for Standard Stirred AN-107 simulant; n = moles of gas in product. Duplicate data are averaged.

3.3.4 Effect of Oxygen

The composition of the gas generated in the tests performed under the cover gas without oxygen (runs 1 and 10) provides information on the thermal decomposition of the simulant. Very similar results were obtained for the stirred (run 1) and nonstirred (run 10) standard simulant. For both experiments, the effect of residual oxygen can be excluded because no air contamination was found by mass spectrometer analyses (argon content was below the detection limit). Hydrogen generation in this case can be attributed to the oxidative decomposition of organic constituents by the nitrite anion at elevated temperature, which is consistent with the high content of N₂O and other nitrogen oxides in the product gas. The nitrogen oxides can be formed by the partial reduction of the nitrite as well as decomposition of the nitrogen-containing organic material (Barefield et al 1996; Pederson and Bryan 1996). Under the same conditions, the mol% of H₂ and N₂O in the gas product of the organic-free simulant (runs 18 and 20, with and without stirring, respectively) was significantly lower, and hydrogen concentration was comparable with the detection limit of the mass spectrometer analysis for hydrogen.

Comparison of the hydrogen content in the product gas of the stirred standard simulant tested using cover gas containing 20 and 100% oxygen (runs 4/5 and 8/9, Table 3.5) reveals that the mol% hydrogen was almost an order of magnitude greater for the 100% oxygen cover gas. The same trend was observed for CO₂, CO, and N₂O product gas constituents. The absolute amount of the product gas was, however, much smaller, which translated into slower component generation rates using 100% oxygen than with 20% oxygen cover gas (Table 3.6). The small amounts of product gas can be explained only speculatively by the nearly complete consumption of oxygen likely in the early stages of the reaction well before it was terminated, which is supported by the abnormally low final gas pressure in the duplicate samples (Table 3.4), and the highest observed rate of oxygen consumption (Table 3.6). Accordingly, it is possible that for the standard stirred simulant tested using 100% oxygen cover gas, the calculated rates of gas component generation are underestimated. Examination of the composition of the product gas suggests that oxygen accelerates formation of hydrogen and hydrocarbons. High concentration of carbon

monoxide (CO) can be attributed to the incomplete oxidation of the organic material due to the insufficient amount of oxygen in the closed reaction system. In this case, CO is an intermediate product of the oxidation reaction.

Drastically different results were obtained using the non-stirred standard simulant and 100% oxygen cover gas (run 13). Only little amount of oxygen was consumed during the reaction, and generation of H₂, CO₂, and N₂O was comparable with that of observed using 20% oxygen cover gas under the same conditions (runs 11/12, Tables 3.5 and 3.6).

3.3.5 Effect of Temperature

The effect of temperature on gas generation using the stirred standard simulant and the cover gas containing 20% oxygen was studied at 60°, 90°, and 120°C (runs 2-7). As the reaction temperature increases, mol% and the rates of H₂ and N₂O generation enhance significantly (Tables 3.5 and 3.6). It was also observed that at 120°C all oxygen was consumed during the reaction. Linear Arrhenius plots were obtained for the H₂ and N₂O produced during the reactions as a function of the inverse temperature, as shown in Figure 3.3. Surprisingly, the analogous plot for the oxygen depletion indicated no dependence on the reaction temperature.

3.3.6 Effect of pH

Neutralization with nitric acid modifies the chemical composition of the simulant. During preparation of neutralized simulants, adding concentrated nitric acid to the AN 107 simulant released a significant volume of product gases. To evaluate whether the organic components of the simulant were oxidized and decomposed by the nitric acid, simulant neutralized to a pH of 3 and <1 was subjected to total carbon analysis. It was found that reduction in TOC in the neutralized simulant (Table 3.4) corresponded to applied dilution factors of 1.3 and 1.56 for simulant samples with a pH of 3 and <1, respectively. It was thus concluded that organic material in the simulant did not undergo complete decomposition, which would lead to a TOC reduction due to release of the gaseous H₂ and CO₂ products. Formation of oxalate is possible because some amount of TOC existed in the precipitate formed during simulant neutralization (Table 3.4). In contrast, TIC of the neutralized simulant was significantly reduced due to removal of the carbonate in CO₂ form.

Neutralized simulants at pH of 4.17, 4.62, 7.35, and 7.55 were tested using 20% oxygen cover gas at 90°C (runs 14-17). Examination of the composition of the gas product given in Table 3.5 suggests the occurrence of the different chemical reactions than using the standard simulant. Hydrogen formation was greatly suppressed, so hydrogen content in the product gas was near or below the detection limit of the analytical method applied. CO₂, CH₄, and other hydrocarbons were found in the product gas at relatively high concentrations. Large amounts of N₂ gas formed during the reaction, evidenced by a significantly larger N₂/Ar ratio than is found in air (84) and higher than that observed in the tests using standard and organic-free simulants. Concentration of N₂O was also high in the product gas. These results point out that oxygen and nitrate extensively react with the organic materials at low pH. Absence of hydrogen in the product gas indicates different mechanism of the oxidation reactions than for the standard high-pH simulant.

4.0 Summary and Conclusions

The WTP flow sheet analysis (Sherwood and Stock 2003) indicated that pulse jet mixing could introduce oxygen into the waste. The Hu correlation (Hu 2002) is designed for predicting hydrogen generation in quiescent anaerobic wastes. Laboratory work was undertaken to determine the influence of oxygen on the hydrogen generation rates in actual wastes because Person (1996, 1998) had shown that the hydrogen generation rates for waste from Tank 241-SY-101 at temperatures over 70°C increased by more than an order of magnitude when exposed to oxygen. While not definitive, other work with wastes and waste simulants also suggests that exposing waste to oxygen could increase hydrogen production.

WTP Project personnel and PNWD selected five Hanford waste tank materials for investigation. Three samples (AN-107, U-106, and AN-102) were selected because of their high TOC content. These wastes also had varying amounts of aluminum, a catalyst for the thermal generation of hydrogen. Another sample (AW-101) was selected because previous study suggested that it might be more reactive than predicted by the Hu correlation. The tests were carried out at 90°C because the hydrogen formation rates would be bounding and the product distributions would provide information about the propensity for methane and C₂ hydrocarbons.

The tests were carried out and discussed in this report. The generation rates of hydrogen and other gases from tank wastes were measured under an inert atmosphere and in the presence of 20% and 100% oxygen. The results were very reproducible, and there were no significant differences in the rates in the two oxygen-containing atmospheres. The following table summarizes these findings.

Table 4.1. Generation Rates for All Major Gases as a Function of Cover Gas

Hanford waste type	Cover gas	H ₂		CO ₂		CH ₄		N ₂		N ₂ O		Total HCs	
		rate, mol/kg/d	std dev	rate, mol/kg/d	std dev	rate, mol/kg/d	std dev	rate, mol/kg/d	std dev	rate, mol/kg/d	std dev	rate, mol/kg/d	std dev
AN-102	100% Ne	4.25E-05	7.90E-06	4.84E-05	9.83E-06	7.49E-06	1.12E-06	2.77E-04	5.54E-05	3.26E-04	6.09E-05	8.33E-06	6.92E-08
	20% O ₂ in Ne	1.89E-04	1.56E-04	1.21E-04	1.24E-04	9.01E-06	8.48E-06	3.46E-03	1.82E-03	3.65E-03	3.25E-03	3.96E-05	1.38E-05
	100% O ₂	1.14E-04	3.27E-05	2.33E-05	--	1.52E-06	8.01E-07	3.58E-03	2.38E-03	4.14E-03	3.95E-03	4.03E-05	3.12E-05
AN-106	100% Ne	8.48E-06	2.44E-06	1.70E-05	--	3.40E-06	--	2.54E-05	7.33E-06	2.55E-05	1.93E-05	--	--
	20% O ₂ in Ne	1.65E-05	9.65E-06	3.54E-05	3.10E-05	4.45E-06	2.89E-06	1.63E-04	3.11E-04	1.55E-05	--	4.18E-06	4.69E-06
	100% O ₂	1.71E-05	7.63E-06	4.48E-05	2.49E-05	--	--	1.84E-05	8.89E-06	--	--	5.47E-06	4.63E-06
AN-107	100% Ne	2.44E-06	1.15E-06	6.27E-05	8.11E-06	2.20E-05	1.49E-05	4.84E-04	4.81E-05	7.65E-04	9.14E-05	6.51E-06	5.90E-09
	20% O ₂ in Ne	3.52E-05	2.10E-05	8.83E-05	5.13E-05	1.28E-05	9.87E-06	1.26E-02	1.10E-02	1.39E-02	1.29E-02	3.66E-05	3.62E-05
	100% O ₂	3.17E-05	2.69E-05	3.88E-05	3.70E-05	5.39E-06	3.48E-06	1.67E-03	2.79E-04	9.41E-04	4.64E-04	2.02E-05	6.86E-06
AW-101	100% Ne	1.88E-04	6.92E-06	2.67E-05	1.86E-05	4.10E-05	2.86E-06	3.94E-04	5.24E-05	5.34E-04	2.38E-04	--	--
	20% O ₂ in Ne	1.17E-04	6.95E-05	3.26E-05	3.39E-05	2.94E-05	4.70E-06	1.79E-04	2.55E-04	1.83E-05	5.69E-06	5.20E-06	9.56E-06
	100% O ₂	1.88E-04	9.57E-05	3.66E-05	1.25E-05	2.81E-05	2.53E-06	1.07E-03	1.54E-03	--	--	--	--
U-106	100% Ne	5.21E-05	8.09E-06	3.31E-05	1.03E-05	6.09E-06	1.31E-06	1.49E-04	3.28E-05	2.49E-04	3.42E-05	6.07E-06	1.14E-06
	20% O ₂ in Ne	2.10E-04	1.22E-04	9.85E-05	1.71E-05	7.03E-06	8.15E-06	5.59E-03	5.64E-03	9.50E-03	1.10E-02	6.10E-05	6.40E-05
	100% O ₂	7.70E-05	3.24E-05	7.55E-05	8.72E-05	2.25E-06	--	3.13E-03	3.59E-03	2.90E-03	4.72E-03	4.54E-05	4.45E-05

The results show that oxygen increases the rates of hydrogen generation for the wastes that have 1.5 to 3% TOC (by factors ranging from 4.0 to 14.4 for high TOC wastes) but does not appreciably alter the rates of hydrogen generation in wastes with low TOC content (factors range from 0.6 to 1.9 for low TOC wastes). These observations are consistent with previous observations by Person (1996, 1998). He found that oxygen accelerated hydrogen generation in Tank SY-101 waste with 3.5% TOC by a factor of more than 10, whereas there was little effect on the hydrogen generation rate for the waste from Tank AN-105 waste with 0.3% TOC. The results also are compatible with previous investigations with waste simulants (Barefield et al. 1996).

The experiments performed using actual waste with moderate to high TOC values indicate that hydrogen generation rates are higher in tank wastes exposed to air (20% oxygen atmosphere) or 100% oxygen atmosphere than in wastes under inert cover gas. The Hu model appears to predict the hydrogen generation rates of these wastes in the presence of oxygen within its prescribed accuracy (Table 2.32 and Figure 2.10). However, it significantly overestimates the hydrogen generation rates from these wastes in the absence of oxygen. This result is incongruous and cause for concern that the agreement may be fortuitous. We suspect the model is obtaining the right answers here for the wrong reasons. Therefore, caution should be exercised in using it to predict hydrogen generation rates in aerated wastes.

A better understanding of the oxygen contribution to gas generation from thermally activated reactions is needed to adapt the Hu model to properly predict its effects on hydrogen generation rates. Using the current Hu model to predict hydrogen generation rates of Hanford wastes under an oxygen atmosphere is, in effect, extrapolating outside the dataset used for the Hu correlation. The effect of oxygen is significant. Oxygen probably is involved in the oxidation of organics (Sherwood and Stock 2003). It scavenges the nitroxyl radical (NO^\cdot) implicated in the generation of nitrogenous gases (Barefield et al 1996; Pederson and Bryan 1996). Whether the aluminate-catalyzed oxidation of organics is relevant when oxygen is present is not known. If the pathway is not competitive, including a parameter for soluble aluminum is not justified. Transition metals, such as chromium, may instead be catalysts when oxygen is present. No studies have been performed of the combined effects of oxygen and transition metals on thermal generation of hydrogen. It should be studied.

This work and previous work demonstrates that the amount of TOC plays a substantial role in hydrogen gas generation, and this work confirms that the amount of TOC directly influences the oxygen depletion rate. However, it would be important to investigate not just the amount of TOC but also the type of TOC contributing to the oxygen consumption/hydrogen enhancement reactions. In the absence of oxygen, the aluminate-catalyzed reaction is selective for compounds such as glycolate, HEDTA, and iminodiacetate and generally complexants with primary or secondary alcohol or amino functional groups. Reactions occurring in presence of oxygen probably will have different selectivities. It should be investigated.

In the presence of oxygen, hydrogen gas is generated at a greater rate, and the N_2/H_2 and $\text{N}_2\text{O}/\text{H}_2$ ratios are much greater than those observed in the absence of oxygen. The relative rate difference between hydrogen and the nitrogenous gas generation is evidence that different mechanisms for gas generation are involved in the presence and absence of oxygen.^(a) The data obtained within this current work under oxygen atmosphere agree with the Hu correlation, but the agreement may be coincidental.

(a) Stock LM and DJ Sherwood. 2003. *The Prediction of Hydrogen Formation in WTP Operations. The Applicability of the Hu Correlation*. Interim Report, Bechtel National, Inc., Richland, WA.

Certainly more experiments are needed to understand the dependence on oxygen, hydroxide, temperature, dose rate, aluminum and/or other catalysts, and type of TOC. Essentially all parameters in the model should be evaluated for statistical significance.

The results for the other flammable gases, methane and the C₂ hydrocarbons (ethane, ethylene, acetylene), show that oxygen has little influence on the methane formation rate. However, oxygen increases the formation rate of C₂ hydrocarbons substantially.

The fact that the C₂ compounds are not formed from simulants that contain complexants (HEDTA, EDTA) and their remnants (NTA, IDA acetate ion, formate ion) under the same reaction conditions implies that the C₂ compounds are produced from other organic compounds in the waste. It is well established that the Hanford wastes contain phosphate esters, hydrocarbons, and their hydrolyzed and oxidized derivatives. These substances are much more plausible precursors of the observed C₂ hydrocarbons than the complexants with CH₂CO₂⁻ fragments or formate ion.

The effect of stirring using simulated wastes under an oxygen atmosphere was studied. The effect of stirring is complex in that it affects several things, including oxygen diffusion in the simulant, the interfacial area between simulant and cover gas, and the state of the simulant itself. Overall, based on the results obtained with the AN-107 simulant, the definitive conclusions on the effects of stirring on gas generation cannot be drawn.

Additional objectives of this work were to document the effects of various parameters on the hydrogen generation rates from Hanford tank wastes. To address the various parameters, six TIRs were written discussing the following topics:

- Modeling Hydrogen Generation Rates in Wastes with Alpha Radiation
- The Influence of Beta and Gamma Radiation on the Rate of Hydrogen Generation
- The Influence of Oxygen on Hydrogen Generation Rates
- The Influence of Hydroxide Ion on the Rate of Hydrogen Generation
- Effect of Permanganate Addition on Predicting Hydrogen Generation Rates
- Effect of Glass Forming Chemicals on Hydrogen Generation Rates.

These TIRs (included as Appendixes A through F) detail the effects of the various constituents on hydrogen gas generation. The conclusions from these TIRs follow.

Modeling Hydrogen Generation Rates in Wastes with Alpha Radiation

The Hu correlation (Hu 2002) developed for predicting hydrogen generation rates in tank wastes at the Hanford Site (Hu 2002) does not consider the influence of alpha radiation. The concentrations of these emitters are much less than those of the beta and gamma emitters in tank waste and the alpha emitters are concentrated in sludge, where the particles have very short ranges. The flow sheet analysis indicated that the situation in the WTP differs because the alpha emitters will be concentrated and suspended in preparation for HLW vitrification. Therefore, it is not evident that their role in hydrogen generation can be neglected.

The literature on generation of hydrogen by alpha radiolysis was reviewed. No publications were found about the alpha radiolysis of alkaline solutions of Hanford waste. However, alpha radiolysis of nitric acid solutions and alpha radiolysis of neutral solutions of scavengers were very relevant. Several

authors had measured the value of $G(\text{H}_2)$ for the alpha radiolysis of nitric acid (Savel'ev et al. 1966; Bibler 1974; Smith 1994). More recently, LaVerne and coworkers at Notre Dame Radiation Laboratory reinvestigated hydrogen generation by alpha radiolysis of water containing a variety of inhibitors including nitrate and nitrite ions (Pastina and LaVerne 1999; LaVerne and Pimblott 2000). They advanced a new mechanism for generation of hydrogen. With the understanding provided by their work, we adapted the Hu model to account for effects of alpha radiolysis in wastes (see Appendix A).

The Influence of Beta and Gamma Radiation on the Rate of Hydrogen Generation

Nitrate and nitrite ions inhibit the radiolytic generation of hydrogen from water. The Hu model includes a term to account for this effect on the yield of hydrogen from beta/gamma radiation in the wastes. However, review and analysis of recent literature shows that the Hu model underpredicts $G(\text{H}_2)$ from water radiolysis. In particular, recent work for the WTP project had measured hydrogen formation from washed solids from Tank AN-102 (Bryan et al. 2002) and washed wastes that have also been treated to remove radioactivity by the strontium carbonate-sodium permanganate operation (Bryan et al. 2003). The hydrogen generation rates of these treated wastes are larger than would be predicted by the Hu model. Being relatively low in soluble TOC, the hydrogen generated by such treated wastes is mainly from water radiolysis. Accordingly, the Hu model for water radiolysis may not be bounding for treated wastes. Therefore, it is not suitable for some of the process streams in the WTP.

As noted above, LaVerne and coworkers at Notre Dame Radiation Laboratory had reinvestigated hydrogen generation by radiolysis of water and advanced a new mechanism for generation of hydrogen (Pastina and LaVerne 1999; LaVerne and Pimblott 2000). In Appendix B, we review their work and apply it to develop a correlation for predicting hydrogen generation rates from beta/gamma radiolysis in WTP process streams. Based on the analysis presented in Appendix B, a new equation is recommended for WTP design calculations specifically concerned with the high-level waste streams that have been treated with permanganate (to precipitate radioactive strontium and TRUs) and/or washed to remove low activity waste components. This equation

$$G_{(\text{H}_2)}^{\beta/\gamma} = 0.34 \frac{1}{1 + 2.4[\text{NO}_3^-] + 0.62[\text{NO}_2^-]} + 0.11 \frac{1}{1 + 120[\text{NO}_3^-] + 43[\text{NO}_2^-]}$$

defines the radiolytic yield of hydrogen in molecules/100 eV absorbed of beta/gamma radiation from an aqueous solution containing nitrate and/or nitrite ion.

The Influence of Oxygen on Hydrogen Generation Rates

The Hu correlation (Hu 2002) was devised for quiescent wastes that are not mixed with air during interim storage. In contrast, operations at the WTP will be aerated by pulse jet mixing. Thus, oxygen will be introduced into the wastes. Previous work with wastes and waste simulants has shown that oxygen may increase hydrogen generation rates in some cases by an order of magnitude. The mechanism of the effect is not well understood, but it appears to alter and enhance thermal degradation pathways that produce hydrogen. Because the Hu model was parameterized to predict hydrogen generation rates from stored tank wastes that are depleted in oxygen, it was decided to perform experimental tests with some representative Hanford tank wastes exposed to oxygen cover gas to quantify the impact of oxygen on hydrogen production in these wastes.

The Influence of Hydroxide Ion on the Rate of Hydrogen Generation

Hydroxide ion plays an important role in the chemistry associated with hydrogen generation in Hanford waste. Because of this and the fact that the ultrafiltration process (UFP) will involve adding large quantities of sodium hydroxide, concerns were raised about applying the Hu model to the WTP. A review of the relevant literature suggests that even though the concentration of hydroxide is not a key parameter in Hu's model, large additions are not likely to invalidate use of the model at the WTP. In developing the correlation, Hu used data from 15 Hanford tanks in which hydroxide concentrations were in excess of 3 M, and the supporting laboratory experiments involved concentrations up to 6 M. Without a concurrent effect of oxygen, varying the hydroxide concentration should not impact the ability of the Hu correlation to provide hydrogen generation rates to within its stated accuracy ($\pm 300\%$).

Effect of Permanganate Addition on Predicting Hydrogen Generation Rates

A UFP in the WTP will add sodium permanganate to precipitate Sr/TRU before the filtration operation. The permanganate ion is a potent oxidizer of organic compounds. The impact of permanganate addition to Hanford waste feed in the WTP was therefore identified as a potential concern for applying the Hu correlation to predict hydrogen generation because organic compounds dominate the behaviors described by the correlation. The effects of permanganate additions to Hanford Envelope C waste have been studied in experiments using simulants and actual waste (Hallen et al. 2000, 2002a, 2002b). We analyzed the results of these tests to assess the potential effect on hydrogen generation rates. Our analyses suggest that that permanganate is not likely to accelerate any of the processes responsible for hydrogen production.

When added to the waste, permanganate is rapidly reduced to lower oxidation states of manganese, primarily Mn[IV]. Experimental data suggest that the organic compounds present in the wastes are the main reductants for permanganate (Gauger and Hallen 2001), but the TOC content is not significantly affected because the levels of permanganate are relatively low (0.075 M) compared with levels of TOC in wastes (~1 M) destined for treatment with permanganate. Nonetheless, organic complexants are partially oxidized by the permanganate addition. Because the resulting compounds are more oxidized, they are expected to generate less hydrogen. Otherwise, adding permanganate ion produces little chemical change in the supernatant fraction of the waste. The Mn(IV) compounds precipitate from solution and are removed by filtration. As a result, the filtered solids contain a significantly higher concentration of Mn than the initial entrained solids. The Hu model should be as valid for permanganate treated wastes as it is for the untreated waste.

Effect of Glass-Forming Chemicals on Hydrogen Generation Rates

Hydrogen production from organic compounds is understood well enough to provide bounding assessments of whether "new" organics (e.g., ion exchange resin, associated degradation products, and sucrose) may affect the Hu correlation's ability to predict hydrogen generation rates within the accepted uncertainty of the model.

Sucrose will be added to the waste stream for denitrification of the waste in the cold cap of the melter. The Hu correlation is focused on waste streams that are rich in organic complexants. The tank wastes have had significant quantities of glycolate ion and gluconate added to them as well as butanol from hydrolysis of tributyl phosphate that entered the tank wastes from the PUREX process (Boldt et al. 1999). Sugar is expected to behave chemically like these constituents. Soluble TOC is a variable in the Hu model. Therefore, it should suffice to combine the TOC from sugar with soluble TOC in the waste to predict the effect of added sugar.

Concerns were also raised that some waste streams may contain degradation products of the organic ion exchange materials. In particular, there was concern about the nitric acid eluate that would also be rich in Cs-137. However, this stream is destined to be concentrated to several molar nitric acid in a reduced-pressure evaporator. These conditions should completely degrade remnants of organic resins and other organic compounds, so downstream effects are expected to be negligible.

Glass forming minerals will be introduced in the high-level waste vitrification-melter feed preparation process. Some of these substances may catalyze the radiolytic generation of hydrogen. Metallic particles in water, hydrated oxide powders, and aqueous suspensions of silica nanoparticles have all been noted to catalyze water radiolysis and increase the yield of hydrogen (LaVerne and Tonnies 2003). However, LaVerne and Tonnies studied the effect of silica particle size on the yields of hydrogen and concluded that the effect in solution is limited to very small particles. For 7- and 22-nm sized SiO₂ particles, they observed hydrogen yields increase with the wt% of silica suspended in water. But for slurries containing 343-nm sized particles, the yield of hydrogen was equivalent to that expected from the water alone. Furthermore, they found that the excess hydrogen derives from reactions of solvated electrons that have occurred with microsecond lifetimes. Scavengers of the solvated electron such as nitrate ion are very effective at inhibiting these reactions. Therefore, enhanced yields of hydrogen are not expected from the process stream.

5.0 References

- Barefield EK, D Boatwright, A Deshpande, F Doctorovich, CL Liotta, HM Neumann, and S Seymore. 1996. *Mechanisms of Gas Generation from Simulated SY Tank Farm Wastes: FY 1994 Progress Report*. PNL-11247, Pacific Northwest National Laboratory, Richland, WA.
- Bibler NE. 1974. *J. Phys. Chem.* 78, 211.
- Boldt AL, GL Borsheim, NG Colton, BA Higley, KM Hodgson, MJ Kupfer, SL Lambert, MD Leclair, RM Orme, DE Place, WW Schulz, LW Shelton, BC Simpson, RA Watrous, and RT Winward. 1999. *Standard Inventories of Chemicals and Radionuclides in Hanford Site Tank Wastes*. HNF-SD-WM-TI-740 Rev. 0C, CH2M Hill Hanford Group, Richland, WA.
- Bryan SA and LR Pederson. 1995. *Thermal and Combined Thermal and Radiolytic Reactions Involving Nitrous Oxide, Hydrogen, and Nitrogen in the Gas Phase: Comparison of Gas Generation Rates in Supernate and Solid Fractions of Tank 241-SY-101 Simulated Wastes*. PNL-10490, Pacific Northwest Laboratory, Richland, WA.
- Bryan SA, LR Pederson, CM King, SV Forbes, and RL Sell. 1996. *Gas Generation from Tank 241-SY-103 Waste*. PNL-10978, Pacific Northwest National Laboratory, Richland, WA.
- Bryan SA, JGH Geeting, RD Scheele, RL Sell, and JE Tanner. 2002. *Thermal and Radiolytic Gas Generation from Washed AN-102 Sludge*. PNWD-3201, Battelle – Pacific Northwest Division, Richland, WA.
- Bryan SA, SJ Bos, JGH Geeting, RD Scheele, RL Sell, and JE Tanner. 2003. *Gas Generation and Energetics Studies of an Envelope C Waste Treated by the Sr/TR Precipitation Process*. PNWD-3257, Battelle – Pacific Northwest Division, Richland, WA.
- Camaioni DM and LM Stock. 2003. *The Influence of Alpha Radiation on the Rate of Hydrogen Generation*. WTP CCN 077982, Bechtel National, Inc., Richland, WA.
- Eibling RE and CA Nash. 2001. *Hanford Waste Simulants Created to Support the Research and Development on the River Protection Project—Waste Treatment Plant*. WSRC-TR-2000-00338, Westinghouse Savannah River Company, Aiken, SC.
- Gauger AM and RT Hallen. 2001. “Individual Reactions of Permanganate and Various Reductants.” *J. Undergraduate Research*, 1:54.
- Hallen RT, PR Bredt, KP Brooks, and LK Jagoda. 2000. *Combined Entrained Solids and Sr/TRU Removal from AN-107 Diluted Feed*. PNWD-3035, Battelle – Pacific Northwest Division, Richland, WA.
- Hallen RT, IE Burgeson, FV Hoopes, and DR Weier. 2002a. *Optimization of Sr/TRU Removal Conditions with Samples of AN-102 Tank Waste*. PNWD-3141, Battelle – Pacific Northwest Division, Richland, WA.
- Hallen RT, JGH Geeting, DR Jackson, and DR Weier. 2002b. *Combined Entrained Solids and Sr/TRU Removal from AN-102/C-104 Waste Blend*. PNWD-3264, Battelle – Pacific Northwest Division, Richland, WA.
- Hu TA. 1997. *Calculations of Hydrogen Release Rate at Steady State for Double Shell Tanks*. HNF-SD-WM-CN-117, Lockheed Martin Hanford Corporation, Richland, WA.

- Hu TA. 2000. *Empirical Rate Equation Model and Rate Calculation of Hydrogen Generation Rate for Hanford Waste Tanks*. HNF-3851 Rev. 0A, CH2M HILL Hanford Group, Richland, WA.
- Hu TA. 2002. *Steady-State Flammable Gas Release Rate Calculations and Lower Flammability Level Evaluation for Hanford Tank Waste*. RPP-5926 Rev. 2, CH2M HILL Hanford Group, Richland, WA.
- King CM, LR Pederson, and SA Bryan. 1997. *Thermal and Radiolytic Gas Generation from Tank 241-S-102 Waste*. PNNL-11600, Pacific Northwest National Laboratory, Richland, WA.
- LaVerne JA and SM Pimblott. 2000. "New mechanism for H₂ formation in water." *J. Phys. Chem. A*, 104(44):9820-9822.
- LaVerne JA and SE Tonnie. 2003. *J. Phys. Chem. B*, Vol. 107, p. 7277, and references cited therein.
- Mahoney LA, ZI Antoniak, JM Bates, and ME Dahl. 1999. *Retained Gas Sample Program*. PNNL-13000, Pacific Northwest National Laboratory, Richland, WA.
- Norton JD and LR Pederson. 1994. *Ammonia in Simulated Hanford double-Shell Tank Wastes: Solubility and Effects on Surface Tension*. PNL-10173. Pacific Northwest Laboratory, Richland, WA.
- Pastina B and JA LaVerne. 1999. "Hydrogen peroxide production in the radiolysis of water with heavy ions." *J. Phys. Chem. A*, 103(11):1592-1597.
- Pederson LR and SA Bryan. 1996. *Status and Integration of Studies of Gas Generation in Hanford Wastes*. PNNL-11297, Pacific Northwest National Laboratory, Richland, WA.
- Person JC. 1996. *Effects of Oxygen Cover Gas and NaOH Dilution on Gas Generation in Tank 241-SY-101 Waste*. WHC-SD-WM-DTR-043, Westinghouse Hanford Company, Richland, WA.
- Person JC. 1998. *Gas Generation in Tank 241-AN-105 Waste with and Without Oxygen Reactions*. HNF-2038 Rev 0, Numatec Hanford Corp., Richland, WA.
- Savel'ev YI, ZV Ershova, and MV Vladimirova. 1966. *Radiokimiya*, 9, 225.
- Sherwood DJ and LM Stock. September 14, 2003. *An Assessment of the Applicability of the Hu Model for Hydrogen Generation to the WTP*. Bechtel National Inc., Richland, WA.
- Smith JR. 1994. *Radiolysis Gases from Nitric Acid Solutions Containing HAS and HAN (U)*. WSRC-TR-94-0525, Westinghouse Savannah River Company, Aiken, SC.
- Tabala Y, Y Ito, and S Tagawa. 1991. *Handbook of Radiation Chemistry*. CRC Press, Boca Raton, FL.

Appendix A

Technical Issue Report

Modeling Hydrogen Generation Rates in Wastes with Alpha Radiation

Leon M. Stock, Donald M. Camaioni, and David J. Sherwood

Appendix A

Technical Issue Report

Modeling Hydrogen Generation Rates in Wastes with Alpha Radiation

Leon M. Stock, Donald M. Camaioni, and David J. Sherwood

The Hu correlation (Hu 1997, 2000, 2002) does not consider the influence of alpha radiation on the hydrogen generation rate (HGR) because the concentrations of these emitters are much smaller than the concentrations of the beta and gamma emitters in tank waste and because the alpha emitters are concentrated in sludges, where the particles have very short ranges. Flow sheet analysis indicates that the situation in the Waste Treatment Plant (WTP) differs because the alpha emitters will be concentrated, and it is not evident that their role in hydrogen generation can be neglected.

The Hu correlation can be modified to predict the hydrogen generation rate from alpha emitters by Eq. (A.1):

$$\text{HGR}^\alpha = H^\alpha f_L F G(\text{H}_2)^\alpha \quad (\text{A.1})$$

where H^α is the heat load of alpha radiation in watts/kg, f_L is the liquid fraction of the waste, the $G(\text{H}_2)^\alpha$ value is expressed in molecules per 100eV of deposited alpha radiation energy, and F is a conversion factor (0.90) to convert (molecules/100 eV)(W/kg) to moles/kg/day.

The $G(\text{H}_2)^\alpha$ value is determined by the sum of the contributions of the G values for the alpha radiolysis of water, $G_0(\text{H}_2)^\alpha$, and the indirect radiolysis of organic compounds, $G_{\text{TOC}}(\text{H}_2)^\alpha$. These terms are evaluated in this appendix.

A.1 Water Radiolysis

The formation of hydrogen by the radiolysis of water and other aqueous solutions has been investigated extensively (Spinks and Woods 1990). Burger (2002) recently summarized the work about alpha radiation. He points out that the principal distinction between alpha and beta radiolysis is that recombination reactions leading to molecular hydrogen and hydrogen peroxide occur much more readily with alpha radiation and that the G values for hydrogen and hydrogen peroxide for alpha radiation [$G(\text{H}_2)^\alpha$ for pure water is 1.4 molecules/100 eV and $G(\text{H}_2\text{O}_2)^\alpha$ is 1.3 molecules/100 eV] are larger than the corresponding values for beta and gamma radiation.

The literature was reevaluated during the preparation of this report. Unfortunately, no publications about the alpha radiolysis of alkaline solutions of Hanford Site waste were found. However, the alpha radiolysis of nitric acid solutions and the alpha radiolysis of neutral solutions of other scavengers, including nitrate and nitrite ions, were found.

First, several authors have measured the value of $G(\text{H}_2)^\alpha$ for the alpha radiolysis of nitric acid (Bibler 1974; Savel'ev et al. 1966; Smith 1994). Smith points out that the data for nitric acid can be described by

$$G(\text{H}_2)^\alpha = 1.217 \frac{1}{1 + 1.702[\text{NO}_3^-]} \quad (\text{A.2})$$

The equation underestimates the accepted $G(\text{H}_2)^\alpha$ value for pure water, but the values predicted for alpha radiolysis of 1 and 2 M nitric acid (0.45 and 0.32 molecules/100 eV) are appreciable.

Second, recent fundamental investigations by LaVerne and coworkers at Notre Dame Radiation Laboratory are directly relevant. They reinvestigated the radiolysis of water by alpha radiation in solutions with a variety of scavengers (Pastina et al. 1999; LaVerne and Pimblott 2000). While the efficiency of hydrogen scavengers varies, the data coalesce when correlated with the scavenging capacity for the precursor to the hydrated electron. LaVerne and Pimblott pointed out that their observations and those of prior investigations with high concentrations of scavengers implied that hydrogen was formed after non-hydrated electrons and water cations (H_2O^+) recombined to form excited water molecules that decomposed to hydrogen and oxygen atoms (Figure A.1):

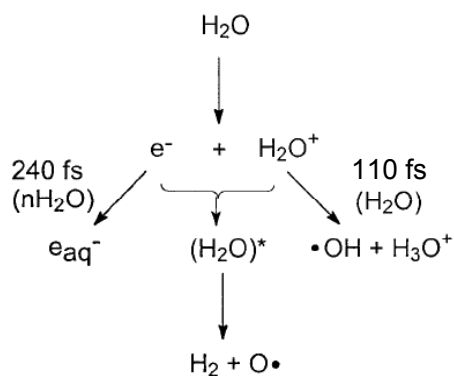
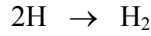


Figure A.1. Mechanism for hydrogen generation involving the non-hydrated electron (LaVerne and Pimblott 2000)

LaVerne and coworkers showed that Eq. (A.3), which is functionally equivalent to Eq. (A.2), describes the yield of hydrogen when scavengers are present at high concentrations, i.e., $[\text{S}] > 0.01 \text{ M}$:

$$G(\text{H}_2)^\alpha = G_0(\text{H}_2)^\alpha \frac{\tau^{-1}}{\tau^{-1} + k[\text{S}]} \quad (\text{A.3})$$

Here, τ is the lifetime for generating hydrogen by the process in Figure A.1, determined by the lifetime of H_2O^+ (110 fs); k is the rate coefficient for scavenging the nonhydrated electron by a solute of concentration $[\text{S}]$ (e.g., $2.2 \times 10^{13} \text{ M}^{-1}\text{s}^{-1}$ for nitrate ion and $0.57 \times 10^{13} \text{ M}^{-1}\text{s}^{-1}$ for nitrite ion); and $G_0(\text{H}_2)^\alpha$ is the estimated maximum yield of H_2 that derives from the process. The equation accurately predicts the values of $G(\text{H}_2)^\alpha$ at high scavenger concentration but fails to predict them at low scavenger concentrations. This is understandable because hydrogen is expected from subsequent reactions that involve the hydrated electron (e_{aq}^-) shown on the left in the figure. These reactions are unimportant at high concentrations of scavengers.



The discrepancy between the predictions of Eq. (A.3) and the experimental results at low scavenger concentrations can be readily resolved by adding a second term to account for hydrogen derived from the hydrated electron (e_{aq}^-). Thus, Eq. (A.3) is transformed into Eq. (A.4):

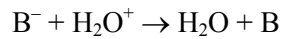
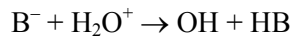
$$G_{(\text{H}_2)}^\alpha = G_{0(\text{H}_2)}^\alpha \frac{\tau^{-1}}{\tau^{-1} + k[\text{S}]} + (G_{(\text{H}_2, [\text{S}] = 0)}^\alpha - G_{0(\text{H}_2)}^\alpha) \frac{\tau_2^{-1}}{\tau_2^{-1} + k_2[\text{S}]} \quad (\text{A.4})$$

where $G_{0(\text{H}_2)}^\alpha$, τ , and k have the same meaning as in Eq. (A.3) and $G_{0(\text{H}_2, [\text{S}] = 0)}^\alpha = 1.4$ H₂ molecules/100 eV is the hydrogen yield in pure water, τ_2 is a lifetime associated with hydrogen generation from e_{aq}^- , and k_2 is the rate constant for the trapping of the solvated electron by the scavenger (e.g., $9.7 \times 10^9 \text{ M}^{-1}\text{s}^{-1}$ for nitrate ion) (Buxton et al. 1988). The results for alpha radiation are displayed in Figure A.1 with $G_{(\text{H}_2, [\text{S}] = 0)}^\alpha = 1.4$ molecules/100 eV, $G_{0(\text{H}_2)}^\alpha = 1.05$ molecules/100 eV, τ is 110 fs, and τ_2 , derived empirically by fitting to the experimental data, is 400 ns. These values define the G value for alpha radiation given by Eq. (A.5):

$$G_{(\text{H}_2)}^\alpha = 1.05 \frac{1}{1 + 2.4[\text{NO}_3^-]} + 0.35 \frac{1}{1 + 3900[\text{NO}_3^-]} \quad (\text{A.5})$$

The results for alpha radiolysis are shown in Figure A.2, where the experimental results are compared with the predictions of Eq. (A.2), (A.3), and (A.5).

We conclude that the amount of hydrogen generated in solutions of nitrate ion during alpha radiolysis is most accurately estimated by Eq. (A.5), the blue solid line in the figure. As shown by the red line, the Smith expression (Eq. A.2) overestimates the G values when the concentration of the scavenger is greater than 0.001 M. Both expressions are conservative in the sense that other scavengers are present in the waste and will also reduce the G value for the alpha radiolysis of water. Two reactions are noted here. First, the high concentration of hydroxide and other basic anions in the waste streams may further inhibit hydrogen formation due to proton or electron transfer with H_2O^+ ions:



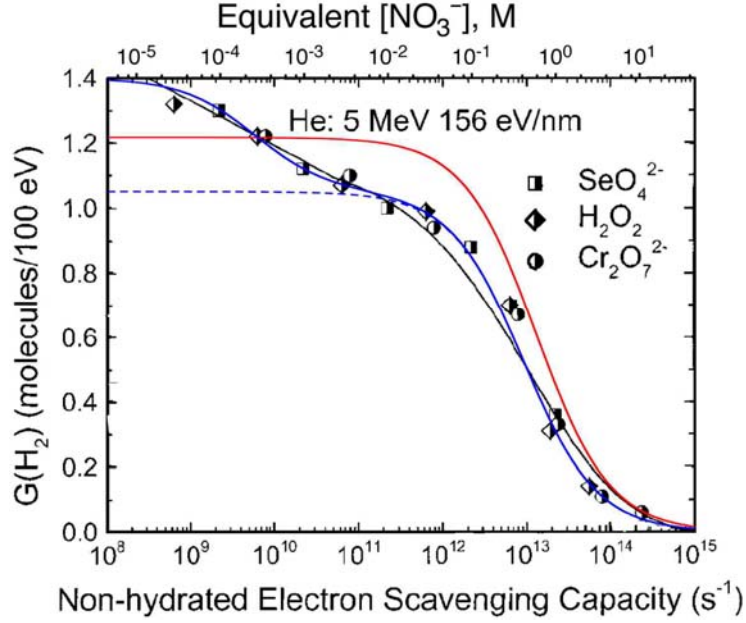


Figure A.2. Comparison of models for predicting the alpha radiolytic yield of molecular hydrogen from aqueous solutions containing scavengers of the non-hydrated and hydrated electrons (graph adapted from LaVerne and Pimblott 2000, Figure 1)

Second, Eq. (A.2) and (A.5) only consider the inhibitory influence of nitrate ion. LaVerne and his associates and many others have shown that nitrite ion and other anions in the wastes would also reduce the rate of hydrogen formation. The role of nitrite ion can be included as shown in Eq. (A.6):

$$G_{(H_2)}^\alpha = G_{0(H_2)}^\alpha \frac{\tau^{-1}}{\tau^{-1} + k[NO_3^-] + k'[NO_2^-]} + \left(G_{(H_2, [S] = 0)}^\alpha - G_{0(H_2)}^\alpha \right) \frac{\tau_2^{-1}}{\tau_2^{-1} + k_2[NO_3^-] + k'_2[NO_2^-]} \quad (A.6)$$

Here, the values of G , k , k_2 , τ , and τ_2 have the same meaning as shown in the previous equations, and k' and k'_2 are the rate constants for the reactions of nitrite ion with the non-hydrated and hydrated electrons, 0.57×10^{12} (Pastina et al. 1999) and $3.5 \times 10^9 \text{ M}^{-1}\text{s}^{-1}$ (Elliot et al. 1990), respectively. Substitution of the numerical values in Eq. (A.6) yields Eq. (A.7):

$$G_{(H_2)}^\alpha = 1.05 \frac{1}{1 + 2.4[NO_3^-] + 0.63[NO_2^-]} + 0.35 \frac{1}{1 + 3900[NO_3^-] + 1400[NO_2^-]} \quad (A.7)$$

Here are some predicted G values for hydrogen formation from a solution with 2 M nitrate and 2 M nitrite ion from alpha radiolysis to make a quick comparison between the three equations presented here:

- Smith with nitrate (Eq. A2), $G_{(H_2)}^\alpha = 0.28$ molecule/100 eV
- Camaioni-LaVerne approach with nitrate (Eq. 5), $G_{(H_2)}^\alpha = 0.18$ molecule/100 eV
- Camaioni-LaVerne approach nitrate and nitrite (Eq. 7), $G_{(H_2)}^\alpha = 0.15$ molecule/100 eV.

Clearly, the Smith equation (A.2) provides a conservative portrayal of hydrogen generation. The expression also underestimates the G value at very low concentrations of nitrate ion (less than $\sim 10^{-4}$ M), but the concentrations of nitrate ion in the waste streams greatly exceed this value. Eq. (A.3) also fails to accommodate the observations at low nitrate ion concentration (less than about 10^{-3} M), but provides a more accurate estimate of the G value at high concentration than the Smith expression. Eq. (A.5) and (A.7) provide an accurate estimate of the G value over the entire concentration range.

The accuracy of Eq. (A.7) depends on summing the scavenging capacity of all scavengers of hydrated and prehydrated electrons in the liquid phase of the waste. While nitrate and nitrite are the dominant scavengers, not including the cumulative effect of other scavengers such as transition metal ions, complexes, and oxy-anions causes errors to be on the conservative side. Also, Eq. (A.7) only applies to the liquid fraction of the waste. Alpha decay energy absorbed by solids may not generate hydrogen. Therefore, a less conservative, more accurate calculation of HGRs using Eq. (A.7) may be obtained by scaling the alpha dose rate by the weight fraction of water in the waste stream.

Eq. (A.7) was determined based on track-averaged yields from 5 MeV alpha particles generated by a linear accelerator. The yield of H_2 is strongly dependent on the initial energy of the alpha particle. Therefore, in making comparisons with/predictions for experimental data obtained from radioactive decay, one may want to scale the G value predicted by Eq. (A.7) to the alpha decay energy of the experiment. For example, Eq. (A.2) was derived from fission of curium-244 (Bibler) and Polonium-210 (Savel'ev). Both have decay energies larger than 5 MeV. Fission of these radionuclides also releases energy in the form of beta or gamma radiation. Therefore, it is understandable that Eq. (A.2) predicts somewhat higher yields of H_2 than Eq. (A.7).

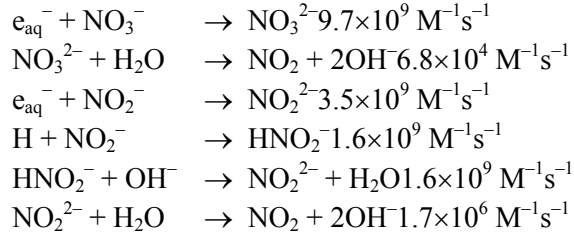
A.2 Organic Radiolysis

The amount of hydrogen produced from radiolytically induced oxidation of organic compounds in aqueous solutions will almost certainly be somewhat lower for alpha radiation than for beta and gamma. This is because the yields of water radicals such as hydrogen atoms and hydroxyl radicals are smaller for 5 MeV He^+ ions than for beta or gamma radiolysis (Spinks and Woods 1990; LaVerne and Pimblott 2000; Chitose et al. 1999, 2001; Hiroki et al. 2002). Hu and coworkers used Eq. (A.8) to compute a G value term for beta/gamma radiolysis of water with dissolved, “reactive” organic compounds:

$$G_{TOC}(H_2) = a_0(f[TOC])\exp(-Q_{rad}/RT) \quad (A.8)$$

In this equation, a_0 is 2.49×10^6 , f characterizes the “reactivity” of the organic compounds in the waste ($f = 0.7$ for DSTs and $f = 0.4$ for SSTs), TOC is the concentration of total organic carbon, Q_{rad} is the activation energy (44,300 J/mole), R is the gas constant, and T is the absolute temperature. Substantial evidence indicates that using this expression to also account for the effect of alpha radiolysis will overestimate HGRs because the higher concentrations of radicals in the spurs induced by alpha radiation lead to their mutual consumption. The high concentrations of nitrite and nitrate in the waste streams dictate that hydrated electrons are essentially all scavenged. The initial product radicals are the corresponding radical dianions, with the nitrate dianion predominating because of its greater scavenging capacity in Hanford waste. The yield of H atoms from water radiolysis is typically much smaller than the yield of electrons. Furthermore, many hydrogen atoms will be scavenged by nitrite ions, initially generating the dihydroxylamine radical ion, which in the alkaline wastes quickly deprotonates to the

nitrite radical dianion (Lyman et al. 2002). The nitrate and nitrite dianions are metastable and decay in a matter of microseconds to oxidizing radicals, NO₂ and NO, respectively. These reactions are summarized below.



Consequently, much of the hydrogen produced through the indirect radiolysis of organic compounds in the waste is formed via oxidations initiated by the surviving NO₂ and OH/O⁻ radicals. The aldehydes such as formaldehyde and glyoxylate ion that are formed in these oxidations undergo thermal decomposition to hydrogen and formate and oxalate ions (Kapoor et al. 1995; Ashby et al. 1994a). Work to elaborate these points through kinetic simulation is in progress.

Experiments and simulations (Chitose et al. 2001) suggest that the yield of radicals surviving intratrack reactions for alpha radiolysis is about 50% of the electron yield. Therefore, the constant *a* in Eq. (A.8) must be reduced by one-half to reflect the less efficient formation of reactive radicals by alpha radiation. Eq. (A.9) provides a more accurate formulation for the evaluation of $G_{\text{TOC}}(\text{H}_2)^\alpha$:

$$G_{\text{TOC}}(\text{H}_2)^\alpha = 0.5a_0(f[\text{TOC}])\exp(-Q_{\text{rad}}/RT) \quad (\text{A.9})$$

It has been pointed out that the high yields of hydrogen peroxide formed during alpha radiolysis might enhance hydrogen generation. Ashby and coworkers (Ashby et al. 1994a, 1994b; Barefield et al. 1995, 1996) have shown that formaldehyde is formed and converted into hydrogen in waste, and Stock (2001) pointed out that hydrogen peroxide can enhance the rate of hydrogen formation from aldehydes. However, LaVerne and coworkers (Pastina and LaVerne 1999; Hiroki et al. 2002) found that $G(\text{H}_2\text{O}_2)$ decreases toward zero with increasing concentrations of OH scavengers. They suggest “OH radical is the sole precursor to H₂O₂.” Using methanol to scavenge OH, they showed that $G(\text{H}_2\text{O}_2)$ from radiolysis with 5 MeV He⁺ drops to about 0.2 molecules/100 eV at 10 M concentration. The yield for gamma with the same methanol concentration, $G(\text{H}_2\text{O}_2)$, is approximately 0.15. Nitrite ion is a 10-fold better scavenger than methanol (Barker et al. 1970), so similar yields would be expected for 1 M nitrite concentrations. Accordingly, hydrogen peroxide generation by alpha radiolysis is of no greater concern than it is for gamma/beta radiolysis.

A.3 Conclusion and Recommendation

The Hu correlation can be modified to predict the hydrogen generation rate from alpha emitters by Eq. (A.1), repeated here:

$$\text{HGR}^\alpha = H^\alpha f_L F G(\text{H}_2)^\alpha$$

where H^α is the heat load of alpha radiation in watts/kg, f_L is the liquid fraction of the waste, the $G(\text{H}_2)^\alpha$ value is expressed in molecules per 100eV of deposited alpha radiation energy, and F is a conversion

factor (0.90) to convert (molecules/100 eV)(W/kg) to moles/kg/day. This “total-alpha G value,” $G(\text{H}_2)^\alpha$, is the sum of contributions from the alpha radiolysis of water, $G_0(\text{H}_2)^\alpha$, and the indirect radiolysis of organic compounds, $G_{\text{TOC}}(\text{H}_2)^\alpha$:

$$G(\text{H}_2)^\alpha = G_0(\text{H}_2)^\alpha + G_{\text{TOC}}(\text{H}_2)^\alpha \quad \text{H}_2 \text{ molecules/100 eV alpha-dose}$$

Smith (1994) proposed an expression for determining $G(\text{H}_2)$ for nitric acid solutions containing alpha emitters. Based on the work of LaVerne and Pimblott, we propose Eq. (A.7), repeated here:

$$G_{(\text{H}_2)^\alpha} = 1.05 \frac{1}{1 + 2.4[\text{NO}_3^-] + 0.63[\text{NO}_2^-]} + 0.35 \frac{1}{1 + 3900[\text{NO}_3^-] + 1400[\text{NO}_2^-]}$$

The molar concentrations of nitrate and nitrite ion are the key parameters in this expression, which can be applied for the evaluation of G values for aqueous solutions that contain high and low concentrations of these substances. It will be most accurate for radionuclides that fission 5 MeV alpha particles. Higher alpha energies will give some greater yields, and lower alpha energies will give smaller yields.

Similarly, Hu provided an expression for evaluating G values from beta/gamma radiolysis of Hanford waste: $G_{\text{TOC}}(\text{H}_2)^{\beta/\gamma}$. Technical considerations indicate that the Hu expression can be adapted for alpha radiolysis if the a term in Hu’s expression for $G_{\text{TOC}}(\text{H}_2)^{\beta/\gamma}$ is reduced by 50%:

$$G_{\text{TOC}}(\text{H}_2)^\alpha = 0.5a_0(f[\text{TOC}])\exp(-Q_{\text{rad}}/RT) \quad (\text{A.10})$$

In this equation, $a_0 = 2.49 \times 10^6$, f characterizes the “reactivity” of the organic compounds in the waste ($f = 0.7$ for DSTs and $f = 0.4$ for SSTs), $Q_{\text{rad}} = 44,300$ J/mole is the activation energy, $R = 8.314$ J/K-mole is the gas constant, and T is the temperature in Kelvin.

A.4 References

- Ashby EC, R Doctorovich, CL Liotta, HM Neumann, CF Yao, K Zhang, and NF McDuffie. 1994a. “Concerning the Formation of Hydrogen in Nuclear Waste. Quantitative Generation of Hydrogen via a Canizzaro Intermediate.” *J. Am. Chem. Soc.*, Vol. 115, p. 1171.
- Ashby EC, A Annis, EK Barefield, D Boatwright, R Doctorovich, CL Liotta, HM Neumann, CF Yao, K Zhang, and NF McDuffie. 1994b. *Synthetic Waste Chemical Mechanism Studies*. WHC-EP-0823, Westinghouse Hanford Company, Richland, WA.
- Barefield EK, D Boatwright, A Desphande, R Doctorovich, CL Liotta, HM Neumann, and S Seymore. 1995. *Mechanisms of Gas Generation from Simulated SY Tank Farm Wastes: FY1994 Progress Report*. PNL-10822, Pacific Northwest National Laboratory, Richland, WA.
- Barefield EK, D Boatwright, A Desphande, R Doctorovich, CL Liotta, HM Neumann, and S Seymore. 1996. *Mechanisms of Gas Generation from Simulated SY Tank Farm Wastes: FY1995 Progress Report*. PNL-11247, Pacific Northwest National Laboratory, Richland, WA.
- Barker GC, P Fowles, and B Stringer. 1970. *Trans. Faraday Soc.* Vol. 66, pp. 1509-1519.
- Bibler NE. 1974. *J. Phys. Chem.* Vol. 78, p. 211.

- Burger LL. 2002. *Decomposition of Hanford Waste Solutions by Alpha and Gamma Radiation*. Pacific Northwest National Laboratory, Richland, WA.
- Buxton GV, CL Greenstock, WP Helman, and AB Ross. 1988. "Critical Review of Rate Constants for Reactions of Hydrated Electrons, Hydrogen Atoms, and Hydroxyl Radicals (OH/O[•]) in Aqueous Solution." *J. Phys. Chem. Ref. Data*, 17, 513–886.
- Chitose N, Y Katsumura, et al. 2001. "Radiolysis of aqueous solutions with pulsed ion beams. 4. Product yields for proton beams in solutions of thiocyanate and methyl viologen/formate." *J. Phys. Chem. A*, 105(20):4902-4907.
- Chitose N, Y Katsumura, et al. 1999. "Radiolysis of aqueous solutions with pulsed helium ion beams. 3. Yields of OH radicals and the sum of e_{aq}⁻ and H atom yields determined in methyl viologen solutions containing formate." *J. Phys. Chem. A*, 103(24):4769-4774.
- Elliot AJ, DR McCracken, GV Buxton, and ND Wood. 1990. "Estimation of Rate Constants for Near-Diffusion-Controlled Reactions in Water at High Temperatures." *J. Chem. Soc. Faraday Trans.* 86, 1539-1547.
- Hiroki A, SM Pimblott, et al. 2002. "Hydrogen peroxide production in the radiolysis of water with high radical scavenger concentrations." *J. Phys. Chem. A*, 106(40):9352-9358.
- Hu TA. 1997. *Calculations of Hydrogen Release Rate at Steady State for Double Shell Tanks*. HNF-SD-WM-CN-117, Lockheed Martin Hanford Corporation, Richland, WA.
- Hu TA. 2000. *Empirical Rate Equation Model and Rate Calculation of Hydrogen Generation Rate for Hanford Waste Tanks*. HNF-3851 Rev. 0A, CH2M HILL Hanford Group, Richland, WA.
- Hu TA. 2002. *Steady State Flammable Gas Release Rate Calculations and Lower Flammability Level Evaluation for Hanford Tank Waste*. RPP-5926 Rev. 2, CH2M HILL Hanford Group, Richland, WA.
- Kapoor S, FA Barnabas, MC Sauer Jr, D Meisel, and CD Jonah. 1995. "Kinetics of Hydrogen Formation from Formaldehyde in Basic Aqueous Solutions." *J. Phys. Chem.*, 99(18):6857-6863.
- LaVerne JA and SM Pimblott. 2000. "New mechanism for H₂ formation in water." *J. Phys. Chem. A*, 104(44):9820-9822.
- Lymar SV, HA Schwarz, and G Czapski. 2002. "Reactions of dihydroxylamine (HNO₂⁻) and hydronitrite (NO₂²⁻) radical anions." *J. Phys. Chem. A*, Vol. 106, p. 7245.
- Pastina B and JA LaVerne. 1999. "Hydrogen peroxide production in the radiolysis of water with heavy ions." *J. Phys. Chem. A*, 103(11):1592-1597.
- Pastina B, JA LaVerne, et al. 1999. "Dependence of molecular hydrogen formation in water on scavengers of the precursor to the hydrated electron." *J. Phys. Chem. A*, 103(29):5841-5846.
- Savel'ev YI, ZV Ershova, and MV Vladimirova. 1966. *Radiokimiya*, Vol. 9, p. 225.
- Smith JR. 1994. *Radiolysis Gases from Nitric Acid Solutions Containing HAS and HAN (U)*. WSRC-TR-94-0525, Westinghouse Savannah River Company, Aiken, SC.
- Spinks JWT and RJ Woods. 1990. *An Introduction to Radiation Chemistry*, Third Edition. John Wiley and Sons, New York.
- Stock LM. 2001. *The Chemistry of Flammable Gas Generation*. RPP-6664 Rev. 1, CH2M HILL Hanford Group, Richland, WA.

Appendix B

Technical Issue Report

The Influence of Beta and Gamma Radiation on the Rate of Hydrogen Generation

Donald M. Camaioni

Appendix B

Technical Issue Report

The Influence of Beta and Gamma Radiation on the Rate of Hydrogen Generation

Donald M. Camaioni

The Hu correlation (Hu 1997, 2000, 2002) was developed for predicting hydrogen generation rates (HGRs) in quiescent tank wastes at the Hanford Site. It has three terms for hydrogen formation: 1) water radiolysis, 2) radiolytically induced organic reactions, and 3) thermally-induced organic reactions. The water radiolysis term predicts the yield of H₂ from water radiolysis based on the aqueous molar concentrations of nitrate and nitrite ions:

$$G(\text{H}_2)^{\beta/\gamma} = 0.45 - 0.56[\text{NO}_3^-]^{1/3} - 0.43[\text{NO}_2^-]^{1/3} \text{ H}_2 \text{ molecules}/100 \text{ eV} \quad (\text{B.1})$$

The nitrate and nitrite ions inhibit the radiolytic generation of H₂. Eq. (B.1) derives from an equation recommended by Tabala et al. (1991) in which the coefficients for nitrate and nitrite ion concentrations are 0.41 and 0.31, respectively. Hu increased the coefficients to match the HGR from Tank 241-AY-102. The waste in this tank was relatively cool and the concentration of organic compounds was quite low. Such conditions favor water radiolysis to be the dominant contributor to H₂ generation. When the concentrations of nitrate and nitrite ion are greater than 1 M, as they are in most Hanford Site wastes, Eq. (B.1) yields very small or even negative *G* values. Thus Hu adopted a default (minimum) value of 0.005 molecules/100eV for these wastes. These adjustments were tested and found suitable for modeling HGRs from stored tank wastes.

Review and analysis of recent data show that Eq. (B.1) is not suitable for some situations in the Waste Treatment Plant (WTP). Recent tests of hydrogen formation from washed solids from Tank 241-AN-102 (Bryan et al. 2002) and washed wastes that have also been treated to remove radioactivity by the strontium carbonate-sodium permanganate operation (Bryan et al. 2003) imply that the *G* values predicted for the radiolysis of water by Eq. (B.1) are too small. While one could revert to using Tabala's coefficients, we have learned that a new and more fundamental understanding of the issue has recently been developed by LaVerne and Pimblott of the University of Notre Dame Radiation Laboratory. On the basis of their work, we already have advanced a correlation for predicting HGRs from alpha radiolysis (Camaioni and Stock 2003). In this appendix we review their work and apply it to develop a correlation for predicting HGRs from beta/gamma radiolysis in WTP process streams.

B.1 Technical Analysis

Since the Hu model was formulated, LaVerne, Pimblott, and coworkers have reinvestigated the production of molecular hydrogen from radiolysis of water (Pastina et al. 1999; LaVerne and Pimblott 2000). They proposed a new mechanism and advanced a simple, yet accurate model for correlating yield data obtained in the presence of a wide variety of inhibitors, including nitrate and nitrite ion. While the

efficiency of hydrogen scavengers varies, LaVerne and coworkers observed that the data coalesce when correlated with the scavenging capacity for the precursor to the hydrated electron (Pastina et al. 1999). LaVerne and Pimblott then suggested that the results could be explained by a mechanism in which the precursor to the hydrated electron (non-hydrated electron) recombines with water cation (H_2O^+) to form an excited water molecule that decomposes to H_2 and oxygen atom (Figure B.1):

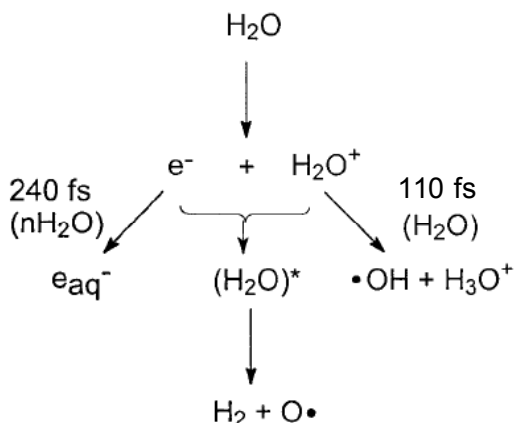


Figure B.1. Mechanism for hydrogen generation involving the non-hydrated electron (LaVerne and Pimblott 2000)

LaVerne and coworkers showed that Eq. (B.2) describes the yield of hydrogen when scavengers are present at high concentrations, i.e., $[\text{S}] > 0.01 \text{ M}$:

$$G_{(\text{H}_2)}^{\beta/\gamma} = G_0(\text{H}_2)^{\beta/\gamma} \frac{\tau^{-1}}{\tau^{-1} + k[\text{S}]} \quad (\text{B.2})$$

Here, τ is the lifetime for generating hydrogen by the process in Figure B.1. It is determined by the lifetime of H_2O^+ (110 fs), k is the rate coefficient for scavenging of the non-hydrated electron by a solute of concentration $[\text{S}]$ (e.g., $2.2 \times 10^{13} \text{ M}^{-1}\text{s}^{-1}$ for nitrate ion and $0.57 \times 10^{13} \text{ M}^{-1}\text{s}^{-1}$ for nitrite ion), and $G_0(\text{H}_2)^{\beta/\gamma}$ is the estimated maximum yield of H_2 that derives from the process shown in Figure B.2. Figure B.2 shows data for several scavengers with Eq. (B.2) plotted for different values of $G_0(\text{H}_2)^{\beta/\gamma}$. The equation accurately predicts the values of $G_{(\text{H}_2)}^{\beta/\gamma}$ at high concentrations of scavengers when $G_0(\text{H}_2)^{\beta/\gamma} = 0.34$.

Eq. (B.3) fails to predict $G_0(\text{H}_2)^{\beta/\gamma}$ at scavenging capacities lower than $\sim 10^{12} \text{ s}^{-1}$. For NO_3^- and NO_2^- , it corresponds to concentrations less than 0.04 and 0.2 M, respectively. This is understandable because hydrogen is expected from subsequent reactions that involve the hydrated electron (e_{aq}^-) shown on the left in Figure B.1.

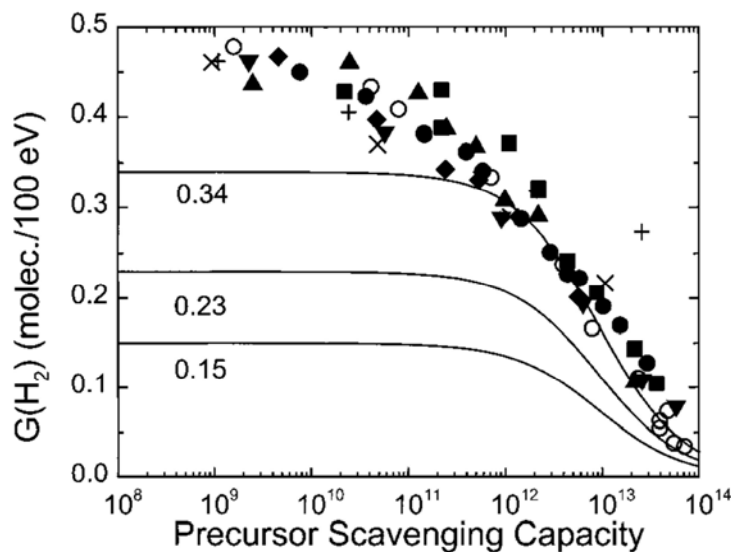
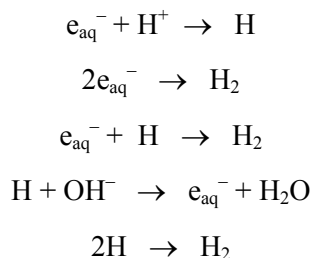


Figure B.2. Molecular hydrogen yields as a function of the scavenging capacity (s^{-1}) of the precursor to the hydrated electron: (\blacksquare) SeO_4^- , (\bullet) MoO_4^{2-} , (\blacktriangle) NO_3^- , (\blacklozenge) NO_2^- , (\blacktriangledown) H_2O_2 , (\circ) $Cr_2O_7^{2-}$, (+) Cu^{2+} , and (\times) Cd^{2+} . The solid lines were obtained using Eq. (B.2) and $G_0(H_2) = 0.15, 0.23, \text{ and } 0.34$. Figure and data from Pastina et al. (1999).



These reactions are unimportant at high concentrations of scavengers.

The discrepancy between the predictions of Eq. (B.2) and the experimental results at low scavenger concentrations can be readily resolved by adding a second term to account for hydrogen derived from the hydrated electron (e_{aq}^-). Thus, Eq. (B.2) is transformed into Eq. (B.3):

$$G_{(H_2)}^{\beta/\gamma} = G_0(H_2)^{\beta/\gamma} \frac{\tau^{-1}}{\tau^{-1} + k[S]} + (G_{(H_2, [S]=0)}^{\beta/\gamma} - G_0(H_2)^{\beta/\gamma}) \frac{\tau_2^{-1}}{\tau_2^{-1} + k_2[S]} \quad (B.3)$$

where $G_0(H_2)^{\beta/\gamma}$, τ , and k have the same meaning as for Eq. (B.3) and $G_0(H_2, [S]=0)^{\beta/\gamma} = 0.45$ H_2 molecules/100 eV is the hydrogen yield in pure water, τ_2 is a lifetime associated with hydrogen generation from e_{aq}^- , and k_2 is the rate constant for the trapping of the solvated electron by the scavenger [9.7×10^9 and 3.5×10^9 $M^{-1}s^{-1}$ for nitrate and nitrite ions, respectively (Buxton et al. 1988; Elliot et al. 1990; see also NDRL/NIST Solution Kinetics Database, <http://kinetics.nist.gov/solution/index.php>)]. Figure B.3 shows data for $G_0(H_2)^{\beta/\gamma}$ from nitrate and nitrite solutions and Eq. (B.3), with $G_{(H_2, [S]=0)}^{\beta/\gamma} = 0.45$ molecules/100 eV, $G_0(H_2)^{\beta/\gamma} = 0.34$ molecules/100 eV, $\tau = 110$ fs, and $\tau_2 = 12.3$ ns derived empirically by fitting to the data.

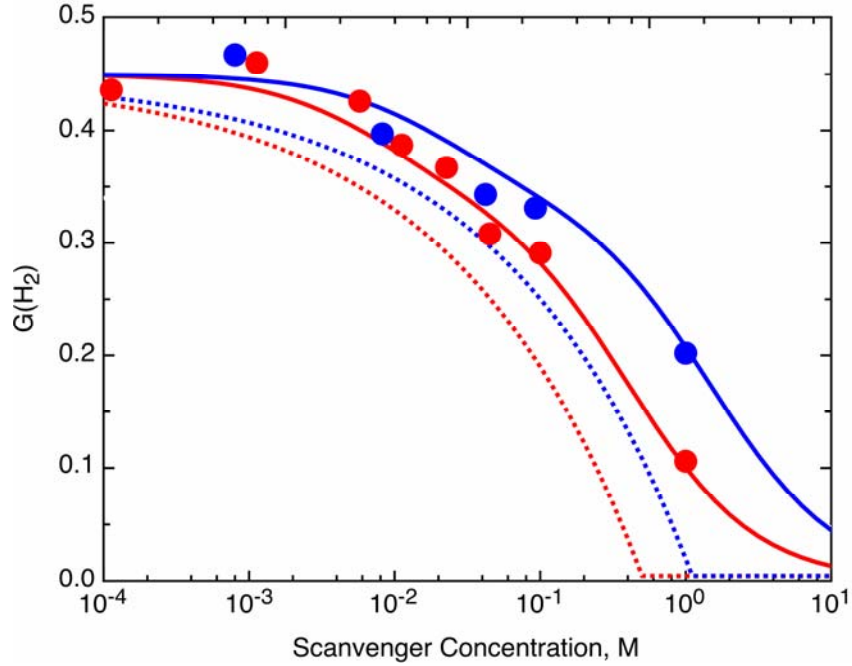


Figure B.3. Dependence of gamma radiolysis yield of H₂ on concentration of NaNO₃ (red) or KNO₂ (blue) and curves for yields predicted by Eq. (4) and Hu model (dotted lines) (data from Pastina et al. 1999)

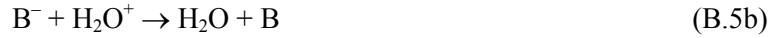
With the fitted parameters for nitrate and nitrite, Eq. (B.3) may be expressed as Eq. (B.4) for beta/gamma radiolysis of solutions containing both scavengers:

$$G(\text{H}_2)^{\beta/\gamma} = 0.34 \frac{1}{1 + 2.4[\text{NO}_3^-] + 0.62[\text{NO}_2^-]} + 0.11 \frac{1}{1 + 120[\text{NO}_3^-] + 43[\text{NO}_2^-]} \quad (\text{B.4})$$

Figure B.3 also shows the Hu model prediction for the same laboratory data. Everywhere it is lower than data from the literature. Perhaps this is as expected because the Hu model was parameterized to predict HGRs from the unique (e.g., high salt/solids) tank wastes. The tank wastes are much more complex and no doubt have other species present in solution that may scavenge electrons and inhibit H₂ generation. However, as the wastes will be processed at the WTP into HLW and LAW waste streams, the solids and Cs-137 will be separated from the supernatant waste fractions, and the solids will be washed of interstitial liquids. These operations will remove other scavengers, and dilute the nitrate and nitrite concentrations. Therefore, the resulting waste fraction may neither be accurately nor conservatively predicted by Eq. (B.1).

Some data indicate that this may be the case. Recent tests measured $G(\text{H}_2) = 0.055$ molecules/100 eV for washed solids from Tank AN-102, and $G(\text{H}_2) = 0.18$ molecules/100 eV for solids from AN-102 and C-104 that were obtained by with sodium permanganate treatment to precipitate radioactive Sr and TRU elements and washed (Bryan et al. 2003). Eq. (B.1) predicts 0.005 and 0.12 molecules/100 eV, respectively, for these treated wastes. Eq. (B.4) predicts 0.13 and 0.30 molecules/100 eV, respectively. While the measured values are bracketed by these estimates, only Eq. (B.4) is bounding.

Steps to increase the accuracy of Eq. (B.3) are possible. For example, identifying other scavengers present in the wastes would allow better definition of the scavenging capacity of the waste. In addition to scavengers of the non-hydrated electron, scavengers of the water cation (H_2O^+) may also contribute. Two reactions are noted here. First, the high concentration of hydroxide and other basic anions in the waste streams may further inhibit hydrogen formation due to proton or electron transfer with H_2O^+ ions:



Hayon (1965) observed that $G(\text{H}_2)$ for water radiolysis is 0.37 in 1 M NaOH. If we assume this results from reactions like (B.5a) or (B.5b), then k for scavenging of H_2O^+ by hydroxide ion is about $2 \times 10^{12} \text{ M}^{-1} \text{ s}^{-1}$. Therefore, a term for scavenging of H_2O^+ by hydroxide ion may be added to Eq. (B.4):

$$G_{(\text{H}_2)}^{\beta/\gamma} = 0.34 \frac{1}{1 + 2.4[\text{NO}_3^-] + 0.62[\text{NO}_2^-] + 0.22[\text{OH}^-]} + 0.11 \frac{1}{1 + 120[\text{NO}_3^-] + 43[\text{NO}_2^-]} \quad (\text{B.4a})$$

Other basic anions present in the wastes could contribute in like manner.

Furthermore, time-dependent effects and ion strength effects on the rate constants for scavenging the hydrated electron could be included (Pastina et al. 1999). The scavenging capacities of anions increase with ionic strength because coulombic repulsion is screened out. However, these effects would come into play in the second term of Eq. (B.3), when the nonhydrated electron scavenging capacity is $< 10^{12} \text{ s}^{-1}$. Also, Eq. (B.3) only applies to the liquid fraction of the waste, and more specifically to the fraction of absorbed energy that ionizes water. Radiation absorbed by solids may not generate hydrogen. Therefore, a less conservative, more accurate calculation of HGRs using Eq. (B.3) may be obtained by scaling the dose rate by the fraction of liquid in the waste stream.

B.2 Conclusion and Recommendation

Based on the analysis presented here, Eq. (B.4) is recommended for use in WTP design calculations specifically concerned with the high-level waste streams that have been treated with permanganate (to precipitate radioactive strontium and TRUs) and/or washed to remove low activity waste components. The data suggest that these waste streams have HGRs that are intermediate between stored wastes and laboratory simulants. Being relatively low in soluble TOC, the H_2 is mainly from water radiolysis. Accordingly, the Hu model for water radiolysis may not be bounding in these situations.

The accuracy of Eq. (B.3) depends on summing the scavenging capacity of all scavengers of hydrated and prehydrated electrons in the liquid phase of the waste. While nitrate and nitrite ions are the dominant scavengers, not including the cumulative effect of other scavengers, *e.g.*, transition metal ions, complexes, and oxy-anions, causes errors to be on the conservative side.

B.3 References

- Bryan SA, JGH Geeting, RD Scheele, RL Sell, and JE Tanner. 2002. *Thermal and Radiolytic Gas Generation from Washed AN-102 Sludge*. PNWD-3201, Battelle – Pacific Northwest Division, Richland, WA.
- Bryan SA, SJ Bos, JGH Geeting, RD Scheele, RL Sell, and JE Tanner. 2003. *Gas Generation and Energetics Studies of an Envelope C Waste Treated by the Sr/TR Precipitation Process*. WTP-RPT-063 Rev. A, Bechtel National, Inc., Richland, WA.
- Buxton GV, CL Greenstock, WP Helman, and AB Ross. 1988. "Critical Review of Rate Constants for Reactions of Hydrated Electrons, Hydrogen Atoms, and Hydroxyl Radicals (OH/O⁻) in Aqueous Solution." *J. Phys. Chem. Ref. Data*, 17, 513–886.
- Camaioni DM and LM Stock. 2003. *The Influence of Alpha Radiation on the Rate of Hydrogen Generation*. WTP CCN 077982, Bechtel National, Inc., Richland, WA.
- Elliot AJ, DR McCracken, GV Buxton, and ND Wood. 1990. "Estimation of Rate Constants for Near-Diffusion-Controlled Reactions in Water at High Temperatures." *J. Chem. Soc., Faraday Trans.*, 86, 1539-1547.
- Hayon E. 1965. "Radical and Molecular Yields in the Radiolysis of Alkaline Aqueous Solutions." *J. Chem. Soc., Faraday Trans.*, 61, 734-743.
- Hu TA. 1997. *Calculations of Hydrogen Release Rate at Steady State for Double Shell Tanks*. HNF-SD-WM-CN-117, Lockheed Martin Hanford Corporation, Richland, WA.
- Hu TA. 2000. *Empirical Rate Equation Model and Rate Calculation of Hydrogen Generation Rate for Hanford Waste Tanks*. HNF-3851 Rev. 0A, CH2M HILL Hanford Group, Richland, WA.
- Hu TA. 2002. *Steady State Flammable Gas Release Rate Calculations and Lower Flammability Level Evaluation for Hanford Tank Waste*. RPP-5926 Rev. 2, CH2M HILL Hanford Group, Richland, WA.
- LaVerne JA and SM Pimblott. 2000. "New mechanism for H₂ formation in water." *J. Phys. Chem. A*, 104(44):9820-9822.
- Pastina B, JA LaVerne, et al. 1999. "Dependence of molecular hydrogen formation in water on scavengers of the precursor to the hydrated electron." *J. Phys. Chem. A*, 103(29):5841-5846.
- Tabala Y, Y Ito, and S Tagawa. 1991. *Handbook of Radiation Chemistry*. CRC Press, Boca Raton, FL.

Appendix C

Technical Issue Report

The Influence of Oxygen on Hydrogen Generation Rates

Leon M. Stock, Donald M. Camaioni, and David J. Sherwood

Appendix C

Technical Issue Report

The Influence of Oxygen on Hydrogen Generation Rates

Leon M. Stock, Donald M. Camaioni, and David J. Sherwood

The Hu correlation (Hu 1997, 2000, 2002) was devised for quiescent wastes that are not mixed with air during interim storage. In contrast, operations at the Waste Treatment Plant (WTP) will introduce air into the waste. The purpose of this appendix is to provide preliminary information on the potential impact of dissolved oxygen on hydrogen generation in Hanford waste. The information is from prior laboratory work sponsored by DOE and is consistent with results reported in the open literature.

C.1 Effects of Oxygen on Thermal Hydrogen Generation Rates

Early observations at Argonne National Laboratory indicated that the oxygen generated in radiolytic reactions was consumed by waste simulants (Meisel et al. 1991). Subsequent investigations of the composition of the stored gases within the tank wastes (Mahoney et al. 1999) revealed that the wastes were essentially free of oxygen. This finding suggests that oxygen, either produced during radiolysis or introduced from the head space, was consumed in the waste.

The influence of oxygen on hydrogen (and other gas) formation rates and on the decomposition rates of organic compounds has been investigated in waste simulants in two laboratories with somewhat different results.

The thermal reactions of sodium *N*-(2-hydroxyethyl)ethylenediaminetetraacetate (HEDTA) were investigated at several temperatures at the Georgia Institute of Technology by Ashby et al. (1994a) and Barefield et al. (1995, 1996). Most of these experiments were conducted under argon, but some were carried out in the presence of oxygen. It was found that oxygen decreased the yields of the three nitrogen-containing gases and reduced the consumption of the nitrite ion. Oxygen also increased the rate of hydrogen formation significantly: Indeed, hydrogen production increased by a factor of 8 in the experiments conducted at 120°C. Oxygen decreased the yield of the formate ion but increased the yield of the oxalate ion.

Camaioni et al. (1996, 1998) tested the effect of oxygen in an inert atmosphere on the product distributions and gas yields from waste tank simulants due to thermal heating and gamma irradiation. The first tests were carried out with a simulant rich in organic solvents, including tributyl phosphate and dodecane, and contained two complexants, ethylenediaminetetraacetate (EDTA), and citrate ions (Camaioni et al. 1996). The second tests used a simulant that contained the major complexants: HEDTA, EDTA, glycolate and citrate ions (Camaioni et al. 1998). Oxygen was consumed despite the fact that the reactors were not stirred, during the radiolytic and thermal reactions. The *G* values for generation of hydrogen were temperature dependent and appeared to increase possibly by a factor of 2 when oxygen

was present. The results of the thermal experiments at 90°C showed that the complexants degraded somewhat more rapidly in the presence of oxygen. However, the rate of formation of hydrogen was little changed.

The influence of oxygen on the hydrogen generation rates (HGRs) in tank waste has also been investigated. Person (1996) observed that the HGR from thermolysis of Tank 241-SY-101 waste at 100°C increased from 0.1 mmole/day hydrogen per liter of waste under a helium atmosphere to between 1.4 and 2.2 mmoles/day hydrogen per liter of waste in a helium atmosphere that contained 20% oxygen. Related experiments with waste from Tank 241-AN-105 revealed that the HGR increased between 5- and 10-fold when oxygen was present in the inert atmosphere (Person 1998).

The gas generation rates reported by Person (1996) for thermolysis of waste from Tank 241-SY-101 in the presence and absence of oxygen and Bryan et al. (1996) for thermolysis of waste from Tank 241-SY-101 and SY-103 are displayed by Figure C.1. The results shown in the figure imply that the gas generation reactions in the presence of oxygen are more rapid and temperature dependent.

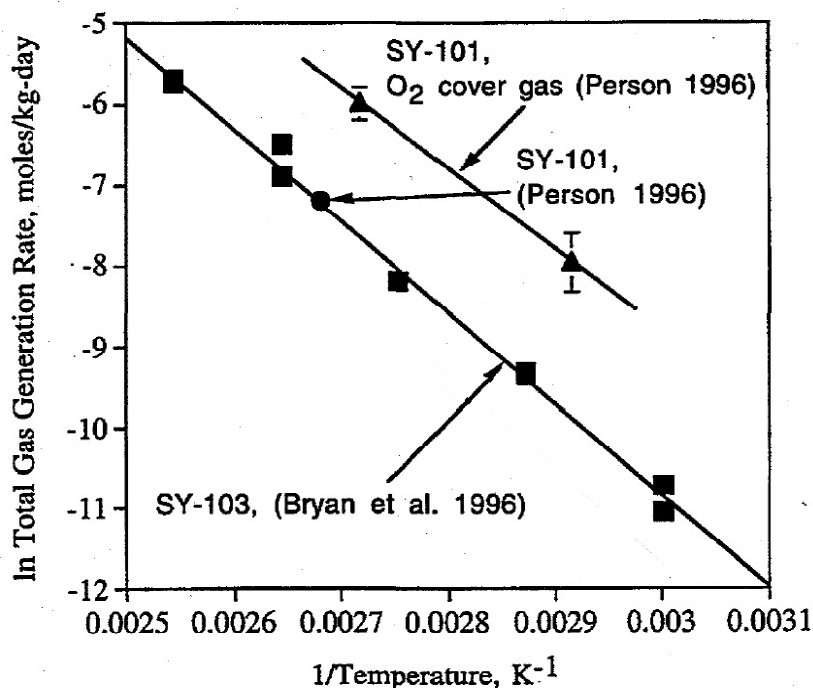


Figure C.1. The temperature dependence of the thermal generation of gas in Tank SY-101 waste in the presence of oxygen and the thermal generation of gas from SY-101 and SY-103 in the absence of oxygen (Person 1996; Bryan et al. 1996)

Stock (2001) points out that these observations are compatible with technical information in the chemical literature from many sources, including the facile air oxidation of organic compounds in alkaline solution, the influence of oxidants such as peroxide on the rate of formation of hydrogen from formaldehyde, and related work concerning the reactions of nitrogen containing intermediates with oxygen. [See, for example, Ashby et al. (1994a), Hudlicky (1990), Carey and Sundberg (1990), Smith and March (2001), and Spinks and Woods (1990).]

C.2 Effect of Oxygen on Radiolytic Generation of Hydrogen

Oxygen reacts very rapidly with solvated electrons and hydrogen atoms (Spinks and Woods 1990), and it is therefore necessary to consider the possibility that dissolved oxygen could reduce the formation rate of molecular hydrogen in aerated solutions. Although the second-order rate constant for reaction of the solvated electron with oxygen is very large, the concentration of oxygen in the solution is small, ranging from about 1.5×10^{-3} M in pure water at 25°C to 1.5×10^{-5} M in concentrated simulated waste solution at 20°C (Norton and Pederson 1994). The impact of oxygen on the *G* value for hydrogen generation can be gauged by comparison of the rate constants for its reaction with the solvated electron with the second order rate constant for the reaction of nitrate ion with the solvated electron (Buxton et al. 1988). The ratio of the rate constants indicates that oxygen is about twice as reactive. Unfortunately, its low solubility contravenes an important role for this substance. For a nitrate concentration of 0.01 M and an oxygen concentration of 0.001 M (the solubility in pure water at 25°C), the inhibitory influence of nitrate ion would be more than five-fold greater than for oxygen. Considerations of this kind imply that oxygen would not materially reduce the rates of the radiolytic reactions under the most favorable conditions, i.e., at its highest solubility, so long as nitrate ion was present.

We also considered the possibility that oxygen might form reactive oxidizing agents, such as hydroxyl radical, that might destroy hydrogen in solution and thereby decrease its concentration. Regrettably, nitrite ion interferes with this chemistry. The rate constant for the reaction of hydroxyl radical with nitrite ion is about 300 times greater than the rate constant for the reaction of hydroxyl radical with molecular hydrogen. Oxygen could not be an effective reagent for the oxidation of hydrogen even at low concentrations of nitrite ion. For example, assuming a nitrite concentration of about 0.01 M for an Envelope B/D UFP07 waste stream, the reaction between dissolved hydrogen, even at its maximum concentration (0.0008 M), and hydroxyl radical could not compete with the more favorable reaction between nitrite ion (0.01 M) and hydroxyl radical. In summary, oxygen could reduce the radiolytic rate of generation of hydrogen, but quantitative considerations imply that its influence will be small.

Oxygen will also influence the rates of the radiolytically induced, hydrogen-generating reactions of the soluble organic compounds in the waste streams. This feature of the chemistry can be addressed by considering the relative rates of the reactions between intermediate organic radicals generated by radiolytic reactions with molecular oxygen and other principal oxidizing agents, NO and NO₂, in the wastes. The reactions between the organic radicals and oxygen are more rapid than the rates of reaction of these radicals with nitric oxide and nitrogen dioxide. In this situation, the organic compounds in the wastes would be oxidized more rapidly in the presence of oxygen than in its absence. Some reaction products, for example, formaldehyde or glyoxylate ion, are potential sources of hydrogen, but other oxidation products like carbonate and oxalate ion are not hydrogen sources. In summary, it is evident that oxygen will reduce the hydrogen content of the organic molecules in the wastes, some reaction products will increase the propensity for hydrogen formation and others will decrease it. Overall, this effect appears negligible.

C.3 The Effect of Aeration on the Thermal Reactions

The WTP flow sheet evaluations (Sherwood and Stock 2003) indicated that pulse jet mixing could introduce oxygen into the waste. Inasmuch as the Hu correlation is designed for predicting hydrogen formation in quiescent, anaerobic wastes, laboratory work was undertaken to determine the influence of

oxygen on the hydrogen generation rates in actual wastes because Ashby and coworkers (Ashby et al. 1994a, 1994b; Barefield et al. 1995, 1996) showed that oxygen influenced hydrogen formation in waste simulants, and Person (1996, 1998) showed that HGRs for waste from Tank 241-SY-101 at temperatures over 70°C were increased by more than an order of magnitude when exposed to oxygen. While not definitive, other work with waste and waste simulants also suggests that exposing waste to oxygen could increase hydrogen formation.

We also considered the possibility that oxygen might form reactive oxidizing agents, such as hydroxyl radical, that might destroy hydrogen in solution and thereby decrease its concentration. Regrettably, nitrite ion interferes with this chemistry. The rate constant for the reaction of hydroxyl radical with nitrite ion is about 300 times greater than the rate constant for the reaction of hydroxyl radical with molecular hydrogen. Oxygen could not be an effective reagent for the oxidation of hydrogen even at low concentrations of nitrite ion. For example, assuming a nitrite concentration of about 0.01 M for an Envelope B/D UFP07 waste stream, the reaction between dissolved hydrogen, even at its maximum concentration (0.0008 M), and hydroxyl radical, could not compete with the more favorable reaction between nitrite ion (0.01 M) and hydroxyl radical. In summary, oxygen could reduce the radiolytic rate of generation of hydrogen, but quantitative considerations imply that its influence will be small.

Oxygen will also influence the rates of the radiolytically induced, hydrogen-generating reactions of the soluble organic compounds in the waste streams. This feature of the chemistry can be addressed by considering the relative rates of the reactions between intermediate organic radicals generated by radiolytic reactions with molecular oxygen and other principal oxidizing agents, NO and NO₂, in the wastes. The reactions between the organic radicals and oxygen are more rapid than the rates of reaction of these radicals with nitric oxide and nitrogen dioxide. In this situation, the organic compounds in the wastes would be oxidized more rapidly in the presence of oxygen than in its absence. Some reaction products such as formaldehyde or glyoxylate ion are potential sources of hydrogen, but other oxidation products like carbonate and oxalate ion are not hydrogen sources. In summary, it is evident that oxygen will reduce the hydrogen content of the organic molecules in the wastes, some reaction products will increase the propensity for hydrogen formation, and others will decrease it. Overall, this effect appears negligible.

C.4 Conclusion and Recommendations

The available information indicates that hydrogen is generated faster in tank waste exposed to air (oxygen) than in waste under inert gases. This factor was not addressed by the Hu model developed for predicting HGRs in what are apparently relatively quiescent, air-free wastes. Assuming that air will be introduced into the wastes during pulse jet mixing and perhaps other WTP operations, the present form of the Hu correlation is not likely to be directly applicable for predicting HGRs for such processes.

It is recommended that HGRs from thermolysis be determined by laboratory experiments for a suite of wastes and temperatures in the presence and absence of oxygen and mixing to provide the necessary information for revising the Hu correlation.

C.5 References

- Ashby EC, R Doctorovich, CL Liotta, HM Neumann, CF Yao, K Zhang, and NF McDuffie. 1994a. "Concerning the Formation of Hydrogen in Nuclear Waste. Quantitative Generation of Hydrogen via a Canizzaro Intermediate." *J. Am. Chem. Soc.*, Vol. 115, p. 1171.
- Ashby EC, A Annis, EK Barefield, D Boatwright, R Doctorovich, CL Liotta, HM Neumann, CF Yao, K Zhang, and NF McDuffie. 1994b. *Synthetic Waste Chemical Mechanism Studies*. WHC-EP-0823, Westinghouse Hanford Company, Richland, WA.
- Barefield EK, D Boatwright, A Desphande, R Doctorovich, CL Liotta, HM Neumann, and S Seymore. 1995. *Mechanisms of Gas Generation from Simulated SY Tank Farm Wastes: FY1994 Progress Report*. PNL-10822, Pacific Northwest National Laboratory, Richland, WA.
- Barefield EK, D Boatwright, A Desphande, R Doctorovich, CL Liotta, HM Neumann, and S Seymore. 1996. *Mechanisms of Gas Generation from Simulated SY Tank Farm Wastes: FY1995 Progress Report*. PNL-11247, Pacific Northwest National Laboratory, Richland, WA.
- Bryan SA, LR Pederson, CM King, SV Forbes, and RL Sell. 1996. *Gas Generation Tank 241-SY-103 Waste*. PNL-10978, Pacific Northwest National Laboratory, Richland, WA.
- Buxton GV, CL Greenstock, WP Helman, and AB Ross. 1988. "Critical review of rate constants for reactions of hydrated electrons, hydrogen atoms and hydroxyl radicals ($\cdot\text{OH}/\cdot\text{O}^-$) in aqueous solution." *J. Phys. Chem. Ref. Data*, Vol. 17, p. 513.
- Camaioni DM, WD Samuels, JC Lenihan, SA Clauss, AK Sharma, KL Wahl, and JA Campbell. 1996. *Organic Tank Safety Program FY96 Waste Aging Studies*. PNL-11312, Pacific Northwest Laboratory, Richland, WA.
- Camaioni DM, WD Samuels, JC Linehan, AK Sharma, ST Autrey, MA Lilga, MO Hogan, SA Clauss, KL Wahl, and JA Campbell. 1998. *Organic Tanks Safety Program Waste Aging Studies Final Report*. PNNL-11909, Pacific Northwest National Laboratory, Richland, WA.
- Carey FA and RJ Sundberg. 1990. *Advanced Organic Chemistry*, Third Edition. Plenum Press, New York.
- Hu TA. 1997. *Calculations of Hydrogen Release Rate at Steady State for Double Shell Tanks*. HNF-SD-WM-CN-117, Lockheed Martin Hanford Corporation, Richland, WA.
- Hu TA. 2000. *Empirical Rate Equation Model and Rate Calculation of Hydrogen Generation Rate for Hanford Waste Tanks*. HNF-3851 Rev. 0A, CH2M HILL Hanford Group, Richland, WA.
- Hu TA. 2002. *Steady State Flammable Gas Release Rate Calculations and Lower Flammability Level Evaluation for Hanford Tank Waste*. RPP-5926 Rev. 2, CH2M HILL Hanford Group, Richland, WA.
- Hudlicky M. 1990. *Oxidations in Organic Chemistry*. ACS Monograph 186, American Chemical Society, Washington, DC.
- Mahoney LA, ZI Antoniak, JM Bates, and ME Dahl. 1999. *Retained Gas Sample Program*. PNNL-13000, Pacific Northwest National Laboratory, Richland, WA.
- Meisel D, H Diamond, EP Horwitz, CD Jonah, MS Matheson, MC Sauer Jr, JC Sullivan, F Barnabas, E Cerny, and YD Cheng. 1991. *Radiolytic Generation of Gases from Synthetic Waste*. ANL-91/41, Argonne National Laboratory, Argonne, IL.

- Norton JD and LR Pederson. 1994. *Solubilities of Gases in Simulated Tank 241-SY-101 Wastes*. PNNL-10785, Pacific Northwest National Laboratory, Richland, WA.
- Pederson LR and SA Bryan. 1996. *Status and Integration of Studies of Gas Generation in Hanford Wastes*. PNL-11297, Pacific Northwest National Laboratory, Richland, WA.
- Person JC. 1996. *Effects of Oxygen Cover Gas and NaOH Dilution on Gas Generation in Tank 241-SY-101 Waste*. WHC-SD-WM-DTR-043, Westinghouse Hanford Company, Richland, WA.
- Person JC. 1998. *Gas Generation in Tank 241-AN-105 Waste with and Without Oxygen*. HNF-2038, Numatec Hanford Corporation, Richland, WA.
- Sherwood DJ and LM Stock. September 14, 2003. *An Assessment of the Applicability of the Hu Model for Hydrogen Generation to the WTP*. Bechtel National Inc., Richland, WA.
- Spinks JTW and RJ Woods. 1990. *An Introduction to Radiation Chemistry*. John Wiley and Sons, New York.
- Stock LM. 2001. *The Chemistry of Flammable Gas Generation*. RPP-6664 Rev. 1, CH2M HILL Hanford Group, Inc. Richland, WA.
- Smith MB and J March. 2001. *Advanced Organic Chemistry*, Fifth Edition. John Wiley and Sons, Inc. New York.

Appendix D

Technical Issue Report

The Influence of Hydroxide Ion on the Rate of Hydrogen Generation

Leon M. Stock, Donald M. Camaioni, and David J. Sherwood

Appendix D

Technical Issue Report

The Influence of Hydroxide Ion on the Rate of Hydrogen Generation

Leon M. Stock, Donald M. Camaioni, and David J. Sherwood

The hydroxide ion plays an important role in the chemistry associated with hydrogen generation in Hanford waste. Large additions of hydroxide in the Ultrafiltration Process were identified as a concern for applying the Hu model to the Waste Treatment Plant (WTP) because of this. Here, effects of various hydroxide concentrations on hydrogen generation are described and related to the applicability of the Hu correlation (Hu 1997, 2000, 2002). It is shown that even very large hydroxide additions are not likely to invalidate use of the Hu correlation at the WTP.

Hydrogen formation in Hanford waste is a complex chemical process that depends on the rates of formation and decomposition of organic “intermediates.” Delegard reported early on that hydrogen formation increased when sodium hydroxide was increased from 0.5 to 1.5 M, and that it decreased by a factor of three when concentration increased from 1.5 to 3.2 M. Later on Bryan and Pederson (1994, 1995) found that gas formation was sensitive to presence of particular organic complexants. In contrast to the results of Delegard (1980), they observed that hydrogen generation for a simulant containing HEDTA increased as the hydroxide ion concentration increased from 0.46 to 2.89 M and increased even more with increases to 4, 5, and 6 M. They also found decreased hydrogen generation in solutions with EDTA and citrate from the initial increase in the hydroxide ion concentration and then increased hydrogen generation at the higher concentrations (4–6 M hydroxide). These curious reactivity patterns have not been explained. However, Delegard showed that HEDTA decomposes much more rapidly than EDTA. Subsequent studies showed that glycolate was also reactive, whereas citrate was not. The curious difference in the way hydroxide influences hydrogen generation is presumably related to how it alters decomposition pathways. Later work in fact concluded that formaldehyde was an intermediate in the oxidative degradation of EDTA and HEDTA and their remnants, and that formaldehyde was efficiently converted to hydrogen in solutions with high hydroxide levels. Other oxidative species (e.g., the OH radical, O⁻ radical ion, or NO₂ radical) decompose formate without producing hydrogen gas.

Four key examples show that while hydroxide concentration influences the course that organic degradation reactions take in Hanford waste, increased levels do not necessarily promote hydrogen formation:

- First, the rate constant for reaction of hydroxide ion with a hydrogen atom is fast enough that at high concentrations, hydroxide may compete with organics for hydrogen atoms and thereby reduce hydrogen production from the usual hydrogen atom abstraction reactions.
- Second, the hydroxide ion converts a hydroxyl radical to its anion, O⁻, which reacts much slower with nitrite ion than hydroxyl radical.

- Third, hydroxide ion is also involved in the dose dependent conversion of nitrogen dioxide into nitrite and nitrate ions.
- Fourth, the effect of hydroxide on radiolytic aging of 0.1 M formate ion in solutions containing 4 M nitrate ion and 2 M nitrite ion is that increasing the hydroxide concentration from 0.1 to 2 M increases the oxidation rate by 400% but decreases the hydrogen generation rate by 20%.

Solvated electrons are the product of the hydroxide ion hydrogen atom reaction; these are rapidly scavenged by nitrate ion to ultimately produce nitrogen dioxide. While nitrogen dioxide has very low reactivity toward formate ion, the oxygen anion radical (O^-) has high reactivity such that a significant fraction of O^- can be scavenged in aged wastes that have relatively high concentrations of formate. The oxidation of formate ion by OH , O^- , or NO_2 does not generate hydrogen gas.

Finally, Albert Hu was aware of the effects of hydroxide on hydrogen generation and did not include it in his correlation because there was no reason to. Hydroxide concentrations in excess of 3 M are observed in 15 Hanford tanks; supporting laboratory experiments involved concentrations up to 6 M.

The Hu correlation (Hu 1997, 2000, 2002) was devised for the estimation of hydrogen generation rates in quiescent wastes that contain a broad array of chemical substances. A preliminary review of the WTP operations indicated that the sodium hydroxide concentration was to be increased to 3 M during solid leaching operations (Stock 2003). Consequently, we examined the role of elevated concentrations of hydroxide ion on the rates of decomposition of organic molecules and the related reactions leading to the generation of hydrogen. The purpose of this document is to provide preliminary information on the potential impact of 3 M sodium hydroxide concentrations on hydrogen generation in Hanford Site waste. The information has been abstracted from technical reports from Hanford and other laboratories.

D.1 Background

D.1.1 Chemical Features

Hydrogen is generated by radiolytic and thermal reactions in Hanford Site waste. The thermal reactions of the organic complexants produce intermediate organic compounds such as formaldehyde that lead to the formation of hydrogen. Similarly, the radiolytic reactions of the inorganic constituents including water, sodium nitrite, and sodium nitrate produce an array of free radicals that oxidize the organic complexants to produce similar intermediates.



Hydrogen formation is therefore a complex chemical process that depends not only on the rates of formation of the intermediates but also upon their rates of decomposition.

Very early work by Delegard (1980) showed that the rate of gas formation at 120°C from an SY-101 simulant containing N-hydroxyethylethylenediaminetriacetate ion (HEDTA) and ethylenediaminetetraacetate ion (EDTA) depended on the concentration of sodium hydroxide in a subtle way. He reported that the rate of gas formation increased as the concentration of sodium hydroxide was increased from 0.5 to 1.5 M. The rate of gas formation then decreased by a factor of 3 as the concentration of sodium hydroxide increased from 1.5 to 3.2 M.

Bryan and Pederson (1994) also examined the effects of hydroxide ion on the thermal gas generation rates with HEDTA, EDTA, citrate ion, and formate ion individually in a SY-101 waste simulant. Formate ion produced only very small amounts of hydrogen; the results for the other complexants are shown in Table D.1.

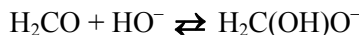
Table D.1. Effect of Hydroxide Ion with Organic Compounds on Hydrogen Generation in Tank SY-101 Waste Simulant

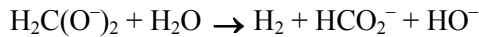
[OH ⁻] (M)	Hydrogen Generation Rate (10 ⁵ moles H ₂ per kg waste per day)		
	[citrate] (M)	[EDTA] (M)	[HEDTA] (M)
0.46	1.9	0.4	1.8
1.66	0.4	0.2	2.0
2.89	0.7		2.7
4.06	3.8	1.2	8.6
5.26	2.2	1.2	17.0
6.46	2.7	5.5	40.4

Bryan and Pederson (1994) found that gas generation rates were dependent upon the nature of the organic complexant in the simulant. In contrast to the results of Delegard, they observed that the hydrogen generation rate with a simulant containing HEDTA increased as the hydroxide ion concentration increased from 0.46 to 2.89 M, and increased even more with hydroxide ion concentrations at 4, 5, and 6 M. But they also found that the hydrogen generation rates with EDTA and citrate ion decreased with the initial increase in the hydroxide ion concentration and then increased as the concentration of hydroxide ion was increased to 4, 5, and 6 M. These curious reactivity patterns have not been explained. While the higher hydrogen generation rates at high hydroxide ion concentrations (4 M) could be attributed to corrosion of the steel reactor vessels, as pointed out by Bryan and Pederson (1994), the variations in the reaction rates, and the obvious dependence of the reactivity pattern on the nature of the complexant at lower hydroxide ion concentrations are probably real.

Several investigators have noted that the rate of hydrogen formation depends on the rate of decomposition of the organic complexant in the waste. Delegard (1980) showed that the rate of decomposition of HEDTA was much more rapid than the rate of decomposition of EDTA. Subsequent studies by Delegard (1987) and Ashby and coworkers (1994a, 1994b) showed glycolate ion was also reactive, whereas citrate ion was not. The reactivity patterns observed by Bryan and Pederson (1994) are compatible with the observations of Ashby and Delegard and their associates. The curious differences in the manner in which hydroxide ion influences the hydrogen generation rates is presumably related to the manner in which hydroxide ion influences the rates of decomposition of the organic molecules.

Later work led to the conclusion that formaldehyde was an intermediate in the degradation of EDTA and HEDTA and their remnants. Ashby and coworkers pointed out that formaldehyde was efficiently converted to hydrogen in strongly alkaline solutions (Ashby et al. 1994a, Ashby et al. 1994b, Barefield et al. 1994, Barefield et al. 1996). This concept was confirmed by work at the Argonne National Laboratory (Kapoor et al. 1995). Hydroxide ion is the key reagent in two steps of the reaction sequence.

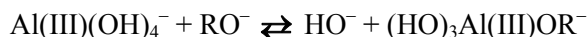




The reaction sequence has been chemically modeled by Kapoor and associates (Kapoor et al. 1995).

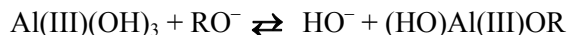
The influence of oxygen on the rates of formation of hydrogen from formaldehyde has been discussed elsewhere (Stock et al. 2003).

The mechanism of the thermal aging of complexants catalyzed by aluminate ion is uncertain. Kinetic studies have shown that the reaction is first-order in aluminate ion. Delegard (1987) proposed a mechanism in which HEDTA, represented as the anion (RO) of an alcohol (ROH), displaced a hydroxyl group from aluminate ion.



He also suggested that the reaction product was oxidized to an aldehyde by nitrite or nitrate ion. The Georgia Tech workers (Ashby et al. 1994b, 1994c) advanced an alternative mechanism to explain the role of aluminate ions. They suggested nitrite and aluminate ions reacted to form a nitritoaluminate species that, in the rate determining step, nitrosates complexants having hydroxyl or secondary or primary amino groups. The resulting nitrite esters and N-nitroso compounds then decompose to formaldehyde or glyoxal and NO^- . Camaioni and Autrey (2000) tested this explanation. They observed that aluminate ion did not accelerate the hydrolysis of nitritoacetate or ethyl nitrite, a model for HEDTA, and therefore could not catalyze the nitrosation reaction. Furthermore, a study of the decomposition of nitritoacetate ($\text{ONOCH}_2\text{CO}_2^-$) in waste simulants showed it to hydrolyze much faster than it decomposes to either glyoxal or formaldehyde (Camaioni et al. 2003 unpublished data). These facts are inconsistent with nitrosation being a rate-determining step in the aging of the complexants.

Delegard's mechanism, in which an organoaluminate ion reacts with nitrite ion is more consistent with the complicated rate dependence on hydroxide ion. Equilibria involving the complexant, represented as ROH, and its anion RO^- , aluminum hydroxide, and aluminate ion concentrations are influenced by the concentration of hydroxide ion as illustrated in the following equations.



Equilibria involving hydroxide ion and aluminum compounds play an important role in determining the solubility of inorganic compounds in Hanford Site waste (Barney 1976; Reynolds and Herting 1984). Consequently, it would not be surprising to find that similar equilibria involving organic compounds play a significant role in determining hydrogen formation rates.

D.1.2 Radiolytic Reactions

The hydroxide ion also affects radiolytic reactions in the waste because it alters the distribution of oxidizing radicals (H, OH, O⁻, and NO₂). Four distinct examples are examined in the following paragraphs. Each illustration is based upon a qualitative analysis of a few key reactions in the complex reaction system that begins with the radiolysis of water and proceeds through the oxidation of organic compounds and ends with hydrogen formation. The preliminary conclusions of this qualitative discussion will be tested by chemical modeling work during the course of this study.

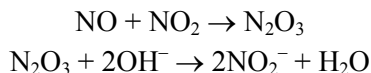
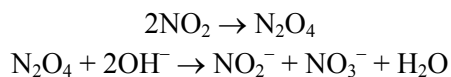
First, the rate constant for reaction of hydroxide ion with hydrogen atom (Han and Bartels 1990),



is fast enough that at high concentrations, hydroxide ion may compete with organic compounds for hydrogen atoms and thereby reduce the production of hydrogen gas from hydrogen atom abstraction reactions. Solvated electrons, the product of the reaction, are rapidly scavenged by nitrate ion to ultimately produce nitrogen dioxide.

Second, hydroxide ion converts hydroxyl radical to its anion, O⁻. This anion radical reacts much more slowly with nitrite ion than hydroxyl radical. Specifically, hydroxyl radical reacts with nitrite ion at the diffusion limit (Buxton et al. 1988), but its anion radical reacts much more slowly ($k \sim 5 \times 10^7 \text{ M}^{-1}\text{s}^{-1}$) (Fessenden et al. 2000). While both reactions produce nitrogen dioxide, the effect on the rate of formation of hydrogen gas is affected because nitrogen dioxide is a key reagent in the oxidation reaction of the complexants that lead to hydrogen-producing aldehydes.

Third, hydroxide ion is also involved in the dose dependent conversion of nitrogen dioxide into nitrite and nitrate ions (Park and Lee 1988; Lee and Schwarz 1981).



Fourth, Camaioni and coworkers have simulated the effect of hydroxide on radiolytic aging of 0.1 M formate ion in a solution containing 4 M nitrate ion and 2 M nitrite ion. The simulations showed that increasing the hydroxide ion concentration from 0.1 to 2 M increases the overall rate of oxidation by 400% but decreases the rate of hydrogen generation by 20%.

These four examples indicate that hydroxide ion will certainly influence the course of the radiolytic reactions that lead eventually to hydrogen generation. It is not evident that an increase in the hydroxide ion concentration will necessarily translate to increased rates of hydrogen generation. Moreover, organic speciation is a major factor in this chemistry. For example, while nitrogen dioxide has very low reactivity toward formate ion, the oxygen anion radical (O⁻) has high reactivity such that a significant fraction of O⁻ can be scavenged in aged wastes that have relatively high concentrations of formate ion (Meisel et al. 2000). The oxidation of formate ion by OH, O⁻, or NO₂ does not generate hydrogen gas. As mentioned,

the rate constants for virtually all the key reactions have been measured and the reaction system will be simulated during the course of this work.

D.1.3 Summary

In summary, hydroxide ion has a complex influence on the thermal and radiolytic gas generation rates. Increasing the concentration of hydroxide ion will certainly accelerate the thermal rate of formation of hydrogen from an intermediate like formaldehyde, but the rates of the reactions that lead from the original complexants to the hydrogen-generating intermediates may actually be slower at 3 M hydroxide ion.

Hydroxide ion alters the distribution of oxidants generated by radiolysis. The oxidants differ significantly in selectivity and reactivity. How the yield and rate of hydrogen production may change depends on the composition of the waste, and in particular on the organic species present in the waste.

D.2 The Hu Correlation

The Hu correlation was developed to assess the rates of hydrogen generation in Hanford tank wastes. It is pertinent to note that hydroxide ion concentrations in excess of 3 M are observed in liquids from 15 tanks (see Table D.2). Consequently, sodium hydroxide concentrations in this range are not unusual.

Table D.2. Waste Tanks with Hydroxide Ion Concentrations Greater than 3 Molar^(a)

Waste Tank	[OH ⁻] (µg/mL)
241-AN-103 ^(b)	104,000
241-AX-101 ^(b)	100,000
241-S-109	89,000
241-AN-104 ^(b)	71,000
241-BY-105	62,000
241-S-106	61,000
241-AN-105 ^{(b,c)‡}	60,000
241-A-101 ^(b,d)	58,000
241-SX-101 ^(b)	57,000
241-AY-101	55,000
241-S-112	55,000
241-AP-105	55,000
241-S-111	55,000
241-BY-103	52,000
241-S-104	51,000
(a) Taken from Best Basis Inventory.	
(b) This tank was included in Albert Hu's evaluations.	
(c) The rate of hydrogen generation was measured by Person (1998).	
(d) The rate of hydrogen generation was measured by Bryan and associates.	

The Hu correlation was developed on the basis of technical information in laboratory investigations of simulants and wastes. Laboratory work with simulants has frequently been carried out with sodium hydroxide concentrations between 2 and 2.5 M (Meisel et al. 1991; Ashby et al. 1994a, 1994b; Barefield et al. 1994, 1996; Camaioni et al. 1996, 1998). As discussed, Delegard (1980, 1987) studied simulants with hydroxide ion concentrations between 0.5 and 3.2 M, and Bryan and Pederson (1994) examined the rates of hydrogen generation from organic complexants in simulants with 0.46 to 6 M hydroxide ion.

The rate data on which the Hu correlation depends were determined by Bryan and associates (Bryan and Pederson 1995; Bryan et al. 1996; King et al. 1998; King and Bryan 1999). They measured the thermal and radiolytic rates of hydrogen generation in seven tank wastes including Tank A-101. Person investigated the rates of hydrogen generation in two additional tank wastes (Person 1996, 1998) including Tank AN-105. These tanks are mentioned because the concentrations of hydroxide ion are approximate 2.5 and 3 M in wastes from AN-105 and A-101, respectively. Therefore, the Hu correlation is based on information from simulants and wastes that contained rather high concentrations of hydroxide ion.

Hu examined the possible reaction variables (including the hydroxide ion concentration) that might influence the reaction rate and concluded that the thermal reaction rate did not depend on the hydroxide ion concentration but did depend upon the concentrations of aluminate ion and total organic carbon (TOC) in the liquid phase (Hu 2002). He empirically established that the available information was best correlated by the adoption of a rate expression in which the thermal reaction rate was first-order in TOC concentration and 0.4-order in aluminum concentration (both in the liquid phase). These features are summarized in the Hu correlation.

$$HGR_{\text{therm}} = a_T (f [\text{TOC}]) [\text{Al}]^{0.4} f_L \exp(-Q_T/RT) \text{ moles H}_2/\text{day per kg-waste.}$$

Here:

$$a_T = 2.76 \times 10^9;$$

$$f = \text{“reactivity coefficient” for organics, } f = 0.7 \text{ for double-shell tank waste, or } f = 0.4 \text{ for single-shell tank waste;}$$

$$[\text{TOC}] = \text{concentration in weight percent of total organic carbon in liquid phase (not the weight fraction: 3 wt\% is 3, not 0.03);}$$

$$[\text{Al}] = \text{weight percent aluminum in the liquid phase;}$$

$$f_L = \text{liquid weight fraction of waste;}$$

$$Q_T = 89.3 \pm 1.93 \text{ kJ/mol, activation energy;}$$

$$R = 8.314 \text{ J/K-mol, the gas constant; and}$$

$$T = \text{the waste temperature in Kelvin.}$$

In a similar fashion, Hu concluded that the G value for hydrogen formation from organic compounds, $G_{\text{TOC}(\text{H}_2)}$, was temperature dependent and also depended on the TOC concentration, but not upon the concentration of aluminum or hydroxide ion:

$$G_{\text{TOC}(\text{H}_2)} = a_0 (f [\text{TOC}]) \exp(-Q_{\text{rad}}/RT),$$

with

$$a_0 = 2.49 \times 10^6;$$

f = “reactivity coefficient” for organics, $f = 0.7$ for double-shell tank waste, or
 $f = 0.4$ for single-shell tank waste;
[TOC] = concentration in weight percent of total organic carbon in liquid phase
(not the weight fraction: 3 wt% is 3, not 0.03);
 Q_{rad} = 44.32 ± 2.04 kJ/mol, activation energy;
 R = 8.314 J/K-mol, the gas constant; and
 T = the waste temperature in Kelvin.

Hu evaluated the rate expression by comparing his predictions with field observations of hydrogen release rates from waste tanks. He focused his attention on the waste tanks for which there was reliable information about the concentrations of the chemical reagents and the rates of hydrogen release from the tank. The finding that the predictions and results agreed within a factor of 2 provided technical support for the general accuracy of the model and the general correctness of its formulation.

The absence of a dependence on the hydroxide ion concentration can be traced, at least in part, to the fact that hydroxide ion does not necessarily increase the rate of hydrogen generation and that the measured hydrogen generation rates for waste from two tanks with quite high hydroxide ion concentrations were used to establish the correlation. The correctness of the decision not to include hydroxide ion in the correlation is affirmed by the apparently successful prediction of the hydrogen generation rates in six waste tanks with $[\text{OH}^-] > 3$ M (Hu 2002).

D.3 Summary

The laboratory work that has been conducted to define the role of hydroxide ion suggests that hydroxide ion plays a complex role in the chemistry. The empirical work seems more definitive. Simply stated, there was no compelling need to include a term for the hydroxide ion dependence in the Hu correlation.

D.4 Conclusion and Recommendations

The available information shows that hydroxide ion has a complex influence on the thermal and radiolytic rates of generation of hydrogen in tank waste. We have adopted the viewpoint that the results obtained in laboratory experiments with concentrations of hydroxide ion greater than 4 M are spurious and should not be used to guide future work. Also, we have focused attention on the observations for reactions with 0.5 to 3.2 M hydroxide ion inasmuch as the concentration of hydroxide ion in WTP unit operations will not generally exceed 3 M $[\text{OH}^-]$.

The laboratory work with simulants suggests that different organic compounds respond in a different manner to changing hydroxide ion concentrations between 0.5 and 3 M. The thermal rates of hydrogen formation from some complexants increase as the concentration of hydroxide ion is increased, but the rates of hydrogen formation from some other complexants decrease as the hydroxide ion concentration is increased.

The effects of hydroxide ion on the radiolytic hydrogen generation rate are equally complex. The examples mentioned in the previous section imply that increases in the hydroxide ion concentration will

alter the chemical reaction sequences, and may therefore actually reduce the hydrogen generation rate in some cases.

The hydroxide concentration was excluded from the Hu correlation because there was no compelling reason to include this term in the thermal or radiolytic rate expressions. Wastes with hydroxide concentrations in excess of 3 M were used to establish the correlation and to test its efficacy. We therefore regard the dependence of the thermal and radiolytic reaction rates on hydroxide concentration as resolved from an empirical viewpoint. While the hydroxide level influences the chemistry of hydrogen generation in waste materials, it is not a key parameter for predicting the hydrogen generation rate with an empirical correlation such as Albert Hu's.

These conclusions lead to the following recommendations.

- First, no laboratory work needs to be planned using simulants or wastes to determine the dependence of the hydrogen generation rate on the hydroxide ion concentration at the present time.
- Second, the radiolytic and chemical reactions leading to hydrogen production should be simulated to provide definite information about the hydroxide rate dependence.
- Third, tank waste samples that are to be examined in the course of this program should be analyzed for hydroxide ion so that the results of hydrogen generation tests can be used to substantiate the concept that the thermal and radiolytic hydrogen generation rates do not depend critically on the hydroxide ion concentration.

D.5 References

Ashby EC, R Doctorovich, CL Liotta, HM Neumann, CF Yao, K Zhang, and NF McDuffie. 1994a. "Concerning the Formation of Hydrogen in Nuclear Waste. Quantitative Generation of Hydrogen via a Canizzaro Intermediate." *J. Am. Chem. Soc.*, Vol. 115, p. 1171.

Ashby EC, A Annis, EK Barefield, D Boatwright, R Doctorovich, CL Liotta, HM Neumann, CF Yao, K Zhang, and NF McDuffie. 1994b. "Synthetic Waste Chemical Mechanism Studies." WHC-EP-0823, Westinghouse Hanford Company, Richland, WA.

Ashby EC, EK Barefield, CL Liotta, HM Neumann, R Doctorovich, A Konda, K Zhang, J Hurley, D Boatwright, A Annis, G Pasino, M Dawson, and M Juliano. 1994c. "Mechanistic Studies Related to the Thermal Chemistry of Simulated Nuclear Waste That Mimic The Contents of a Hanford Site Double-Shell Tank." *ACS Sym Ser*, Vol. 554, p. 247.

Barefield EK, D Boatwright, A Desphande, R Doctorovich, CL Liotta, HM Neumann, and S Seymore. 1995. "Mechanisms of Gas Generation from Simulated SY Tank Farm Wastes: FY1994 Progress Report." PNL-10822, Pacific Northwest National Laboratory, Richland, WA.

Barefield EK, D Boatwright, A Desphande, R Doctorovich, CL Liotta, HM Neumann, and S Seymore. 1996. "Mechanisms of Gas Generation from Simulated SY Tank Farm Wastes: FY1995 Progress Report." PNL-11247, Pacific Northwest National Laboratory, Richland, WA.

Barney SA. 1976. *Vapor-liquid-Solid Phase Equilibria of Radioactive Sodium Salt Wastes at Hanford*. ARH-ST-133, Atlantic Richfield Hanford Company, Richland, WA.

- Bryan SA and LR Pederson. 1994. *Composition, Preparation, and Gas Generation Results from Simulated Wastes of Tank 241-SY-101*. PNL-10075, Pacific Northwest National Laboratory, Richland, WA.
- Bryan SA and LR Pederson. 1995. *Thermal and Combined Thermal and Radiolytic Reactions Involving Nitrous Oxide, Hydrogen, and Nitrogen in the Gas Phase: Comparison of Gas Generation Rates in Supernate and Solid Fractions of Tank 241-SY-101 Simulated Wastes*. PNL-10490, Pacific Northwest National Laboratory, Richland, WA.
- Bryan SA, LR Pederson, CM King, SV Forbes, and RL Sell. 1996. *Gas Generation in Tank 241-SY-103 Waste*. PNL-10978, Pacific Northwest National Laboratory, Richland, WA.
- Buxton GV, CL Greenstock, WP Helman, and AB Ross. 1988. "Critical review of rate constants for reactions of hydrated electrons, hydrogen atoms and hydroxyl radicals ($\cdot\text{OH}/\cdot\text{O}^-$) in aqueous solution." *J. Phys. Chem. Ref. Data*, Vol. 17, p. 513.
- Camaioni DM and T Autrey. 2000. "Thermochemical Kinetic Analysis of Mechanism for Thermal Oxidation of Organic Complexants in High-Level Wastes." *Nuclear Site Remediation, First Accomplishments of the Environmental Management Science Program*. EPG Eller and WR Heineman, eds. *ACS Symp. Ser.*, Vol. 778, p. 299. American Chemical Society, Washington, DC.
- Camaioni DM, WD Samuels, JC Lenihan, SA Clauss, AK Sharma, KL Wahl, and JA Campbell. 1996. *Organic Tank Safety Program FY96 Waste Aging Studies*. PNL-11312, Pacific Northwest Laboratory, Richland, WA.
- Camaioni DM, WD Samuels, JC Linehan, AK Sharma, ST Autrey, MA Lilga, MO Hogan, SA Clauss, KL Wahl, and JA Campbell. 1998. *Organic Tanks Safety Program Waste Aging Studies Final Report*. PNNL-11909, Pacific Northwest National Laboratory, Richland, WA.
- Delegard C. 1980. *Laboratory Studies of Complexed Waste Slurry Volume Growth in Tank 241-SY-101*. RHO-LD-124, Rockwell International, Richland, WA.
- Delegard CH. 1987. *Identities of HEDTA and Glycolate Degradation Products in Simulated Hanford High-Level Waste*. RHO-RE-ST-55P, Rockwell Hanford Operations, Richland, WA.
- Han P and DM Bartels. 1990. *J. Phys. Chem.* Vol. 94, p. 7294.
- Fessenden RW, D Meisel, et al. 2000. "Addition of Oxide Radical Ions (O^-) to Nitrite and Oxide Ions (O^{2-}) to Nitrogen Dioxide." *J. Am. Chem. Soc.* Vol. 122, pp. 3773-4.
- Hu TA. 1997. *Calculations of Hydrogen Release Rate at Steady State for Double-Shell Tanks*. HNF-SD-WM-CN-117, Lockheed Martin Hanford Corporation, Richland, WA.
- Hu TA. 2000. *Empirical Rate Equation Model and Rate Calculation of Hydrogen Generation Rate for Hanford Waste Tanks*. HNF-3851 Rev. 0A, CH2M HILL Hanford Group, Inc., Richland, WA.
- Hu TA. 2002. *Steady-State Flammable Gas Release Rate Calculations and Lower Flammability Level Evaluation for Hanford Tank Waste*. RPP-5926 Rev. 2, CH2M HILL Hanford Group, Inc. Richland, WA.
- Kapoor S, FA Barnabas, MC Sauer Jr, D Meisel, and CD Jonah. 1995. "Kinetics of Hydrogen Formation from Formaldehyde in Basic Aqueous Solutions." *J. Phys. Chem.*, 99(18):6857-6863.
- King CM and SA Bryan. 1999. *Thermal and Radiolytic Gas Generation Tests on Material from Tanks 241-U-103, 241-AW-101, 241-S-106, and 241-S-102: Status Report*. PNL-12181, Pacific Northwest National Laboratory, Richland, WA.

- King CM, LR Pederson, and SA Bryan. 1998. *Thermal and Radiolytic Gas Generation from Tank 241-SY-102 Waste*. PNL-11600, Pacific Northwest National Laboratory, Richland, WA.
- Lee YN and HA Schwarz. 1981. "Reaction Kinetics of Nitrogen Dioxide with Liquid Water at Low Partial Pressures." *J. Phys. Chem.* Vol. 85, pp. 840-848.
- Meisel D, H Diamond, EP Horwitz, CD Jonah, MS Matheson, MC Sauer Jr, JC Sullivan, F Barnabas, E Cerny, and YD Cheng. 1991. *Radiolytic Generation of Gases from Synthetic Waste*. ANL-91/41, Argonne National Laboratory, Argonne, IL.
- Meisel D, DM Camaioni, and T Orlando. 2000. "Radiation and Chemistry in Nuclear Waste: The NO_x System and Organic Aging." *Nuclear Site Remediation, First Accomplishments of the Environmental Management Science Program*, EPG Eller and WR Heineman, eds. *ACS Symp. Ser., Vol. 778*, pp. 342-361. American Chemical Society, Washington, DC.
- Park JY and YN Lee. 1988. "Solubility and Decomposition Kinetics of Nitrous Acid in Aqueous Solution." *J. Phys. Chem.*, Vol. 92, pp. 6294-6304.
- Person JC. 1996. *Effects of Oxygen Cover Gas and NaOH Dilution on Gas Generation in Tank 241-SY-101 Waste*. WHC-SD-WM-DTR-043, Westinghouse Hanford Company, Richland, WA.
- Person JC. 1998. *Gas Generation in Tank 241-AN-105 Waste with and Without Oxygen.*" HNF-2038, Numatec Hanford Corporation, Richland, WA.
- Reynolds DA and DL Herting. 1984. *Solubilities of Sodium Nitrate, Sodium Nitrite, and Sodium Aluminate in Simulated Nuclear Waste*. RHO-RE-ST-14P, Rockwell International, Richland, WA.
- Stock LM. 2003. "An Evaluation of the Hu Model for Calculating Hydrogen Generation Rates in the Hanford Waste Treatment and Immobilization Plant." Report to the WTP Project R&T Department, CCN 062957.
- Stock LM, DM Camaioni, and DJ Sherwood. 2003. "The Influence of Oxygen on the Rate of Hydrogen Generation" Technical Information Report, WTP CCN 067390.

Appendix E

Technical Issue Report

Effect of Permanganate Addition on Predicting Hydrogen Generation Rates

Richard T. Hallen, Donald M. Camaioni, Leon M. Stock, and David J. Sherwood

Appendix E

Technical Issue Report

Effect of Permanganate Addition on Predicting Hydrogen Generation Rates

Richard T. Hallen, Donald M. Camaioni, Leon M. Stock, and David J. Sherwood

E.1 Summary

The ultrafiltration process employs sodium permanganate additions to remove Sr/TRU before the filtration operation. The permanganate ion is a potent oxidizer of organic compounds. The impact of permanganate addition to Hanford waste feed in the WTP was therefore identified as a potential concern for applying the Hu correlation to predict hydrogen generation, because organic compounds dominate the behaviors described by the correlation. Here, the potential effects of permanganate additions on hydrogen production in Hanford Envelope C waste are evaluated. Permanganate is not likely to accelerate any of the processes responsible for hydrogen production. However, a study has shown that the radiolytic yield of hydrogen gas is higher following treatment. This result is attributed to the fact that nitrate and nitrite, which inhibit radiolytic H₂ generation, are separated from the waste in the subsequent wash steps. The Hu model's water radiolysis term should be reviewed for this condition.

Hydrogen formation in Hanford waste results from complex chemical processes, which depend partly on the rates of formation and oxidative decomposition of organic "intermediates." Bryan and Pederson found that gas formation was sensitive to the presence of particular organic complexants such as EDTA and HEDTA. These complexants are responsible for the elevated levels of Sr-90 and TRU in the Envelope C wastes requiring the permanganate additions. Permanganate additions will have little impact on the total organic carbon (TOC) content of the waste, but the organic compounds are more oxidized ("aged") as a result of permanganate (Mn[VII]) reduction to lower oxidation states of manganese (Mn[IV]).

The impact of permanganate addition can be summarized as:

- Permanganate(Mn[VII]) is rapidly reduced to lower oxidation states of manganese (primarily Mn[IV]). Permanganate is only present for a few minutes after addition to tank waste; reduced Mn is the most stable oxidation state and the reduced forms of Mn precipitate from solution after reduction. Experimental results suggest that the organic compounds present in the waste are the main reductants for permanganate.
- The TOC is not significantly impacted, because the levels of permanganate are relatively low (0.075 M) compared to the levels of TOC in the waste treated (~1 M). However, the TOC is oxidized by the permanganate addition. The resulting TOC would be more aged and is therefore expected to provide for less hydrogen generation than untreated waste.
- Additions of permanganate compounds produce little chemical change in the bulk waste. These compounds are precipitated from solution and then removed by filtration. As a result, the filtered solids contain a significantly higher concentration of Mn than the initial entrained solids.

- The filtered precipitate from a Sr/TRU removal test with an actual waste sample was washed and used for gas generation tests. The result was: $G(H_2) = 0.18$ molecules/100 eV, which is consistent with analyses that showed significantly lower concentrations of nitrate and nitrite in the sample due to the washing process.

E.2 Introduction

Stock (2003) identified the permanganate addition during the Sr/TRU precipitation operation for the Ultrafiltration Process as a potential concern for using the Hu correlation to predict hydrogen generation rates (HGRs) in the WTP. This issue is evaluated here.

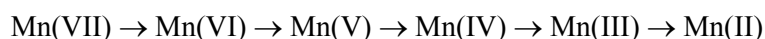
Soluble Sr-90 and TRU elements will be removed from Envelope C waste by adding 1) nonradioactive Sr for isotopic dilution and precipitation of Sr-90 as $SrCO_3$, and 2) sodium permanganate ($NaMnO_4$) to partially and selectively oxidize the organic complexants and co-precipitate the soluble TRU elements with the (reduced) Mn precipitates. Only two Hanford tanks, AN-102 and AN-107, are currently designated as Envelope C waste and require the Sr/TRU removal before the supernatant can be vitrified as LAW.

The aqueous chemistry of permanganate ions and organic complexants is briefly described here. No processes could be identified which would lead to increased production of hydrogen gas or any complications with using the Hu correlation for predicting hydrogen generation rates in the WTP. It is interesting to note that potassium permanganate was employed for both the Bismuth Phosphate (Jones 1994) and REDOX (Long 1967) operations at the Hanford Site. So, while levels in the waste feed to the WTP may be low, permanganate is not an entirely new addition to the Hanford waste.

E.3 Background

Permanganate ion, Mn(VII), has been used as an oxidizing agent in organic chemistry for over a century (Fatiadi 1987). It is one of the most versatile and vigorous of the commonly used oxidants and has been employed extensively across the range of pH. Many books and reviews summarize the reaction chemistry of permanganate with a wide variety of organic compounds, including alkanes, alkenes, alcohols, aldehydes, ketones, and other organic nitrogen- and sulfur-containing compounds (Smith and March 2001; Hudlicky 1990). Permanganate is a powerful oxidant under basic conditions, $E^\circ = +1.23V$ (Fatiadi 1987), in contrast to other common oxidants like cerium, Ce(IV), or chromate, Cr(VI), which are good oxidants under acidic conditions but are stable under the basic conditions characteristic of Hanford tank wastes.

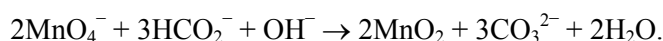
The permanganate oxidation of tank waste results in the reduction of Mn(VII) to lower oxidation states, with the potential for complete reduction to Mn(II), as shown here:



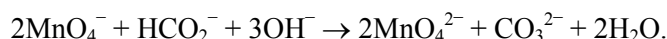
However, under basic conditions, the most stable oxidation state is Mn(IV), while under acidic conditions, Mn(II) is the most stable oxidation state. The Mn(IV) is typically insoluble in base and

precipitates from such solutions as a hydrated manganese dioxide^a (Lilga et al. 2003). At high hydroxide concentrations permanganate can disproportionate, which makes it difficult to determine whether the oxidation proceeds via a one- or two-electron process (Fatiadi 1987).

The reduction of permanganate, Mn(VII), is rapid in tank wastes, only taking minutes for reduction and precipitation from solution as Mn(IV). For example, a sample taken 10 minutes after the permanganate addition showed TRU removal by precipitation was already completed (Hallen *et al.* 2002a). Many compounds present in tank waste have the potential to reduce permanganate. Lilga *et al.* (2003) and Gauger and Hallen (2001) reported results from studies directed at understanding the mechanisms of the Sr/TRU removal process. One of the simplest reactions of permanganate with tank waste can be represented by the oxidation of sodium formate:



The oxidation proceeds quickly with high concentration of reagents via a stepwise process, with manganate, Mn(VI), as an intermediate in the overall oxidation process:



Permanganate is reduced by many of the known or suspected organic compounds in tank waste with the exception of oxalate, which does not reduce permanganate under basic conditions. For example, formate oxidation produced carbonate, glycolate oxidation produced oxalate, and glycine oxidation produced oxalate and ammonia. Nitrite was *not* oxidized by permanganate under the basic conditions tested.

Orth et al. (1995) first demonstrated supernatant decontamination of Hanford tank waste (from Tank SY-101) using permanganate treatment. The waste was diluted 3:1 and treated with 0.11 M permanganate. For SY-101 waste and under these reaction conditions, TOC destruction was observed; Cr was dissolved from the sludge; Sr-90 and TRU were removed from the supernatant; and nitrite oxidation was observed.

E.3.1 Gas Generation Results with Washed Sr/TRU Process Solids

Bryan et al. (2003) measured gas generation from washed Sr/TRU solids. Their results are summarized in Table E.1. They concluded that:

- Activation energies for AN-102/C-104 Sr/TRU and AN-102 washed solids samples are 64 and 63 kJ/mol, respectively; essentially identical.
- $G(\text{H}_2) = 0.18$ molecules/100eV for the AN-102/C-014 Sr/TRU sample and $G(\text{H}_2) = 0.055$ molecules/100 eV for the AN-102 washed solids.
- This increased G value for the AN-102/C-104 Sr/TRU sample using the external gamma source is due to lower concentrations of nitrate and nitrite in the treated and washed sample.

(a) Lilga et al. (2003) references to manganese dioxide and the formula MnO_2 are used for simplicity. The actual precipitate from Mn(VII) reduction with aqueous formate solutions was determined by analysis to be the deprotonated, hydrated form of manganese dioxide, $\text{NaMn}(\text{O})(\text{OH})(\text{O}) \cdot x\text{H}_2\text{O}$. The composition from other reaction solutions may differ.

Table E.1. Thermal and Radiolytic Rate Parameters for Gas Generation from AN-102/C-104 Sr/TRU Precipitate Samples in 0.01M NaOH ^(a)

Parameter	H ₂	N ₂ O	N ₂	CH ₄	Overall rate
E_a , kJ/mol ^(b)	64(±62)	79(±26)	14(±7)	147(±82)	60(±32)
A , mol/kg/day ^(c)	790	6.9×10^5	2.3×10^{-3}	3.6×10^{14}	2.0×10^3
ln(A)	7(±21)	13(±9)	-6(±2)	34(±27)	8(±11)
R ²	0.458	0.902	0.934	0.861	0.699
G value at 32,000 R/h ^(d)	0.18 (±0.02)	0.0041 (±0.004)	-- ^(e)	0.0006 (±0.001)	0.19 (±0.023)
G value at 687 R/h	0.025 (±0.016)	0.004 (±0.004) >45°C 0.053 (±0.002) 45°C	-- ^(e)	0.005 (±0.003)	0.04 (±0.03)

(a) Values in parentheses indicate 95% confidence interval.
(b) Thermal activation parameter.
(c) Arrhenius pre-exponential factor.
(d) The G value, or gas generation efficiency, is defined as the number of molecules produced per 100 eV of radiation absorbed by the media.
(e) Indicates values not determined.

E.3.2 Potential Impacts of Permanganate Addition

Effects of permanganate addition on some factors affecting hydrogen generation are described in this section.

Dose Rate: The Sr/TRU removal process precipitates approximately 90% of the Sr-90 and 80% of the TRU from solution. Thus, concentrations of beta and alpha emitters should be decreased in the solution and increased in the washed solids. On the other hand, no decontamination of gamma emitters (e.g., Cs-137 and Co-60) occurred except for approximately 70% of Eu-154 (Hallen et al. 200b).

Aluminum: Soluble aluminum is present in both the AN-102 and AN-107 wastes, with significantly higher amounts in the former. The entrained solids in AN-102 are mostly Al, whereas the solids in AN-107 are largely Fe and Mn. The Al does not precipitate on permanganate treatment. Because of the caustic addition step associated with the Sr/TRU removal process, soluble Al may increase on treatment of AN-102 wastes.

TOC: The amount of added permanganate is actually quite low (0.05 M) relative to the TOC in the waste (~ 2 M at 6 M Na). The result of using permanganate for Sr/TRU removal from Envelope C wastes will be some amount of organic oxidation, similar to that which occurs during long-term waste storage (aging); i.e., the organic compounds will be more oxidized, but overall TOC will likely decrease very little.

Hallen et al. (2000) reported that on treatment of AN-107 with 0.05 M permanganate, very little of the organic carbon was destroyed (supernatant [TOC] = 13600 µg/g); a 6% reduction was reported, but analytical error is expected to be 10% for this analysis. The TIC was reduced by 14%; taking into account the amount required to precipitate the added Sr(NO₃)₂ as SrCO₃, carbonate decreased by 6%. These data indicate that very little TOC is destroyed on permanganate treatment and provide no indication of complete oxidation to carbonate. The nitrate in this test increased by approximately 7%, and the nitrite

was reduced by approximately 10%, indicating that permanganate, or the heat-digest of the precipitate, resulted in some nitrite oxidation to nitrate. However, these values are also within the expected $\pm 10\%$ error for the ion chromatography (IC) analytical method.

The washed solids from the treatment of AN-107 waste by the Sr/TRU process are low in TOC (1625 $\mu\text{g/g}$ dry solids), and the oxalate value (by IC) was quite high, 23300 $\mu\text{g/g}$. If all oxalate is considered TOC, then the solids TOC concentration should be at least 6350 $\mu\text{g/g}$. It is possible that some oxalate decomposition occurred during analysis and was reported as TIC. These results would suggest that most of the TOC in the washed solids are oxalate.

The TIC/TOC/TC was not analyzed in detail for the AN-102 wastes. However, in the appendix of Hallen et al. (2002b) the analytical data are included for both the treated supernatant and the resulting washed solids from AN-102/C-104 blended waste. Much less permanganate was used in treating this waste blend, 0.02 M. The supernatant was 11900 $\mu\text{g/g}$ TOC. The washed solids had a TOC of 6580 $\mu\text{g/g}$. These washed solids appear to be high in oxalate, 36200 $\mu\text{g/g}$ by IC, which would correspond to 9900 $\mu\text{g/g}$ TOC. Therefore, the relatively low TOC value for the washed solids relative to the high oxalate concentration suggest that oxalate is the primary TOC in the washed solids. These solids were also analyzed by thermal analysis (Bryan et al. 2003) and no apparent exotherm was observed.

Simple model compound studies (Gauger and Hallen 2001; Lilga et al. 2003) conducted to investigate the mechanism of permanganate decontamination of wastes showed that inorganic compounds (nitrite and oxalate) were unreactive to permanganate oxidation. The organic complexants and their degradation products were, on the other hand, easily oxidized by permanganate. For example, formate was oxidized to carbonate, glycolate was oxidized to oxalate, and glycine was oxidized to oxalate and ammonia. Mn(VII) was stepwise reduced to Mn(IV) and even lower oxidation states. When Mn(II) was added to waste simulant mixtures, it was found to air oxidize to higher oxidation states, forming similar solids as with a permanganate addition. The organic complexants such as gluconate (with alpha hydroxy carboxylate groups) promote the reduction of Mn(IV), leading to the incorporation of lower oxidation states of Mn in the precipitate. The reduced states of Mn are susceptible to air oxidation back to Mn(III) and/or Mn(IV). Permanganate appears to promote the air oxidation of complexants through continued reduction and air oxidation of species between the various oxidation states Mn(II), Mn(III), and Mn(IV).

Use of permanganate for oxidative leaching will likely have little impact, since the sludges are washed prior to leaching and only solids are oxidized. The Envelope D wastes are also typically low TOC wastes. The waste from C-106 (now in AY-102) may be a problem sludge waste, but it will likely be recommended that this tank not be caustic leached, let alone leached with permanganate.

Hydroxide: The baseline Sr/TRU removal process specifies addition of 1 M NaOH to as-received waste (6 M Na). Hydroxide levels in the tanks were originally quite low, for example, approximately 0.2 M AN-102, and AN-107 was even caustic deficient (no free OH^- and bicarbonate present). (AN-107 had consumed free hydroxide during storage.) Additional hydroxide has been added to these tanks after samples were taken for the WTP Project.

The ultrafiltration process permanganate treatment consumes very little free hydroxide; it is generally equivalent to the amount of added permanganate. This would correspond to less than 10% reduction in free hydroxide for baseline treatment conditions of 1 M added hydroxide and 0.05 M added permanganate.

Other waste components: The permanganate treatment process has little impact on the major chemical species present in the waste. Permanganate treatment primarily results in the precipitation of Mn(IV) compounds from solution. With the exception of iron in AN-107 (~1000 µg/g), most of these ions are in very low concentration in the waste. The anions remain relatively unchanged in solutions with small changes in carbonate and nitrate as a result of adding Sr(NO₃)₂ (0.075 M in the baseline flow sheet). Nitrite, phosphate, and sulfate levels remain relatively unchanged after permanganate additions.

Generic to any treated waste with permanganate, solids will have elevated concentrations of Mn, most likely as NaMn(O)(OH)(O)•xH₂O. Acid cleaning of the filter elements could result in some soluble Mn(II), which on neutralization would precipitate as Mn(OH)₂ and eventually air oxide to similar Mn solids from the original treatment, NaMn(O)(OH)(O)•xH₂O.

E.4 Conclusions and Recommendations

Permanganate is short lived in the WTP. Once added to tank waste it is rapidly converted to reduced forms of Mn, ultimately forming Mn(IV) precipitates. Permanganate treatment is not expected to accelerate gas generation, or impact the Hu correlation's ability to provide bounding predictions of hydrogen generation. Wastes treated with permanganate should generate less hydrogen gas from organic aging, because some oxidation of the organic compounds will likely occur. The additional hydroxide (1 M) added to Envelope C wastes is within the range that wastes have been evaluated for gas generation. Therefore, the Hu model's thermal hydrogenation term is likely to be applicable at this level of free hydroxide. The radiolytic yield of H₂ is higher following treatment. This result is attributed to the fact that nitrate and nitrite, which inhibit radiolytic H₂ generation, are separated from the waste in the subsequent wash steps. The Hu model's water radiolysis term should be reviewed for this condition.

E.5 References

- Bryan SA, SJ Bos, JGH Geeting, RD Scheele, RL Sell, and JE Tanner. 2003. *Gas Generation and Energetic Studies of an Envelope C Waste Treated by the Sr/TRU Precipitation Process*. WTP-RPT-063, Battelle – Pacific Northwest Division, Richland, WA.
- Fatiadi AJ. February 1987. "The Classical Permanganate Ion: Still a Novel Oxidant in Organic Chemistry." *Synthesis*, pp. 85-127.
- Gauger AM and RT Hallen. 2001. "Individual Reactions of Permanganate and Various Reductants." *J. Undergraduate Research*, Vol. 1, p. 54.
- Hallen RT, PR Bredt, KP Brooks, and LK Jagoda. 2000. *Combined Entrained Solids and Sr/TRU Removal from AN-107 Diluted Feed*. PNWD-3035, Battelle – Pacific Northwest Division, Richland, WA.
- Hallen RT, IE Burgeson, FV Hoopes, and DR Weier. 2002a. *Optimization of Sr/TRU Removal Conditions with Samples of AN-102 Tank Waste*. PNWD-3141, Battelle – Pacific Northwest Division, Richland, WA.
- Hallen RT, JGH Geeting, DR Jackson, and DR Weier. 2002b. *Combined Entrained Solids and Sr/TRU Removal from AN-102/C-104 Waste Blend*. PNWD-3264, Battelle – Pacific Northwest Division, Richland, WA.

- Hudlicky M. 1990. *Oxidation in Organic Chemistry*. American Chemical Society, Washington, DC.
- Jones T. 1994. *Hanford Technical Exchange Program: Process Chemistry at Hanford (Genesis of Hanford Wastes)*. PNL-SA-23121 S, Pacific Northwest Laboratory, Richland, WA.
- Lilga MA, RT Hallen, KM Boettcher, TR Hart, and DS Muzatko. 2003. *Assessment of the Sr/TRU Removal Precipitation Reaction Mechanisms Using Waste Simulant Solutions*. PNWD-3263, Battelle – Pacific Northwest Division, Richland, WA.
- Long JT. 1967. *Engineering for Nuclear Fuel Reprocessing*. Gordon and Breach Science Publishers, New York.
- Orth RJ, AH Zacher, AJ Schmidt, MR Elmore, KR Elliott, GG Neuenschwander, and SR Gano. 1995. *Removal of Strontium and Transuranics from Hanford Tank Waste via Addition of Metal Cations and Chemical Oxidant - FY 1995 Test Results*. PNL-10766, Pacific Northwest National Laboratory, Richland, WA.
- Smith MB and J March. 2001. *Advanced Organic Chemistry*, 5th Ed., John Wiley & Sons, New York.

Appendix F

Technical Issue Report

Effect of Glass Forming Chemicals on Hydrogen Generation Rates

Donald M. Camaioni and Leon Stock

Appendix F

Technical Issue Report

Effect of Glass Forming Chemicals on Hydrogen Generation Rates

Donald M. Camaioni and Leon Stock

Glass-forming chemicals will be introduced in the HLW Vitrification Melter Feed Preparation Process. The process receives HLW concentrate from the pretreatment plant. The concentrate is blended with glass formers and fed to the melter to produce a vitrified product that meets waste form qualification requirements. The HLW glass former recipe may include the following glass forming chemicals: silica (SiO_2), zinc oxide, lithium carbonate, boric acid (H_3BO_3), borax ($\text{Na}_2\text{B}_4\text{O}_7$), Fosterite olivine magnesium silicate (Mg_2SiO_4), and Wollastonite (CaSiO_3) (Lee and Binsfield 2003). The low activity waste glass former recipe may include, in addition to the above, titanium dioxide, ferric oxide, aluminum silicate, zirconium silicate. Sucrose, which prevents foaming in the melter, may also be added to the glass former mix. We are not aware of any direct studies of H_2 generation by Hanford wastes or waste simulants mixed with glass formers.

Some of the glass-formers may catalyze the radiolytic generation of hydrogen. Metallic particles in water, hydrated oxide powders, and aqueous suspensions of silica nanoparticles have all been reported to catalyze water radiolysis and increase the yield of H_2 (see LaVerne and Tonnie 2003 and references therein). For metal oxide particles suspended in solution, recent work suggests that the effect depends strongly on particle size.

LaVerne and Tonnie (2003) studied the effect of silica particle size on the yields of H_2 and concluded that the effect in solution is limited to very small particles. For 7- and 22-nm sized SiO_2 particles, they observed H_2 yields increased with the wt% of silica suspended in water. But for slurries containing 343-nm sized particles, the yield of H_2 was equivalent that expected from the water alone. Furthermore, they showed that the “excess” yield of H_2 caused by small particles is due to the generation of “excess” solvated electrons, which can be scavenged by mM concentrations of nitrate ion. Therefore, yields of H_2 should not be enhanced by energy absorbed by silica particles in waste streams that have as much or more nitrate and nitrite.

The presence of solid oxides can catalyze oxidation of organics to precursors of H_2 . The gamma radiolysis of aqueous EDTA is catalyzed by TiO_2 (Su et al. 1998). Addition of feldspar, an aluminosilicate, to a neutral solution containing nitrate and acetate increased yield of H_2 from gamma radiolysis (Pikaev et al. 2002). Such phenomena have received relatively little study and it is not possible to predict quantitatively the yields. As is the case for direct generation of H_2 , the effect should be strongly dependent on physical properties of the particles, e.g., particle size and porosity.

Considering that a variety of solids are already present in the wastes, the Hu model term for organic radiolysis, having been parameterized on actual wastes, may include the effect.

With respect to the effect of sucrose, we note that the tank wastes have had significant quantities of similar chemicals added to them. For example, glycolate ion and gluconate were added (Boldt et al. 1999) and butanol is present from hydrolysis of tributyl phosphate that entered the tank wastes from the PUREX process. Sugar is expected to behave chemically like these constituents. The Hu correlation was developed from waste tank data and soluble TOC is a variable in the Hu model. Therefore, it should suffice to combine the TOC from sugar with soluble TOC in the waste to predict the effect of added sugar.

References

Boldt L, GL Borsheim, NG Colton, BA Higley, KM Hodgson, MJ Kupfer, SL Lambert, MD Leclair, RM Orme, DE Place, WW Schulz, LW Shelton, BC Simpson, RA Watrous, and RT Winward. 1999. Standard Inventories of Chemicals and Radionuclides in Hanford Site Tank Wastes. HNF-SD-WM-TI-740 Rev. 0C, CH2M HILL Hanford Group, Richland, WA.

Su Y, Y Wang, JL Daschbach, TB Fryberger, MA Henderson, J Janata, and CHF Peden. 1998. "Gamma-Ray Destruction of EDTA Catalyzed by Titania." *J. Advan. Oxid. Technol.* Vol. 3, pp. 63-69.

LaVerne JA and SE Tonnie. 2003. *J. Phys. Chem. B*, Vol. 107, p. 7277 and references therein.

Lee E and M Binsfield. 2002. *Flowsheet Bases, Assumptions, and Requirements*. 24590-WTP-EPT-PT-02-005 Rev.1, Richland, WA.

Pikaev AK, GN Pirogova, et al. 2003. "Radiation-chemical aspects of radioactive waste management." *High Energy Chemistry*, 37(2):60-72.

Distribution

**No. of
Copies**

**No. of
Copies**

OFFSITE

ONSITE

1 Savannah River National Laboratory
Richard Edwards
Westinghouse SA
Aiken, South Carolina 29808-0001

14 Battelle – Pacific Northwest Division
S. A. Bryan (5) P7-25
D. M Camaioni P7-28
T. G. Levitskaia P7-28
B. K. McNamara P7-28
D. E. Kurath P7-28
R. L. Sell P7-25
Project File (2) P7-28
Information Release (2) K1-06

4 Bechtel National, Inc.
J. F. Doyle (2) H4-02
R. A. Peterson H4-02
D. J. Sherwood H4-02